CHAPTER 2.5

# Modeling and Simulation

Khosrow Nikkhah, David Wiseman, Michael J. Dry, and Hsin-Hsiung Huang

In mineral processing and extractive metallurgy, process modeling can be summarized as the numerical analysis of process data, generating the information required for the design of process equipment and the calculation of capital and operating costs for one or more configurations of unit operations for processing ore or concentrate from a given deposit. Process modeling is also a powerful tool for analyzing and optimizing an existing or a conceptual process and evaluating potential improvements.

Taking a mineral deposit from discovery to reality begins with quantification of the amount of ore present and the concentrations of valuable elements. This work includes drilling and analysis of samples, or re-compilation of results from earlier work. The results can be conveniently summarized as a total amount of ore and an elemental analysis, which, in conjunction with relevant prices, leads to an estimate of the potential value of the deposit. When the potential value is deemed to be sufficient, attention turns to the work needed to further quantify the deposit, generate appropriate samples, and evaluate the extraction technology.

This chapter covers process modeling and simulation for mineral processing and extractive metallurgy in hydrometallurgical and pyrometallurgical processes. Process modeling has a broad range of applications in these fields. It is an effective technique for better understanding of processes and their design, and it can be used to maximize the efficiency of the process and to minimize costs. In an operating plant, process modeling allows understanding of the process, thereby enabling better operation of the plant. Applications of process modeling can be categorized by both field of operation (mineral processing, hydrometallurgy, and pyrometallurgy) and the stage of project (conceptual study, feasibility, and detailed design).

Mining and metallurgical operations are commercial ventures, governed by the rules of investment for profit, safety, and environmental compliance. Within this framework, the objective of technology selection, therefore, must be to maximize the commercial benefit to be had from the deposit in question. Preliminary selection of technology for any given deposit is based on knowledge of the technology applied to similar deposits and sometimes also on information about novel technology. Although appropriate technology might be mineral processing, hydrometallurgy, or pyrometallurgy, within these categories are many individual combinations of unit operations. For the purposes of this chapter, the assumption is that the technology falls into one or more of these domains, but the principles illustrated would apply equally to all domains even though the unit operations differ from one domain of extractive metallurgy to another.

Modern computers and commercially available software for process simulation enable the evaluation of existing and envisaged circuits much earlier than was previously feasible, substantially enhancing the efficiency of the work required for the development of new ventures. This power also enables much more detailed study of existing circuits, leading to improved plant operation and uncovering improvements with considerably less risk than would otherwise be possible.

Although sophisticated software is available for process modeling, acquiring and mastering it entails appreciable cost, time, and effort. It is also possible to use spreadsheet calculations for preliminary evaluation of envisaged circuits for processing ore or concentrate.

## SIMULATION AND MODELING IN MINERAL PROCESSING

To arrive at the best design and sizing of mineral processing plants and improve efficiency of operations, process modeling can be used to efficiently study the effect of a variety of process concepts, design criteria, and capacities. In addition, process modeling can be used to evaluate process economics for different design alternatives and at the same time show flaws in process design, thus avoiding unnecessary problems during commissioning and plant operation. Having proven the

Khosrow Nikkhah, Senior Process Engineer, AMEC Foster Wheeler, Vancouver, British Columbia, Canada
David Wiseman, Principal, David Wiseman Pty Ltd., Blackwood, South Australia, Australia
Michael J. Dry, Owner, Arithmetek Inc., Peterborough, Ontario, Canada
Hsin-Hsiung Huang, Professor, Department of Metallurgical & Materials Engineering, Montana Tech, Butte, Montana, USA

soundness of the process design, it can be used in raising of capital for the intended development.

In modeling of mineral processing plants, sizing of equipment and optimization of mineral processing circuits are the usual goals. These plants have large capital and operating costs, with electrical power consumption in comminution plants being a significant factor. This necessitates the use of process modeling for sizing of equipment to arrive at increased capacity and improved particle size distribution, while at the same time reducing capital and operating costs. Process modeling in mineral processing uses characterization of feed material, known plant data, and test work to size and specify equipment and optimize flow sheets and operating conditions.

The uses and requirements for modeling and simulation by those in academia and education and by those in industry differ. Although research and training are important in advancing the technology, this chapter focuses mostly on the current "state of the art" of the availability and use of modeling and simulation tools for mineral processing industry practitioners.

## Historical Perspective

Herbst et al. (2002) provide a comprehensive overview of the historical background to modeling and simulation in the minerals processing sector of the industry.

The *SME Mineral Processing Handbook* (Weiss 1985) included a simulation and modeling section, specific to comminution circuits, covering much material also published earlier by Lynch (1977), which detailed model equations for grinding mills and hydrocyclones, and suggested that such models could be implemented in programming languages such as Fortran. However, it is unlikely that such use occurred outside of academia and the advanced research departments of larger companies.

Almost coincidental with the publication of the 1985 handbook (Weiss 1985) was the introduction and commercialization of a generation of "general-purpose," "user-friendly" simulation systems specifically aimed at minerals processing applications, which included CANMET-SPOC (Argyropoulos et al. 1984), MODSIM (Mineral Technologies International 2010), JKSimMet (JKTech 2018), and USIM PAC (Caspeo 2018). By providing a prebuilt simulation structure and suitable models, these simulation systems aimed to remove the need for specialized programming skills on the part of those interested in applying the models. After further development, by the time of the 2002 SME Mineral Processing Plant Design, Control and Practice conference in Vancouver, British Columbia, Canada (Herbst et al. 2002), these were reported as the "de facto industry standards."

The period between these two SME publications, from 1985 to 2002, also saw the publication of several important monographs that provided the background for the various data handling, process models, and modeling approaches. These included monographs by Austin et al. (1984), Napier-Munn et al. (1996), Wills (1997), and King (2001). A third contributing factor to changes in approach that occurred during this period was the introduction and subsequent ubiquity of personal computers, which resulted in increased accessibility to the models and the developing simulation frameworks. Coincident with the introduction of personal computing was the advent of general-purpose spreadsheet applications that largely replaced both calculators and mainframe computing and programming languages for mineral processing calculations.

## Current Status

In the intervening years since 2002, the modeling and simulation of mineral processing landscape has seen additional changes. Apart from specialized academic and research applications, with the introduction of commercial packages, user programming of complex simulation calculations has largely ceased. For simpler and ad hoc calculations, spreadsheets (typically Microsoft Excel) and general-purpose engineering calculation packages such as MATLAB (MathWorks 2018) and Mathcad (PTC 2018) have become the norm.

In the commercial sphere, there have also been changes to the four reported "de facto industry standards":

1. The CANMET-SPOC applications appear to be no longer in general use, although the mass balancing component of that system now forms part of the commercial data reconciliation and material balancing package Algosys Bilmat and Algosys Metallurgical Accountant from Triple Point (2018a, 2018b).
2. A free version of the MODSIM software was released on a CD with King's 2001 monograph. Current support is through Minerals Technologies Inc., a spin-off from the Utah Comminution Center at the University of Utah.
3. USIM PAC development has kept pace with these changes to the underlying system environment and continues to be commercially available through Caspeo in France, offering around 150 process models for a wide range of minerals.
4. JKSimMet remains in active development and provides support with a focus on simulation of comminution and classification circuits. Its latest version is commercially available and includes a flotation-specific analysis and simulation package in JKSimFloat and a two-dimensional (2-D) size by assay mass balancer in JKMultiBal. The JKMetAccount simulation-based approach to metallurgical accounting was spun off to Mincom/ABB and is now part of the ABB Ventyx suite (JKTech 2018; ABB 2018).

Further developments in the commercial realm include application in the minerals processing area of general-purpose simulation systems originally developed for use in other domains, including the following:

- Aspen Plus (Aspentech 2018), originally chemical/hydrocarbon process focused
- IDEAS (Andritz 2018), originally for pulp and paper and then developed for mining and metals
- METSIM (Proware 2018), originally for pyrometallurgical processes
- SysCAD (2018), originally for dynamic control system validation and operator training
- HSC SIM (Lishchuk 2016), graphical and spreadsheet type process unit models. This package can be used to model many types of processes in metallurgy and mineralogy.
- IGS (Integrated Geometallurgical Simulation) (Lishchuk 2016). This tool minimizes risk using a geometallurgical model of the ore body by integrating geometallurgical data with process simulation. It combines these data with mining, operational, and environmental inputs that affect the process simulation results, capital, and operating costs. The equipment for mineral processing and the associated capital and operating costs can then be optimized based on the geometallurgical inputs. Utilization of

the geometallurgical models of the ore body are becoming the standard for development of both steady-state and dynamic models of mineral processing plants.

With the use of spreadsheets becoming more commonplace, several other spreadsheet-based applications have also emerged. These include the following:

- Moly-Cop Tools (Moly-Cop 2018). Now in version 3.0, this package consists of a set of Excel spreadsheets covering individual process models and calculations for most of the common comminution circuit unit processes as well as their combination in flow sheets. It is available free of charge.
- Limn—The Flowsheet Processor (Maelgwyn Mineral Services Ltd. 2009). Originally developed as a general-purpose simulation system that could model almost any process, this Excel-hosted package has found a niche in the simulation of physical separation processes, thus finding widespread use in the coal, diamond, iron ore, and mineral sands industries. It is under active development and support. Also available are several products aimed more at the aggregates industry but that may find mineral processing applications, particularly in the comminution area. These include Metso's Bruno (Metso 2008) packages and the AggFlow package from BedRock Software Inc. (AggFlow 2018).

## Aspects of Commercialization

Most simulation work in the industry is performed using commercial packages. Although low-cost or no-cost "open-source" software has received some backing, particularly in the academic sphere, without a commercial arrangement, support and updating of applications in the fast-moving computer software and hardware environment is unlikely.

Such commercial arrangement can take the form of free or relatively low-cost software supported as part of a corporate identity (e.g., Moly-Cop Tools, Metso Bruno, MinOOcad [Herbst and Pate 2018], and ProSim [2018]), by the commercial arms of research groups, or spun off into new companies (e.g., MODSIM, JKSimMet, USIM PAC), or by small groups of focused individuals producing software targeted at a particular market niche (e.g., METSIM, Limn [Maelgwyn Mineral Services Ltd. 2009]).

With commercialization comes the need for competitive advantage, and this is evidenced most in the area of process models. Unlike much of chemical engineering and perhaps also some areas of pyrometallurgy and hydrometallurgy, where general theoretical principles can be more readily applied, or extractive test work and pilot-plant results be used to confirm chemical species, equations, and degree of conversion, the detailed models of processing units available to mineral processors are typically more empirically based.

Although many papers have been written over the years describing modeling approaches and model development, the most successful application of models has come from those that have been implemented in a suitable simulation framework.

Where a model development group possesses such a simulation framework, there is no incentive for model developers or "owners" within that group to make those models available to other parties for use in other frameworks. This represents a considerable impediment to entry into the mineral processing simulation area by software originally developed for other domains, for example, Aspen Plus, IDEAS, and SysCAD.

This also means that users, rather than purchasing multiple simulation systems to gain access to specific specialized models, often need to use consultants and specialists (including those within the simulation system supplier organization) to carry out the actual simulation studies, using the appropriate software. Given the specialized nature of some of the models and the reliance on experience and accumulated databases of parameters, and lack of cost and time-effective in-house expertise, this may be entirely appropriate.

## Mineral Processing Simulation Regimes

In the minerals processing area, there are three main simulation regimes of interest: steady-state, dynamic, and general multiphysics numerical modeling techniques (e.g., computational fluid dynamics–discrete element method).

Historically, steady-state simulation has been the most common area of application, and although this continues to be the case, the rapid rise of computer power has seen increasing use of dynamic simulation and multiphysics approaches.

### *Steady-State Simulation*

A simulation at steady state produces a representation of the plant or subprocess in a condition that is unlikely to arise in practice, that is, the condition where the sum of inputs equals the sum of outputs both for the overall plant and for each individual unit process.

Despite this, steady-state simulation remains extremely useful and represents the most widely used form of simulation in industry. The complexity and degree of accuracy required of steady-state models can be tailored to match the outcomes desired. The Pareto principle applies, in that if little data are available, simple models can still be used to get a useful basic understanding of a circuit. If more-detailed or more-accurate results are required, more (often considerably more) effort can be directed to fine-tune and validate more comprehensive unit models.

With appropriate models, steady-state simulation finds application in the following, for example:

- Detailed equipment assessment for design
  - Crusher selection: cone versus HPGR (high-pressure grinding roll)
  - Screen aperture selection
  - Ball and AG/SAG (autogenous grinding/semiautogenous grinding) mill sizing
  - Hydrocyclone component selection
- Production of process balances for design
  - Multiple scenarios and what-if analysis for equipment envelope definition
  - Evaluation of throughput options for operating envelope definition
  - Examination of effect of multiple feed types on design
- Evaluation of circuit operations for alternative equipment selection
  - Spirals versus teeter bed separation versus flotation
  - Jig versus dense medium separation versus ore sorting
  - Wet versus dry processing
- Assessment of circuit operations for alternative flow configuration
  - Rearrangement of existing grinding capacity

  - Variation of size cut points to examine effect on downstream density separation
- Evaluation of proposed circuit modifications
  - Effect of additional regrinding capacity on flotation
  - Effect of upgrading water recovery devices on plant water balance
- Optimization of equipment settings
  - Selection of relative density cut points for heavy medium circuits
  - Selection of screen and hydrocyclone apertures to match changes in ore type
- Benchmarking of operations: Comparison of current operation with predefined "best practice" for current plant, other similar plants within the company, or similar global operations
- Geometallurgy and future ore test work
  - Estimation of future plant performance for mine and plant design
  - Evaluation of design modifications for existing plants
- Mine planning and production scheduling
  - Mine design
  - Production schedule optimization
  - Treatability studies
  - Blending strategy evaluation
- Online product estimation for grade control
  - Mine planning
  - Plant feed scheduling
  - Plant product estimation
- Online in-plant parameter estimation to calculate
  - Milling circuit product size
  - Optimum separation circuit cut points for current feed conditions

#### *Dynamic Simulation*

Dynamic simulation aims to produce a system that replicates the dynamic behavior of a process unit or of an overall circuit. Similar models to those applied in steady-state simulations may be used where the unit process residence time is less than the time increment of interest (e.g., hydrocyclones within a grinding circuit). However, internal dynamics need to be addressed where residence times are significant (e.g., within a SAG mill).

Whereas in steady-state simulations, material transfer between unit processes (via pumps, conveyors, pipes, etc.), is ignored, in dynamic simulation these interprocess aspects are of similar importance to the units themselves. Setting up a dynamic simulation thus requires significantly more effort than is required for steady-state simulation, and this has contributed to somewhat restricted use in industry.

In the mineral processing domain, examples of the use of dynamic simulation include the following:

- Ore flow modeling for design and analysis of
  - Conveyor systems
  - Stockpiles and stockyards
  - Feed and product bins
  - Train loadouts
- Examination of blending strategies for
  - Mine planning
  - Plant feed stockpiles
  - Bulk commodity (e.g., coal, iron ore) rail and port facilities
  - Conveyor systems
- Dynamic plant models to assist in plant control implementation
  - Test bed for control system programming and commissioning and determining stop–start logic and safety interlocks
  - Preliminary loop tuning
  - Plant controllability testing and validation
- Modeling of circuits for control, for example,
  - Grinding circuit mill load control
  - Flotation plant circulating load control
  - Slurry pumping
- Modeling of circuits for operator training, for example,
  - Plant familiarization, *ab initio* training
  - Start-up/shutdown training
  - Unusual operating modes training
  - Safe operations training

#### *Multiphysics Numerical Modeling Techniques*

Multiphysics numerical modeling techniques encompass such techniques as computational fluid dynamics (CFD), smooth particle hydrodynamics, discrete element method, and discrete particle method techniques, as well as their combinations.

Because of its computation, intensive nature, and the time taken for solution, the multiphysics approach is not one that currently lends itself to direct application in minerals processing plant operations.

Although commercial packages (e.g., ANSYS Fluent [ANSYS 2018] and EDEM [EDEM 2018]) and open-source solutions (LIGGGHTS, CFDEM [CFDEM Project 2018], and OpenFOAM [OpenCFD Ltd. 2017]) exist, the specific difficulties presented in modeling of many processes in the mineral processing regime (particulate slurries at high percent solids, particles in dense media, etc.) mean that much manual configuration/modification is required. However, consultants and specialist service providers do offer services in several areas applicable to minerals processing, particularly in the bulk materials handling area, including the following:

- Stacker/reclaimer design
- Ore flow and bin design and validation
- Conveyor and transfer point design and validation

On the process hardware side, these techniques have also found use within equipment design and manufacturing companies to assist in design optimization in areas such as the following:

- Crusher liner profile optimization
- Grinding mill pulp lifter design
- Flotation agitator design
- Slurry pump design
- Studies of erosion and wear

### Mineral Processing Modeling Implementation

Where circuit or plant-wide simulation implementation is required, two main approaches to steady-state simulation have been used: the equation-solving method and the sequential modular method.

#### *Steady-State Regime*

The equation-solving method involves writing the equations for the relationships between all simulation components across the circuit (e.g., in a flotation circuit, the relationships between the individual masses of copper and gangue minerals

and the mass of water at each point in the circuit—both mass balance and separation equations) as well as the constraint and specification equations. These equations are then solved using standard mathematical techniques for the solution of sets of nonlinear equations. Although solution can be relatively efficient, the number of equations for solution of even a modest circuit can be daunting to set up, and the approach does not lend itself readily to incorporation into a prepackaged simulation system.

The sequential modular approach involves linking individual unit models by data structures representing process streams and having those unit models determine the composition of output streams based on the input streams and the unit model parameters. As each unit model is calculated in sequence, output streams from some unit models become inputs to the further downstream process models. As recycle material subsequently alters the feed streams to processes back upstream, the process unit calculations are repeated for successive iterations until some suitable completion criterion is achieved. (The approach is analogous to starting up a real plant and waiting until steady-state operation is achieved.) Although generally slower in solution than the equation-solving approach, advances in computing power have made speed of solution less of an issue.

Largely because of ease of implementation and the way prebuilt process unit models can be robustly implemented in modular form, the sequential modular approach is by far the most commonly applied.

Of the simulation packages mentioned, JKSimMet/JKSimFloat, Limn—The Flowsheet Processor, and USIM PAC primarily target steady-state simulation. JKSimMet has the strongest set of predictive comminution models, whereas JKSimFloat focuses on flotation. Moly-Cop Tools, Bruno, and AggFlow also have a comminution focus.

Limn—The Flowsheet Processor and USIM PAC are broader in application, covering general minerals processing plant operations, but generally with simpler, more basic public domain models, often sourced from the published literature. Although not specifically targeted at minerals processing applications, IDEAS, METSIM, and SysCAD also have steady-state capability and have been used in this area, again with more general public domain models.

The output requirements from steady-state simulation are relatively modest (e.g., tables of flows and component assays), and most commercial packages have both built-in data displays and export facilities to a spreadsheet to allow further analysis as required.

#### *Dynamic Domain*

The two steady-state approaches can be extended into the dynamic domain as well, with the sequential modular methodology being the most widely adopted.

The additional computing load required by dynamic simulation has been somewhat addressed by the exponential rise in computing power indicated by Moore's law, which states that overall processing power for computers will double every two years. The trade-off between solution time and fidelity of results (which generally translates to the magnitude of the time increment between successive simulation "slices") remains an issue, however. The use of computing hardware other than the personal computer (e.g., online "software-as-a-service" and cloud-based systems such as Microsoft's Azure) or personal computer–hosted numerical calculation enhancements (e.g., graphics processing units or GPU-accelerated computing) has provided some benefits in this area.

IDEAS and SysCAD focus strongly on dynamic simulation. METSIM and Aspen Plus also have dynamic simulation capability.

The display requirements for dynamic simulation are much more extensive than those required for steady-state work and include trend charting and operator interfaces. In some cases, this is handled by a pseudo-SCADA (supervisory control and data acquisition) system built into the simulator. Configuration of these subsystems contributes to the higher setup levels required for dynamic simulation. In operator training systems, the dynamic simulator may even be connected to a version of the actual plant human–machine interface hardware and software. Facilities for data export to spreadsheets are also commonly available.

#### *Multiphysics Approaches*

The numerically intensive multiphysics approaches depend on the availability of suitable computing platforms, with solutions taking hours to days rather than the seconds to minutes typically observed in steady-state and dynamic simulations. Similar approaches to cloud-based and accelerated computing options that apply to dynamic simulation also find use in the multiphysics area. Where personal computer use for these applications is driven by cost or availability, because end use tends to not be time limited, the calculations can be run on dedicated machines over extended time periods.

The results of multiphysics simulations lend themselves well to false color images and three-dimensional (3-D) graphics, and users can make good use of the advances in these fields.

### Process Models

This section applies largely to models used only in the steady-state and dynamic simulation categories.

#### *Stream Data Structures*

Whereas the calculations that describe the process (the process unit models) determine the overall simulation results, the process stream data structures define the components of the system over which those calculations must be applied.

Mineral processing modeling and simulation is dominated by concerns about tracking particles, and although some of the multiphysics approaches do address individual particles, within the constraints of current hardware and software, the number of particles present precludes such approaches in general steady-state and dynamic modeling. The work-around is to combine particles into appropriate groupings or classes and to use the average properties of each class as the property for all particles within such a class.

The classes used usually match the physical groupings of interest within the processes, which are themselves often driven by the analysis techniques available. If one considers, for example, particle size, although there are techniques that report actual particle size, sizings are generally reported as the fractional (or percentage) mass of material falling between two sieve sizes in a series or range of such sieves. For calculation purposes, all particles within the size fractions are assumed to have the geometric mean size of that sieve interval. In cases where the raw analysis data are sparse, or intervals

are irregular, interpolation is often performed to regularize the data.

Particle size is important in almost all mineral processing unit operations and in commercial simulation systems that focus on comminution circuits; it forms the main property of interest. In these cases, the stream data structure becomes a single vector, tracking the amount of material in each size fraction, plus additional individual components such as water, which may be included as required. Such stream data structures are said to be one dimensional, or 1-D.

Where an ore has multiple phases (e.g., hard and soft, kimberlite and clay, heavy mineral and gangue, coal and rock), even in comminution circuit simulation it is sometimes necessary to extend the 1-D approach to accommodate the difference in properties and hence the comminution response. In that case, the data structure becomes 2-D, with each size fraction further separated according to the phase properties of interest.

Moving beyond the comminution sections of a mineral processing plant, other properties of the process stream also become important, and the use of a multidimensioned stream structure approach is more common. For example, in coal, iron ore, mineral sands, and diamond plants, where separations based on relative density are important, the stream structure is extended to include a density distribution for particles in each size interval.

Although most simulation systems treat size as a distributed property describing a continuum of sizes, the second dimension tends to be more diverse. Thus, although it may be possible to model a mineral sands circuit using relative density as a continuous distributed property within each size fraction, it may also be possible to model it using the size distributions of the individual minerals present.

Higher dimensions are also possible. For example, in a flotation circuit, the data may be expressed as particles within a size range, of a particular mineral type, each having a range of floatability indexes, thus making a 3-D stream structure. Similarly, in a diamond processing circuit, the distributed properties of size and relative density may be tracked, and within each of those categories, a diamond size distribution may be tracked.

Simplification, to minimize the calculation load and/or data handling requirements, can sometimes be applied. In modeling a coal plant, it is often assumed that a single "washability" applies across the plant (i.e., if a particle is found anywhere within the circuit, if it has a certain size and a certain relative density, it will be assumed to have the same assay). This simplifying assumption means that a 3-D problem can been handled as a 2-D problem.

### *Liberation*

Because different plant sections tend to be analyzed in different ways, it is common practice to simulate the different plant sections separately also, changing streams data structures to suit.

Crossing the boundary from one stream data structure to the other often requires more information to be added (e.g., going from a 1-D comminution circuit to a 2-D flotation circuit structure) or information to be compressed (e.g., from a 2-D size by density structure to the 1-D comminution structure required by a re-crush circuit model in a diamond processing plant). The major issue in such cases is determining how properties in one of the dimensions vary with changes in another dimension. For example, a breaker in a coal circuit and regrind mills in flotation circuits both result in a movement of particles from coarser sizes to finer sizes. Because of this, the resulting progeny particles will have different secondary or second-dimension properties from their parent particle.

Describing this liberation of material and allocating the progeny particles to the correct secondary property class remains one of the difficulties for simulation of mineral processing plants. Although improvements in analysis methods and advances in the theory have been made, their application in commercial simulation systems remains scarce. No standard approach to the problem of liberation has emerged, and apart from some basic heuristic and rudimentary empirical methods, applied particularly where comminution equipment is embedded within separation circuits, the problem remains largely unsolved, contributing to the tendency to model the separate plant sections individually.

### *Unit Process Models*

Unit process models include models for comminution, classification, and separation as well as those for mineral recovery and based on mass recovery approach.

**Comminution.** Comminution remains the costliest component of many minerals processing plant flow sheets; consequently, considerable effort has been expended in model development in this area. The most common comminution simulation approach in both steady-state and dynamic simulation is the size-based "matrix model" population balance approach (Austin et al. 1984; Napier-Munn et al. 1996; Wills 1997).

***Jaw and cone crushing (after Whiten).*** The Whiten (1972) crusher model was one of the earlier matrix comminution models developed at the Julius Kruttschnitt Mineral Research Centre (JKMRC) in Queensland, Australia, and remains in widespread use. It has been published in sufficient detail by Lynch (1977) to be effectively in the public domain and has been included in most of the comminution-focused simulation systems (e.g., JKSimMet, Limn). The basic model was extended by Andersen to form the Whiten–Andersen crusher model (Andersen 1988). This model uses a series of regression equations to relate ore and machine parameters to the underlying model parameters. Although it is present in several simulation systems in this form, in the absence of sufficient data to populate the regression equations, it is most often used in the simpler form originally published by Whiten (1972). Although the default breakage characteristics published for use with this model are generally sufficient, the model has the ability to make use of ore specific breakage data from ore testing via the JKMRC drop weight test. Estimation of the machine characteristics, however, requires a suitable database of "typical" parameters, or backfitting to measured data from operating crushers. Where backfitting is used, the model is not predictive for the effect of changes in machine geometry and is then only used to estimate the effects of changes in feed material type and size distribution.

***Other jaw and cone crushing.*** In a greenfield situation, where no other data are available, the Whiten model approach has limitations. In such a case, models based on a manufacturer's "grading curves" can be used. Although these models are built into some packages (e.g., Bruno, AggFlow), they can be implemented in most simulation systems by simply entering tables of data extracted from the available manufacturer's literature. In some cases, multiple curves are available for different feed rate or crusher settings and these can be incorporated into such tables. Care does need to be taken using this

approach, as it applies a predetermined distribution to the product stream, taking no account of feed size distribution, ore type, and so on.

***Impact crushing (vertical shaft impactor and hammer mill).*** Both the Whiten crusher model and the manufacturer's grading curve approaches can be applied to impact mills.

***Rolls crushing, toothed roll and sizers.*** Both the Whiten crusher model and the manufacturer's grading curve approaches can again be applied.

***Rolls crushing (HPGR).*** The Whiten crusher model has been extended by Daniel and Morrell (2004) to handle modeling of HPGR crushing. In this case, the device is divided into three sections, pre-, bed, and edge crushing, and an individual basic Whiten model applied in each section. For simulation systems that implement the Whiten model but not the specific HPGR version, with reference to the Daniel and Morrell (2004) paper, the HPGR model can be implemented using three instances of the basic crusher model, with the precrusher in series with the bed and edge crushers operating in parallel.

***AG/SAG.*** The general-purpose Whiten perfect mixing mill model (Whiten 1974) was incorporated into an energy-based, ore-specific AG/SAG model by Leung (1987). Further extended with power modeling calculations due to Valery and Morrell (1995) and implemented in the JKSimMet package, this model is believed to be the most widely used for design and optimization of SAG circuits. Although the model has been published in sufficient detail to allow implementation by others, it does not appear to be available in any of the other referenced commercial packages. Where other packages include calculations for AG/SAG mills, they appear to follow a more general approach such as that outlined by King (2001). In the absence of a suitable database of operations on which to base parameter selection, both the JKMRC model and the more general versions require backfitting of parameters from operating data. This has limited the application of the models for design. Coupled with the requirement for a deep understanding of the model limitations and experience in the design and operation of the physical equipment, most simulation work in this area remains the province of consultants and specialists.

***Rod mill grinding.*** With rod mill use declining, development of new models in this area has been limited. The original Calcott–Lynch matrix model (Valery and Morrell 1995) is available in commercial packages such as JKSimMet and Limn and in the public domain (Lynch 1977; Napier-Munn et al. 1996) but does require backfitting to obtain useful parameters. For greenfield design situations, simple tables of estimated product size distribution will often suffice, since these units rarely operate in closed circuit.

***Ball mill grinding.*** The Whiten perfect mixing model (Whiten 1974) also forms the basis of the most commonly used ball mill model. It is available in the public domain (Napier-Munn et al. 1996) and is widely used in commercial simulation systems. It has the facility for ore-type specific breakage information (appearance function) to be used but does require back calculation of combined breakage/discharge rate parameters from survey data. Although variations in mill size are accounted for in the model form, the fitted, combined breakage/discharge rate parameters can be further scaled to allow for variation in mill load, mill speed, and ball size. The more general approaches (King 2001) are also available in the public domain and have been implemented in commercial systems and in spreadsheets by some practitioners.

***Stirred grinding (tower mill and IsaMill).*** The Whiten ball mill model (Whiten 1972) has been successfully used to model these devices.

***New developments.*** A major issue with the use of the matrix comminution models for both design and optimization is the requirement to backfit breakage parameters to plant survey data to tune the model to particular applications. Daniel and Morrell (2004) have described an energy-based approach to comminution modeling, which, in conjunction with an extensive database from which the specific equation parameters have been derived, shows promise as a design strategy for comminution machine selection. The published approach and equations are in the public domain; however, the individual specific parameters are proprietary. When combined with a simulation system (the current implementation is used in conjunction with Limn—The Flowsheet Processor), the system may be used for overall comminution circuit design. Commercial use of the package CM-DOCC (Tian and Morrell 2015) is in its infancy but is available as a service through CITIC-SMCC Process Technology (2018).

**Classification and separation.** Although comminution is a high-cost component of plant flow sheets, the ultimate aim of a mineral processing plant is to upgrade the valuable components of the feed ore. Modeling of the separation stages required to achieve this has historically received less input compared with comminution, although more recently, considerable effort has been expended on modeling the flotation process.

Three main methods are typically applied to the modeling of separation devices:

1. Efficiency or partition curve approach,
2. Mineral recovery/mass recovery approach, and
3. Kinetic approach.

***Partition curve approach.*** The partition curve approach reflects the reality that in any separation process, a particle must report to only one of the product streams. Where the measured property of interest driving the separation (e.g., particle size, density, color, X-ray fluorescence) is discretized into suitable groups or classes, the term *partition number* (also *partition coefficient*, *recovery factor*, *separation number*, *split factor*) is used to describe the fraction of material in that class that reports to the product stream of interest.

In simulation systems where the stream structure for input and output (feed and product) streams is defined in terms of those property classes, a similarly structured table in a unit model can be filled with the partition numbers for each class or grouping. Where a unit process has more than two products, the model can be set up as multiple partition tables, arranged in series or parallel as required to describe the process.

This partition table forms the most basic model of separation. However, with a single parameter for each property class, such models are not particularly useful.

To reduce the overall number of parameters, it is usual to attempt to link the partition numbers in some logical manner related to the physical separation process. Where the property classes represent subranges within a distribution (size ranges, density intervals), the partition numbers can be related by a sigmoidal or S-shaped curve. At one extreme of the property distribution, most particles in that property class report to one product; at the other extreme, most particles report to the alternate product; and at some intermediate property value, there will be equal numbers of particles reporting to both products.

The literature contains many examples of equations to describe partition curves (King 2001). The application of the basic partition equation forms of these "second-level" models has proven successful for obtaining reasonably detailed balances useful for benchmarking and mine-planning type studies. They find application in the physical separation processes, such as separations by size and density, where the few model parameters describing the basic curve shape do not tend to vary with ore/material properties and are reasonably well understood. The basic configuration of the Limn package (Maelgwyn Mineral Services Ltd. 2009) makes extensive use of models at this level in modeling, for example, coal, diamond, iron ore, and mineral sands circuits. The models are also relatively easily implemented in stand-alone spreadsheets.

After a partition curve has been defined (or a set of partition curves defined in a 2-D simulation framework), the parameters of that curve can themselves be related to machine operating characteristics. These higher-level relationships often comprise empirical equations whose parameters require backfitting from test data.

The two most commonly encountered examples of this "multilevel model" approach are size separation on screens, such as outlined in the Vibrating Screen Manufacturers Association handbook (VSMA 2014), or in hydrocyclones (Nageswararao 1990) and in comminution circuits and density or gravity-based separations, such as those operating in spirals or dense medium cyclones (Luttrell et al. 2005).

***Mineral recovery–mass recovery approach.*** Apart from the partition curve approach, there are many other ways to represent separation data (Drzymala 2007). The approach of Holland-Batt (1989) has been implemented in at least one commercial simulation system (Fourie 2007) and appears useful for modeling gravity separators, particularly those found in mineral sands circuits. Based on the relationship between cumulative mineral recovery versus cumulative overall mass recovery, it provides a description of the process operating "separation window" and uses the concepts of separation efficiency and proportionality of efficiency to allow scaling for changes in feed grade. It is, however, an empirical approach and does require test work to derive the requisite relationships.

***Kinetic approach.*** Although partition curve and mineral/mass recovery techniques are applicable to all separation processes, it is the layers built upon those base techniques that provide the framework for a more deterministic understanding of the underlying process.

Particularly in the modeling of flotation unit processes, an understanding of the kinetics of the process is important, and most of the commercially available flotation models are based on process kinetics, usually assuming a first-order rate equation. Different rate constants may be applied by size, mineral, floatability class, or liberation class. At least one proprietary simulation package, SUPASIM (Hay 2005), has been reported as successful in applying simple laboratory test work determined rate constants together with experiential heuristics in process unit and circuit models to build a better understanding of the issues in running the circuits.

Much research work has focused on measurement of many cell and bank operational parameters and in relating those parameters to the rate constants, resulting in significantly increased model complexity. The research effort from the JKMRC (JKTech 2018) and associated Australian Mineral Industries Research Association (AMIRA) (Schwarz et al. 2006) collaborative projects in this area is embodied in the commercially available JKSimFloat package (Schwarz and Richardson 2013). Calibration of the models remains a nontrivial exercise, and simulations of this nature are typically performed with a combination of experienced plant personnel and expert consultant assistance.

**Ancillary processes (dewatering, water recovery, medium recovery devices, etc.).** Although detailed theoretical phenomenological models exist for many of these devices, the implementation and incorporation in a circuit simulation of such models is not straightforward. They are typically modeled in only a most basic form in most commercial simulation packages and their role even ignored in certain instances. This is entirely appropriate where the goal of the simulation is, for example, to determine the likely plant recoveries for various ore blends in a geometallurgical or mine planning study.

Where inclusion of such unit processes is important (e.g., determining a water balance for a process design, or evaluating medium losses in a dense medium circuit), simple recovery-type models are often used.

**Material handling (conveyors, pumps, bins, stockpiles, blending/ore handling).** Generally, models of these process items are not required in steady-state simulations. Where needed to complete a flow sheet, a simple mixer is usually sufficient.

The most common dynamic simulations using these unit processes are longtime slice ore-flow-type simulations. The models are usually spatially related with internal data storage of property information at a spatial resolution to match the required output information.

## Example of Steady-State Simulation

With the availability of commercial simulation packages, the task of the process engineer becomes one requiring an understanding of the simulation process, data requirements, and potential shortcomings, rather than one requiring the ability to program in a computer language or to have a deep understanding of the mathematical approaches behind the provided models. As an example, the following section describes the use of a typical steady-state simulation package to examine the potential for inclusion of a flash flotation unit within a grinding circuit. It is based on work described by Yan et al. (2005). Although this study details the modeling work, the example described here focuses on the simulation task and the user inputs and analysis required.

### *Project Planning*

Prior to beginning a simulation exercise, whether it is performed personally, by an in-house specialist group, or by an external consultant, several basic steps are required.

**Use expected outcomes to select the simulation environment.** With any simulation project, the first question is: "Why am I doing this?" The answer to that question will determine the appropriate level of complexity required and generally point to appropriate tools to apply. For example, if the aim of the project is simply to produce a solids and water balance about a circuit, a simulation environment that requires size distribution data, grinding rates, and complex flotation models is probably not necessary and quite simple models may be suitable. Alternatively, if estimation of maximum mill throughput is one of the desired outcomes, more-detailed mill models are probably required.

In the example project covered here, the aim is to see whether flash flotation units will benefit an existing grinding

and flotation circuit. Because particle size is expected to be important, the models must be able to take that into account. The existing plant produces a bulk sulfide concentrate, so for being an initial study, one probably does not need to track individual minerals but will, at a minimum, need to distinguish between sulfide and gangue species. The simulation system therefore must be capable of handling the size distributions of the two species present in each stream.

**Choose flow sheet extent and detail.** Focusing on just those processes that affect the required or expected outcomes can considerably simplify the tasks of collecting data and setting up the simulation. In a steady-state simulation, bins, conveyors, pumps, sumps, and pipes do not affect the outcome; therefore, omitting them will simplify the simulation with no loss of fidelity.

Similarly, if the focus is on the grinding and flotation sections, the feed to the grinding circuit can perhaps be taken as a constant, removing the need to simulate the crushing plant. Any considerations of dewatering units or other downstream processing may also be ignored.

In some cases, it is also possible to ignore certain aspects of the process streams. For example, in a mine planning or plant design study to determine the effect of ore block variability on a dense medium circuit and the consequent effect that will have on product quality and production rate over the life of the mine, it may be possible to simulate the ore solids only. Where necessary, percent solids, medium density, ore to medium ratio, and similar metrics can be used as model parameters to determine the requirements for these stream components in a particular process unit model, but it may not be necessary to include them in the overall circuit balance. Simplifying the stream description by removing any requirement to balance the accompanying water and dense medium components of the stream will simplify the overall simulation calculations and eliminate the need to include models for the water and medium recovery aspects of the circuit.

In the example flow sheet shown in Figure 1, the aim is to perform a qualitative assessment of the addition of flash flotation cells within the grinding circuit, and the following definitions, choices, and simplifications have been made:

- The simulated circuit ore feed is the feed to the fine grinding (ball mill) circuit.
- The circuit products will be the combined flotation concentrate and tailings.
- Simulation of conveyors, pumps, and sumps is not required.
- The stream ore description will include size distributions for two subspecies.
- Simulation of both solids and water stream components is required.
- Water addition points will be required.

**Draw the flow sheet.** Having made initial decisions regarding flow-sheet extent and detail, it is useful to begin to draw the flow sheet at this point because that task will direct attention to the important aspects of the simulation study.

A graphical flow sheet or process flow diagram forms the primary interface between the user and the simulation system. Most modern commercial simulation systems provide a means of defining the flow sheet in graphical form. This usually takes the form of a basic drawing package with a library of shapes representing items of process equipment and some facility for joining these shapes using lines to represent process flows.

The drawn flow sheet will reflect the decisions made in the project planning stage, ideally being as simple as possible, while still addressing the reason for conducting the study.

For the example task, the simplified flow sheet required to allow assessment of the effect of adding a flash flotation unit in the grinding circuit is shown in Figure 1.

**Select suitable unit process models.** Having drawn the flow sheet, the process units that will have to be modeled have been identified. Of course, model choice is driven by the availability of specific models in the selected simulation package. Compromises may need to be made. In the minerals processing arena, most models in regular actual use are empirical in nature and require some form of fitting to plant data, or tuning, before they can be applied. Availability of such data will also drive model choice.

***Appropriate models.*** Most commercial simulation packages have a set of available process models. Some systems explicitly associate a model with the flow-sheet picture chosen to represent the process unit. Other systems associate a class of models with the picture, offering a limited choice, whereas some systems are completely general, relying on the user to make appropriate choices.

Where a suitable model does not exist, most systems have mechanisms to allow user-developed models to be incorporated, either as a standard part of the package or as an add-on "model developer's kit."

Where suitably detailed models do not appear to be present in any available simulation package, the user will need to choose between the additional costs required to develop such models (perhaps by some external consulting or research group) versus the loss in verisimilitude associated with choosing a more general model of lower accuracy.

The difficulty of implementing a simulation model from published papers should not be underestimated. Among other issues, the paper may have too narrow a focus for the intended application of the m3odel, may be reporting work in progress, or, for intellectual property reasons, may publish the broad framework of a model but omit detailed values for parameters that are only obtainable from a proprietary database. Similarly, models detailed in academic theses may require significant additional work to make them suitable for use in solving a real-life problem.

***Appropriate levels of detail.*** As with the flow sheet itself, the models for the individual process units should be chosen to be as simple as possible while meeting the overall project goals. For example, although models exist that will allow optimization of cyclone physical size and orifice dimensions, they may require more data for tuning than are readily available, or be overly complex when compared with the result sought. In such cases, it may be more sensible to use simpler separation curve–type models with fewer parameters that can be estimated from a basic understanding of the process.

### Models for the Example Flow Sheet

The flow sheet shows that models are required for the following:

- **Ball mill.** It is assumed that particle size will be an important property in determining how effective the flash flotation units will be and that removal of sulfide material in those units may affect the grinding process.

  The ball mill model will therefore need to respond appropriately to changes in feed size distribution. It

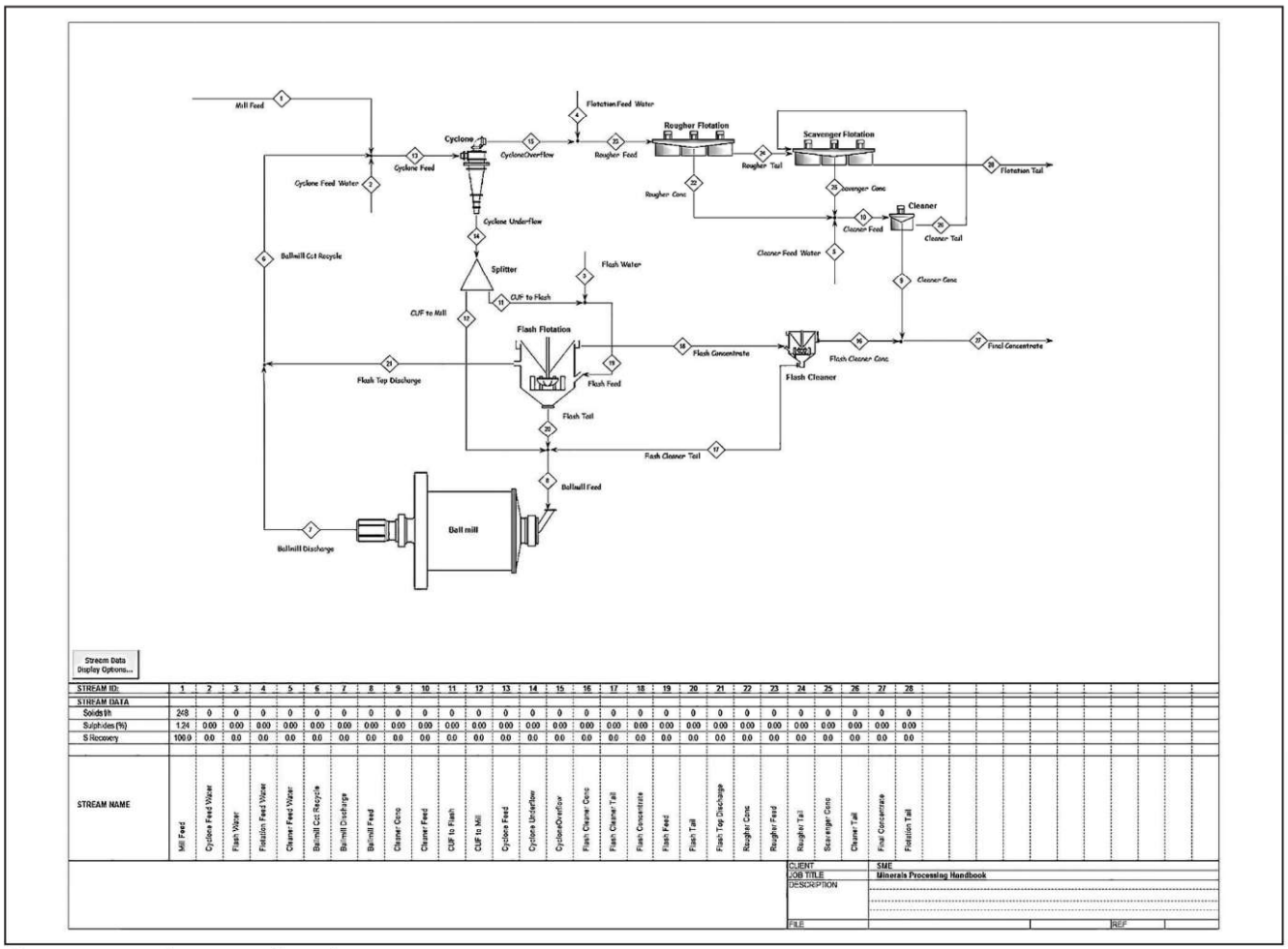


**Figure 1 Example process flow sheet**

will need to handle at least two ore subspecies with different grinding behavior.

The Whiten perfectly mixed ball mill model (Whiten 1972), using separate appearance functions determined from ore testing of each ore subspecies, was chosen for the example.

- **Cyclone.** If percent solids values are maintained in a similar range, the cyclone could be expected to behave in a similar manner under all regimes to be simulated. Consequently, a relatively simple "efficiency curve" model should be adequate.
- **Splitter.** The splitter model for steady-state simulation is trivial, requiring just a single split value to determine product stream makeup.
- **Primary and cleaner for flash flotation**. A size-by-size, two-parameter single-rate equation, recovery-based flash flotation model with the addition of solids and liquid bypass streams as in plant practice, was described by Mackinnon et al. (2003) and used for the flash flotation units in the example flow sheet given here.
- **Rougher, scavenger, and cleaner for conventional flotation.** A similar model to that used for flash flotation (without the bypass streams) was also used for the conventional flotation units.

**Data collection.** The choice of model will generally indicate the data required to tune or adapt the model to the circuit of interest. Good data are expensive and in any simulation study will invariably be in short supply.

***Existing equipment.*** If the flow sheet or part of the flow sheet encompasses an existing plant, there may already be data available that can be used. Alternatively, fresh test work may be commissioned to obtain data explicitly directed at tuning the models for the proposed simulation task. Generally, each model has its own data requirements for tuning, and a series of specific targeted surveys about individual process units to meet these requirements may be a better use of resources than a complete circuit survey. If the test work is focused on one or more individual unit processes, achieving overall circuit steady-state conditions is less of a consideration.

***New equipment.*** Where the process units in the flow sheet do not form part of an existing plant, either because the flow sheet represents part of a greenfield study or because the individual units are proposed new additions to an existing circuit, laboratory or pilot-plant test work may be required. Some

experience with the model to be used will be invaluable in planning this test work.

***Industry standard operational data.*** In some cases, it may be possible to use "industry standard" parameters as an alternative to generating them for a study. This is particularly the case for a separation process relying on physical separations, for example, size and density-based separations in coal or iron ore upgrading plant operations. In these cases, the equipment is expected to operate within a range of efficiencies and the parameters that represent these efficiencies and can, as a useful starting point, be considered as independent of plant operation, feed type, or equipment manufacturer and installation.

***Potential for progressive improvement in model accuracy.*** As always, the decision about the level of data required should be driven by the cost/value trade-off for the level of accuracy required given the answers sought.

There can also be a benefit in performing initial simulation runs using more general models or more general model parameters to get a "feel" for how the available data fits the existing circuit, as well as a better understanding of the areas in which the data are deficient.

### Data Collection for the Models in the Example Flow Sheet

For the example, the following data were available or obtained:

- **Ball mill.** From the work leading to the Mackinnon et al. paper (2003), a set of ball mill feed and product data is available to allow estimation of the breakage rate parameters for the Whiten ball mill model.

  Ideally, test work (drop weight breakage testing) to determine the ore-specific appearance functions for the sulfide and gangue components should be performed. In this case, it was not available and published "typical" values were used.
- **Cyclone.** The survey results used for the ball mill also included sufficient data to model the cyclone.
- **Splitter.** The splitter model split is a user-controlled value and no data are required.
- **Primary and cleaner flash flotation.** The Mackinnon et al. (2003) paper had described a model suitable for use for the flash cells.
- **Rougher, scavenger, and cleaner conventional flotation.** The work by Yan et al. (2005) describes the laboratory flotation test work that was required to enable application of the two-parameter, single-rate flotation model used for the flash units to also be applied to the conventional cells. These data were available for use in the example shown here.

Although the data available for the example are limited, it is of an appropriate level to address the reason for carrying out the simulation: a qualitative assessment of the addition of flash flotation cells within the grinding circuit.

**Fit or tune models to match available process data.** The empirical nature of most minerals processing unit models means that fitting those models to data is usually a necessary step.

Many simulation packages incorporate parameter estimation/model fitting routines (usually nonlinear, least squares based) within their framework. Other packages rely on external tools such as Microsoft Excel's Solver, Solver extensions from Frontline Systems Inc., or similar software.

There are advantages in having the parameter estimation routines available as part of the simulation package, since the actual models to be used are available in that environment without transcription to other tools. Also, where fitting of multiple units in a circuit is required, it is often advisable to fit them simultaneously to allow the effects of circulating loads to be included in the parameter estimation.

***Multiple data sets.*** When using simple empirical models, where relationships between model parameters and operating variables are required (e.g., screening efficiency versus feed rate), it becomes necessary to fit multiple sets of data. Typically, each data set is fitted to the basic model, and regression equations are then determined between the fitted parameters and the measured operating variables. Again, there are trade-offs to be made between cost of test work and analysis against expected improved versatility of the model.

### Model Fitting for the Example Flow Sheet

Because data were limited to the results of a single plant survey, it was not possible to derive higher-level relationships for the ball mill model in the example case.

The Whiten efficiency curve (Whiten 1972), however, can be extended to include an estimation of the effect of relative density of ore components using the relationship reported by Napier Munn et al. (1996), thus minimizing the number of parameters that need to be fitted to account for the two ore components being considered. This is shown in Figure 2.

Keeping in mind the reason for performing the study, the researchers felt that, provided percent solids and circulating load values could be kept similar between the measured data set and the simulation runs, this would not impinge on the broader desired outcomes and there was no incentive to collect additional data to model fit more complex models for mill or cyclone.

Because the laboratory flotation test work had been performed at four different aeration rates, it was possible to incorporate these data into an interpolative aeration rate model calculation layer built over the simple two-parameter, single-rate flotation model.

**Determine input conditions.** After the flow sheet has been drawn, and models have been selected (or developed) and suitably tuned by extracting parameters from data sourced from operating plants or laboratory test work, the remaining task is to input the process stream data to the simulation.

***Ore feed streams***. Depending on the simulation task to be undertaken, the input or feed streams to the simulation may be a single typical/representative set of component values or a set of data extracted from a table of such component values via an index, thus allowing the simulation of the circuit with multiple feed compositions.

A single scenario or data set for the feed stream is most typically used when the process itself is under scrutiny. Multiple scenarios or data sets for the feed are used, for example, to examine the treatment of the total ore body in a chosen plant configuration.

***Ancillary feed streams.*** Additional input streams may be required where component makeup is required at various places in the circuit. Water makeup is the most obvious, but there may also be a requirement to include addition points

**Model for Unit: Cyclone**

| Model Summary | | | | |
|---|---|---|---|---|
| | Feed | Product 1 | Product 2 | Audit Check |
| Solids t/h | 953.881 | 246.314 | 707.566 | OK |
| Water t/h | 655.36 | 455.79 | 199.57 | OK |
| % Solids | 59.275 | 35.082 | 78.00 | - |
| Pulp SG | 0.948 | 0.451 | 1.54 | - |
| Volume m3/h | 1,006.256 | 546.707 | 459.55 | OK |
| Sulphides (%) | 1.473 | 0.741 | 1.727 | - |
| Gangue (%) | 98.527 | 99.259 | 98.273 | - |
| Sulphides (tph) | 14.046 | 1.826 | 12.22 | OK |
| Gangue (tph) | 939.834 | 244.489 | 695.346 | |

| Model Parameters | |
|---|---|
| Water Split | |
| Required % Solids in Underflow | 78.00 |
| Water split to Product 1 | 0.695 |
| Efficiency Curve Parameters - to Product 1 | |
| Nominal d50c | 160.00 |
| d50c Scale Factor - K2 | 1.166 |
| Alpha - sharpness of cut | 1.736 |
| rf - bypass fraction | 0.395 |
| Feed SG Average | 2.718 |

| | | Species | |
|---|---|---|---|
| | SG specific d50c | Sulphides 59.719 | Gangue 162.023 |
| Size (µm) | | | |
| +6700 | 7,978.10 | 0.000 | 0.000 |
| +4750 | 5,641.37 | 0.000 | 0.000 |
| +3350 | 3,989.05 | 0.000 | 0.000 |
| +2360 | 2,811.76 | 0.000 | 0.000 |
| +1700 | 2,003.00 | 0.000 | 0.000 |
| +1180 | 1,416.33 | 0.000 | 0.000 |
| +850 | 1,001.50 | 0.000 | 0.000 |
| +600 | 714.14 | 0.000 | 0.001 |
| +425 | 504.98 | 0.000 | 0.012 |
| +300 | 357.07 | 0.000 | 0.057 |
| +212 | 252.19 | 0.002 | 0.152 |
| +150 | 178.33 | 0.016 | 0.271 |
| +106 | 126.10 | 0.066 | 0.375 |
| +75 | 89.16 | 0.166 | 0.451 |
| +53 | 63.05 | 0.285 | 0.502 |
| +38 | 44.88 | 0.384 | 0.535 |
| +25 | 30.82 | 0.462 | 0.558 |
| -25 | 20.00 | 0.518 | 0.576 |

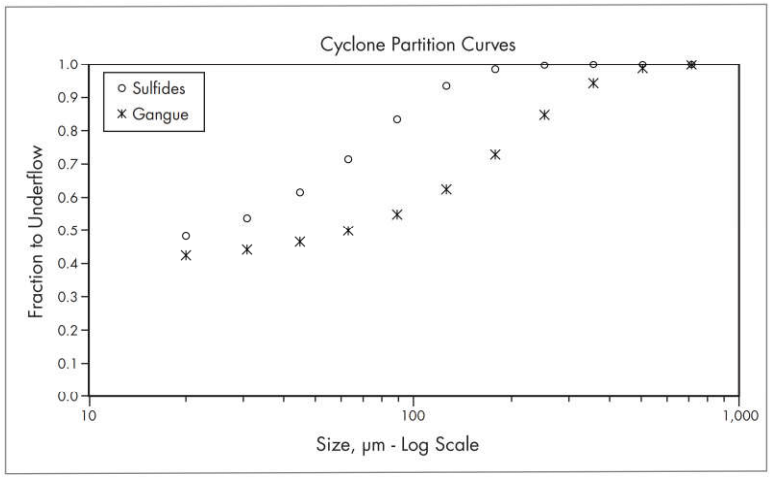


**Figure 2 Fitted hydrocyclone model (Whiten efficiency curve equation for multiple minerals)**

for reagents, medium solids makeup in a dense medium plant or carbon in a gold plant. Such requirements will depend on the degree of detail required for the simulation task to be undertaken.

### Input Streams for the Example Flow Sheet

Because the example flow sheet simulation is to be used to assess large-scale circuit changes and given that the data available are limited, only a single "typical mill feed" ore stream was used. To maintain stream densities, water addition points were also included. The chosen simple models do not allow or require reagent additions or other such components.

**Setup constraints.** In any simulation, there are typically conditions that must be achieved or operational regimes that must be adhered to if the simulation results are to be realistic. In initial simulation runs, this may be achieved manually by observing the results and adjusting the inputs (and possibly unit parameters) to drive the simulation into the domain of interest.

After the simulation system is running in approximately the correct manner, however, it is an advantage to have available some form of constraint control built into the simulation system, which can ensure that the required regime is maintained. There are two main approaches to achieving this:

1. **Direct calculation of required values.** It is sometimes possible to build direct calculations into the models such that the required operating points become parameters of the model. For example, it would be possible to specify the percent solids of both the concentrate and tailings in a flotation model and to use this to determine the feed water additions required to achieve the water balance deriving from those percent solids constraints. However, if such a facility is not available within the model, the calculations must be performed in some other manner, perhaps via an ad hoc calculation facility built into the simulation system.
2. **Generic constraint controllers.** An alternative approach that has proven successful and useful is to provide constraint control via a separate model that is solved as part of the simulation sequence. A simple implementation of this is a controller acting in much the same manner as a conventional plant controller. The user specifies the dependent variable to be monitored, the independent variable to adjust, and the required value or set point for the constrained value. Based on the difference between the current and required constraint value, the simulation system adjusts the independent variable as part of the solution, such that the constraint calculation converges along with overall simulation model convergence.

### Constraints for the Example Flow Sheet

In the example flow sheet, a generic constraint controller facility was used to control water additions to the ball mill

and cyclone, as well as allow control of final concentrate grade if required.

**Refine models and simulation conditions.** During the preceding initial steps, the simulation model generally will have been run many times to identify areas that needed adjusting and to begin to understand the response of the overall simulation system to the available inputs.

If deficiencies are identified, or it is obvious that the system will not produce suitable answers to the questions posed of it, the deficiencies must be corrected and the models further refined, which may require additional test work, model fitting, and so on. This should be regarded as normal practice; development of a useful simulation model tends to be an iterative process.

**Investigate operational scenarios.** After the base case simulation runs have been performed and all stakeholders in the exercise are comfortable with the results, the true power of the simulation study will become apparent. Where "back of the envelope" studies can give an indication of results from a limited range of conditions, a properly structured simulation study can be used to examine the full envelope of options quickly, consistently, and with a high degree of confidence that mistakes have not been made in manual calculations or transcriptions, and that errors have not been made during cut-and-paste operations typically required in extending spreadsheet or similar software calculations to handle multiple inputs to the model.

Although all simulation systems will allow the user to enter a new set of equipment parameters or input conditions, rerun the simulation, and store the results, many systems also have built-in arrangements to automate the process of examining simulation scenarios. A table of inputs and conditions may be specified, simulation runs automatically performed over all the sets of conditions, and results logged for later analysis.

### Example Scenarios

For the example shown here, the scenarios manager tool available in the simulation system used was set up to examine a range of cyclone underflow split to flash rougher cell values from 0%–70%. Figure 3 shows a summary of scenarios for the example flow sheet and its models.

**Assess results.** The state of the art of modeling of unit processes in the minerals processing arena remains largely empirically based. Thus, the results of any simulation study will only be a good as the data used in the modeling process. Models are usually limited in the range of applicability, and where processes themselves are ore-type dependent, the associated models are often restricted to one or, at best, a limited number of different sets of feed conditions.

With these factors in mind, there is a need to critically examine the results of the simulation runs by asking such questions as: Are they reasonable? Do they involve large extrapolations from the base data? Do they answer the original question?

### Example Circuit Results

Figures 4 and 5 show the results from the multiple runs performed at varying cyclone underflow split to the flash flotation. As the split to the flash circuit increased, a slight increase in grade is observed, accompanied by a sizeable increase in sulfur recovery. Increases in size and recovery are unusual in normal flotation circuit operation, so it appears that the flash flotation unit has moved the simulated plant to a new operating point.

If the example was for a new plant design, given the reduction in sulfur recovery in conventional flotation indicated by the simulation, appropriate sizing of flash and conventional flotation sections for the recovery originally targeted could result in capital savings in the overall design.

Apart from the grade aspects, the simulation can also give an indication of the changes in size distributions within the circuit as well as the changes in flows.

**Iterate the aforementioned steps as necessary.** If the simulation predicts an answer to the question that is sufficiently attractive to justify additional work, the next step is to examine the models to determine where that work should take place. Most commonly, this will take the form of collecting more data—or more accurate data—to improve the veracity of the models. It may also take the form of additional laboratory or even pilot-scale test work to verify the simulation results. Further simulation can then be performed using this additional data and the process repeated until the original question is answered to the satisfaction of all concerned.

### Example Circuit

The increase in recovery predicted would appear to be sufficient to encourage further work.

The flotation models particularly have been derived from limited test work and contain significant simplifying

Run the Scenarios

| | *Variables* | | | *Results* | | | | | | | | | |
|---|---|---|---|---|---|---|---|---|---|---|---|---|---|
| ***Cell Address*** | 0.25 | 1.00 | 22.677 | 6.0057 | 63.4142 | 22.677 | 79.0998 | 1.9254 | 36.3976 | 42.6676 | 1.4856 | 44.8408 | 40.5582 |
| | | | | | Final Conc | | | Flash Conc | | | Flash Cleaner Conc | | |
| ***Cell Description*** | Split to Flash | Concentrate Grade Controller Enabled | Concentrate Grade Setpoint | Cleaner Air Rate | Solids Flow t/h | %S Grade | %S Recovery | Solids Flow t/h | %S Grade | %S Recovery | Solids Flow t/h | %S Grade | %S Recovery |
| | 0.70 | 0 | - | 6.00 | 61.38 | 22.53 | 85.15 | 3.61 | 28.38 | 62.44 | 2.44 | 39.21 | 58.18 |
| | 0.625 | 0 | - | 6.00 | 61.30 | 22.68 | 84.50 | 3.37 | 29.37 | 60.30 | 2.31 | 39.99 | 56.35 |
| | 0.60 | 0 | - | 6.00 | 61.28 | 22.72 | 84.26 | 3.29 | 29.72 | 59.52 | 2.27 | 40.26 | 55.67 |
| | 0.50 | 0 | - | 6.00 | 61.15 | 22.90 | 83.19 | 2.94 | 31.27 | 56.03 | 2.09 | 41.41 | 52.62 |
| | 0.40 | 0 | - | 6.00 | 60.98 | 23.04 | 81.84 | 2.57 | 33.06 | 51.71 | 1.88 | 42.67 | 48.79 |
| | 0.30 | 0 | - | 6.00 | 60.78 | 23.12 | 80.06 | 2.16 | 35.18 | 46.16 | 1.63 | 44.07 | 43.76 |
| | 0.20 | 0 | - | 6.00 | 60.51 | 23.09 | 77.55 | 1.67 | 37.75 | 38.46 | 1.32 | 45.66 | 36.66 |
| | 0.10 | 0 | - | 6.00 | 60.16 | 22.79 | 73.47 | 1.05 | 40.98 | 26.28 | 0.87 | 47.51 | 25.18 |
| | 0.00 | 0 | - | 6.00 | 59.70 | 21.54 | 64.59 | 0.00 | 0.00 | 0.00 | 0.00 | 0.00 | 0.00 |

**Figure 3 Scenarios run for the example flow sheet and models**

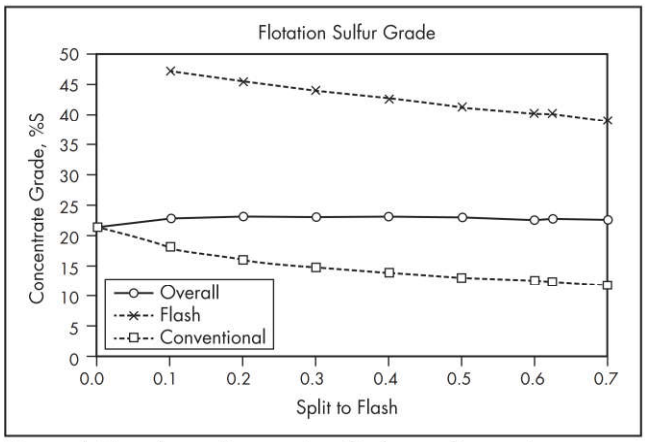


**Figure 4 Flotation sulfur grade with increasing cyclone underflow split to flash flotation**

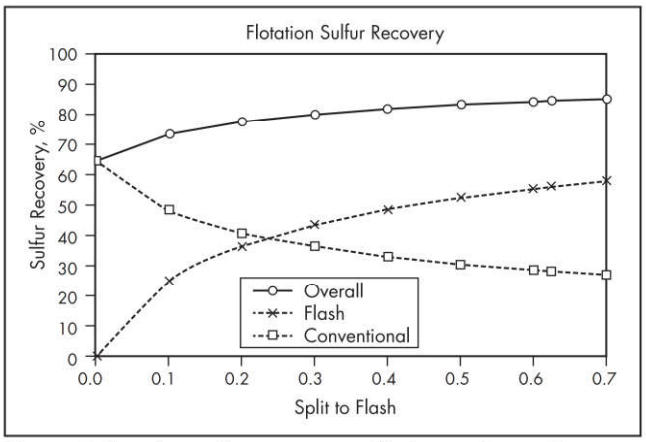


**Figure 5 Flotation sulfur recovery with increasing cyclone underflow split to flash flotation**

assumptions, namely, that the flotation rates in the conventional cells do not change as the split to the flash circuit is increased. This is clearly unlikely and would require additional test work at varying feed grades to the conventional flotation circuit to produce a more accurate model.

The models of the grinding circuit were also based on a single survey, and additional test work, particularly with ore of reduced feed sulfur if possible, would help to pin down the effect of removing sulfides from the grinding circuit circulating load.

Of course, if the results are of such magnitude and the models are conservative, the simulation could provide justification to proceed to installation of a pilot flash unit in the cyclone underflow that would provide further information. The simulation could then be repeated and used to justify (or discourage) the idea of proceeding to a full-scale installation.

## COMPUTER MODELING IN EXTRACTIVE METALLURGY

Process modeling in extractive metallurgy can start with determining chemical speciation based on known process conditions and test work followed by detailed chemical and physical models of unit operations to provide a more accurate representation of the extractive metallurgy in the process plant.

### Modeling of Chemical Speciation in Extractive Metallurgy

Initial use of simulation packages for modeling of extractive metallurgy involving hydrometallurgical and pyrometallurgical processes is beneficial in clarifying the chemical speciation associated with the process concept. Although test work and information from operating plants are used to develop the conceptual chemistry as well as heat and mass balance, in addition or alternatively at initial stages of design, process modeling can be used to perform chemical and equilibrium calculations for aqueous and solid systems. Still, pilot plants and test work are important in providing information for rates of chemical reaction and non-ideality of solutions.

Establishing the process chemistry for hydrometallurgical reactions is fundamental in understanding the process and its conditions. For this reason, computer modeling of aqueous thermodynamics is used for understanding system chemistry and determining preliminary information on the behavior of

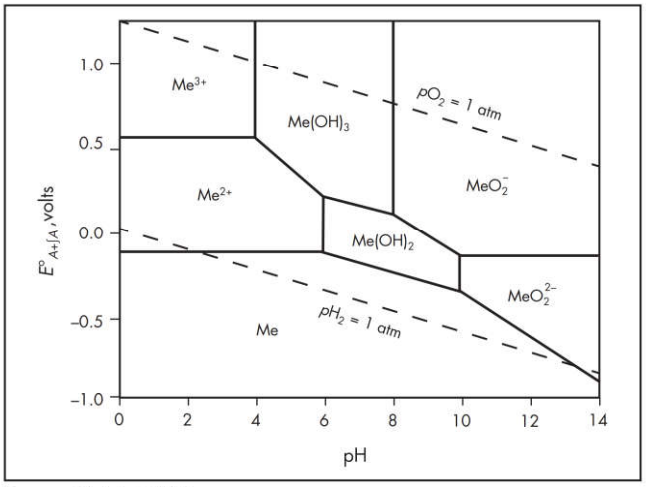


Source: Gilchrist 1989

**Figure 6 Eh–pH diagram for the system metal Me–water as a function of pH and reduction potential**

aqueous/solid systems in the form of Eh–pH diagrams. In hydrometallurgy, a Pourbaix diagram, also known as an Eh–pH diagram, outlines stable (equilibrium) phases of an aqueous electrochemical system. Predominant ion boundaries are represented by lines. An Eh–pH diagram is like a standard phase diagram and does not contain any information on reaction rate or kinetic effects.

Figure 6 shows a characteristic Eh–pH diagram for a typical metal Me for which the standard half-cell potentials are represented as follows:

$$Me^{n+} + ne^- = Me \quad \textbf{(EQ 1)}$$

$$Me^{m+} + (m - n)e^- = Me^{n+} \quad \textbf{(EQ 2)}$$

$$Me\,(OH)_n + nH^+ + ne^- = Me + nH_2O \quad \textbf{(EQ 3)}$$

The third potential is a function of pH, assuming unit activity for Me and Me $(OH)_n$. For a given metal, these potentials may be plotted in an $E°_A$ versus pH diagram. This is represented in Figure 6 for the arbitrary metal Me.

The lines in Eh–pH diagrams show the equilibrium conditions, where the activities are equal, for the species on each

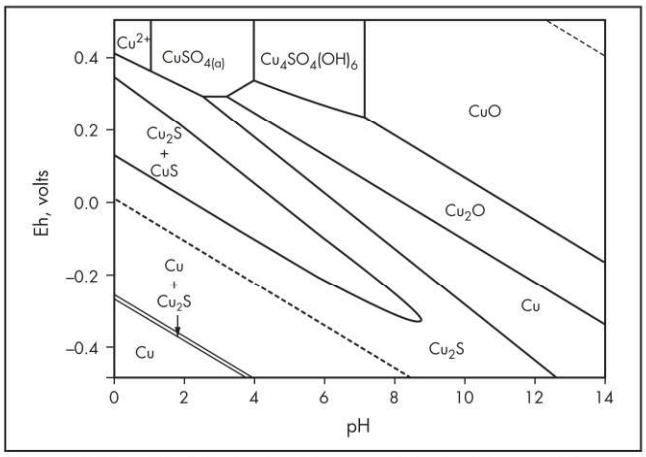


**Figure 7 Eh–pH of Cu-S showing coexistent of two solids in one area**

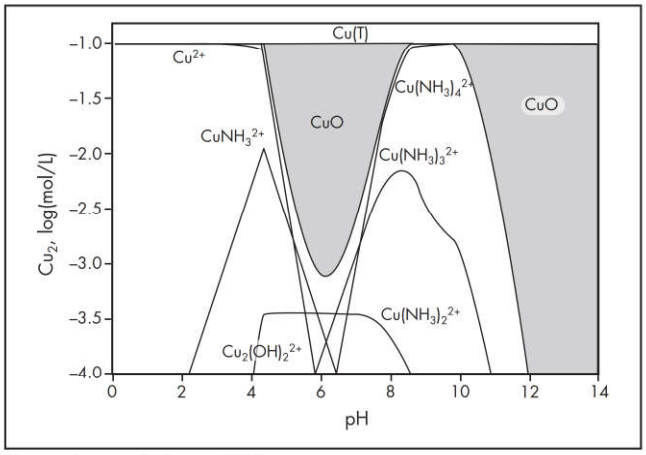


Source: Baes and Mesmer 1976

**Figure 8 Distribution pH of Cu(II) with $NH_3$ generated by Stabcal program**

side of that line. On either side of the line, one form of the species is predominant.

STABCAL (2015) (stability calculation for aqueous and nonaqueous systems) is an integrated Windows program that performs comprehensive stability calculations for complex systems for hydrometallurgical, pyrometallurgical, and environmental engineering; geochemistry; and chemistry for academic research and industrial applications. The program is broken down into two separated groups: aqueous and nonaqueous. Each group function independently has its own computer code and databases taken from the literature.

STABCAL can produce Eh–pH diagrams showing the coexistence of several solids in one area. For instance, the Eh–pH diagram in Figure 7 shows that both covellite (CuS) and chalcocite ($Cu_2S$) are stable in a large area of the Eh–pH diagram of Cu-S-$H_2O$ system.

Another important diagram for aqueous system is the distribution versus pH (Baes and Mesmer 1976). Besides showing the hydrolysis of metal ions on the diagram, STABCAL reveals the formation of complexes from metal with ligands such as Cu(II) and $NH_3$. This is shown in Figure 8.

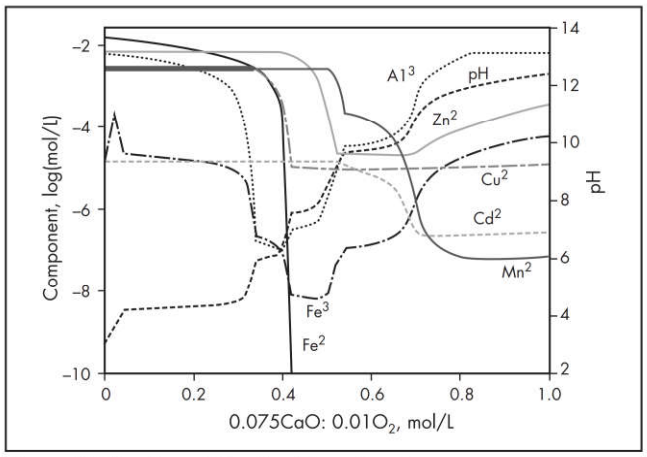


**Figure 9 Titration of the Berkley pit water**

STABCAL is also capable of simulation of systems where chemicals are added to an aqueous solution. For instance, by addition of CaO and $O_2$ stepwise to the Berkeley pit water (Butte, Montana, United States), as depicted in Figure 9, the program will show how the metal hydroxides precipitate, and while Fe(II) is being oxidized, Eh and pH change.

Another program with similar capability in simulation of speciation in extraction of metals and mineral processes is HSC Chemistry by Outotec (Lishchuk 2016). It can show this information by drawing simple Eh–pH diagrams for systems as basic as an element and water, as well as more complicated diagrams with several elements.

## Fundamentals of Heat and Mass Balance in Extractive Metallurgy

In extractive metallurgy, steady-state computer modeling and simulation is usually limited to producing a heat and material balance based on known process design criteria. Process design criteria for well-defined operations include process conditions such as temperature and pressure, feedstock and fuel flow rates and compositions, physical properties including thermochemical properties for each input and output material stream, and the extent of chemical reactions based on the known chemical stoichiometry for the process. Knowing the extent of chemical reactions for a commercial or pilot-plant operation means that reaction kinetics are well known or have already been determined from test work or similar operating plants. The heat and mass balance is then determined based on the following criteria:

- Mass flow rates

$$\text{rate of mass in} = \text{rate of mass out} \qquad \textbf{(EQ 4)}$$

- Chemical reactions and their extent and phase changes for each process unit
- Stoichiometry (for chemical-reacting systems in addition to the law of conservation of mass)

The non-steady-state form for the rate of an individual component, $j$, is as follows:

$$\frac{dmj}{dt} = \sum_{i=1}^{n\,\text{in}} \frac{dmj}{dt},\ \text{in},\ i\ - \sum_{i=1}^{n\,\text{out}} \frac{dmj}{dt},\ \text{out},\ i + rp, j - rc, j \qquad \textbf{(EQ 5)}$$

where

$m$ = unit mass
$j$ = representative component in all input and output streams
$rp, j$ and $rc, j$ = its rates of production and consumption by chemical reactions

Similarly, for steady states, the component mass balance equation is reduced to

$$\sum_{i=1}^{n\,\text{in}} \frac{dmj}{dt},\ \text{in},\ i + rp, j = \sum_{i=1}^{n\,\text{out}} \frac{dmj}{dt},\ \text{out},\ i + rc, j \qquad \textbf{(EQ 6)}$$

In extractive metallurgy where there is chemical or physical change, system energy can be gained or lost from the following sources:

- Sensible heat for each input and output material
- Latent heat because of phase change
- Heats of reaction for all chemical reactions
- Heat inputs and outputs to and from the system by a heat source or cooling

Energy balance at a steady state is defined as total heat input minus heat output. Sources of heat input considered are heat of reaction at 298 K, heat of fusion and evaporation (latent heat), and sensible heat in reactants. Heat balance is an important exercise, and it is used to determine the theoretical temperature reached during the extractive metallurgy process step. Knowledge of heat balance and temperature reached is useful in determining the materials of construction in hydrometallurgy as well as refractory material and overall roaster or furnace design in pyrometallurgy.

The non-steady-state form of energy balance is given as

$$\frac{d(mh)}{dt} = \left(\frac{dm}{dt}\right)_{\text{in}} \cdot h_{\text{in}} - \left(\frac{dm}{dt}\right)_{\text{out}} \cdot h_{\text{out}} + rh\,p = rh\,c \qquad \textbf{(EQ 7)}$$

where

$m$ = unit mass
$h$ = associated enthalpy
$rh\,p$ and $rh\,c$ = rates of heat production and consumption because of chemical reactions, heat input to the system, or cooling

For steady-state balance, the energy balance reduces to

$$\left(\frac{dm}{dt}\right)_{\text{in}} \cdot h_{\text{in}} + rh\,p = \left(\frac{dm}{dt}\right)_{\text{out}} + rh\,c \qquad \textbf{(EQ 8)}$$

Understanding the energy balance as part of extractive metallurgy process design is important. For example, in pyrometallurgy, concentrates are often roasted with coal to convert metal sulfide into oxide. Heat generated by roasting and combustion raises the temperature of the products of coal combustion and roasting. In this case, one goal of pyrometallurgical process simulation is to calculate the temperature under adiabatic conditions, that is, no heat input or loss. This calculated temperature can then be adjusted by incorporating heat losses. The steady-state process simulation would then consider an adiabatic process of roasting with the following heat sources: heat of combustion, heat of reaction, and the sensible heat in reactants. The products consist of solids and gases.

The rate of change of enthalpy of a substance with temperature at fixed pressure is called the heat capacity at constant pressure, $Cp$. Given the function $Cp\ (T)$, the change in enthalpy of a substance as its temperature is raised:

$$\sum_{j=1}^{n} (H_T - H_{298}) = \sum_{j=1}^{n} (H_T\ \frac{dmj}{dt}\ , \quad Cpj \int_{298}^{T} Cp\ (T)\ dT \qquad \textbf{(EQ 9)}$$

where $T$ is the adiabatic temperature attained in a pyrometallurgical process.

Thus, for adiabatic roasting and combustion, Equation 9 can be used together with the liberated or consumed heats of reaction and combustion. If the material balance for roasting is known, as well as temperatures of fuel and air, heat capacity ($Cp$), and heat of reaction, the temperature of the process can be calculated a part of a steady-state process model. The final step in this case is accounting for the input and output components, and determining heat and mass balance by calculating the difference between input and output streams.

In hydrometallurgy, water is a major system component, and the latent heat of evaporation of water is an important variable in the heat balance. In processes operating at temperatures greater than the atmospheric boiling point of water, the pressure is elevated and the design of equipment for such processes is strongly dependent on the vapor pressure of water at the required temperature.

## Application of Process Modeling in Hydrometallurgy

In its simplest form, hydrometallurgy can be described as a technique within the field of extractive metallurgy involving the use of aqueous chemistry for the recovery of metals from ores, concentrates, solutions, and recycled or residual materials. In hydrometallurgy, although sophisticated software is available for process modeling, acquiring and mastering it entails appreciable cost, time, and effort. It is also possible to use spreadsheet calculations for preliminary evaluation of envisaged circuits for processing ore or concentrate.

The modeling software METSIM (Proware 2018), used extensively in extractive metallurgy, comes with models that include chemical reactions and hydrometallurgical unit operations to simulate leaching, autoclaves, solid–liquid separation, precipitation tanks, and numerous other pieces of equipment such as tanks, pumps, bins, stockpiles, dryers, kilns, furnaces, boilers, and steam and gas handling equipment. In METSIM, an interface to FactSage is also available to access Fact's extensive databases.

METSIM is also used for development of simulation models for heap leaching that include a mine block and plan that take into consideration the geometry of heap, its leach cycles, and metal recovery in conjunction with gold carbon-in-circuit and copper solvent extraction and electrowinning operations. The results of such models would be dynamic mass balances over extensive periods of heap leaching operation.

Marsden and Botz (2017) have given a complete review of current approaches to metal production forecasting in heap leach modeling. In their review, heap leaching models are divided into six categories based on type and functionality. The first three categories are Excel based, with the most basic having no scale-up or time delay functionality and the other two as having empirical scale-up and time delays and in-heap inventory-adjusted production estimation. The fourth category consists of off-the-shelf heap leach modeling software capable of some of the aforementioned capabilities.

Off-the-shelf heap modeling includes METSIM and SysCAD described previously. At this level, geometry of the

heap is represented in the model. The heap is represented as many "blocks" or "reactors" that contain solids, liquids, and gases. These models can depict the chemical reactions based on test work such as leach test curves. Drainage factors are also used to calculate moisture contents within each block of the heap.

The last two categories, known as "phenomenological" modeling, are based on use of CFD, thermodynamics, and kinetics of the reactions involved and with the most advanced version having 3-D heap geometry capability.

Another software package that can be used during all stages of a hydrometallurgical plant for numerical analysis and process evaluation is IDEAS (Andritz 2018). This software package includes unit operation objects in libraries that enable users to effectively simulate a nickel laterite plant. IDEAS libraries feature a flexible and easily customized database that contains the material properties for components commonly used in the mineral industry. IDEAS has powerful steady-state capabilities. It performs steady-state mass and energy balances; tracks components, compounds, and element flow and concentration; and handles particle size distributions. IDEAS has been used to model complex plants that include high-pressure acid leaching, heat recovery circuits, neutralization, countercurrent decantation (CCD), autoclaves, precipitation, filtration, separation, solvent extraction, and electrowinning.

Steady-state models created in IDEAS can be easily converted to a dynamic environment to include detailed dynamic specifications and process control logic. By using IDEAS for control logic verification, plants can reduce costly design errors that could otherwise delay start-up. In fact, studies have shown that using simulation to help with start-up can correct a great percentage of control logic problems before field implementation.

The dynamic simulator can also be used for operator training. Working just like a flight simulator, IDEAS allows trainees to gain realistic, hands-on experience without inflicting harm on themselves, the environment, or the plant.

### *Example of Process Modeling in Hydrometallurgy*

This section uses an example to best illustrate the hands-on use of process modeling software and spreadsheet-based calculations in hydrometallurgical process development. The example chosen for this exercise is the processing of laterite. This example is generic and simplified, but the principles illustrated can be applied to actual projects. The exact numbers used are less important than the principles illustrated.

**Laterite processing.** This example is based on general process knowledge and published information, including the results of laboratory leaching tests (Dutwa Project 2018). The key finding of the experimental work was that this particular laterite ore responds well to leaching at low temperature and reasonably low additions of sulfuric acid, leading to the speculation that lower-cost atmospheric leaching might be appropriate in this instance, rather than the more established high-pressure acid leaching (HPAL) route.

**Mineralogy.** In spreadsheet calculations and in process modeling using specialized software, the elemental analysis of the feed ore or concentrate must first be translated into a suite of valuable and gangue minerals, such that the mineral suite accounts for the total mass of the feed and correctly reflects the available data. Modeling software such as METSIM and Aspen Plus can be used as a better alternative to spreadsheets to model a variety of processes in extractive metallurgy. In this example, feed assay and acid leach data are available. Selecting the minerals in this suite would initially be guided by the geology of the deposit, and later refined via mineralogical analysis and other experimental data. Knowledge about how the various minerals respond to different chemical environments can then be used to compile one or more conceptual processes for extracting the valuable elements. While in spreadsheets, the user must compile the thermochemical properties of the elements and components that are used in the heat and mass balance; the commercial modeling software provide the advantage of having an associated compilation thermochemical database.

Table 1 contains the available information on the composition of the laterite ore used in this example. In laboratory leaching tests this laterite was found to consume 210 kg $H_2SO_4$/t (metric ton) of dry laterite ore and to release 92% of the nickel into solution during the leach.

Typically, nickel occurs in laterites as nickel oxide incorporated in goethite-type minerals and in magnesium silicate. The iron is usually present as goethite (FeOOH) and hematite ($Fe_2O_3$), the relative proportions depending on the degree of weathering of the ore. Magnesium is generally present as magnesium silicate minerals. Acid leaching generally decomposes the magnesium silicate minerals and the goethite but not the hematite, so the proportions of goethite and hematite influence the overall consumption of acid. The silicate in the magnesium silicate minerals is converted to silica in the solid residue. Table 2 shows the acid leach chemistry in simplified form. Table 3 shows a simple representation of the laterite as

**Table 1 Laterite assay, mass percentage**

| Laterite Assay | Mass Percentage |
|---|---|
| Ni grade | 1.1 |
| Co grade | 0.034 |
| Cu grade | 0.007 |
| Fe grade | 8.5 |
| Mg grade | 3.5 |

Source: Dry 2013

**Table 2 Acid leach chemistry**

| |
|---|
| $NiO + H_2SO_4 \rightarrow NiSO_4 + H_2O$ |
| $CoO + H_2SO_4 \rightarrow CoSO_4 + H_2O$ |
| $CuO + H_2SO_4 \rightarrow CuSO_4 + H_2O$ |
| $MgSiO_3 + H_2SO_4 \rightarrow MgSO_4 + H_2O + SiO_2$ |
| $2FeOOH + 3H_2SO_4 \rightarrow Fe_2(SO_4)_3 + 4H_2O$ |

Source: Dry 2013

**Table 3 Laterite representation, mass percentage**

| Laterite Representation | Mass Percentage |
|---|---|
| NiO | 1.40 |
| CoO | 0.04 |
| CuO | 0.01 |
| MgO | 5.80 |
| FeOOH | 3.22 |
| $Fe_2O_3$ | 9.26 |
| $SiO_2$ | 80.18 |

Source: Dry 2013

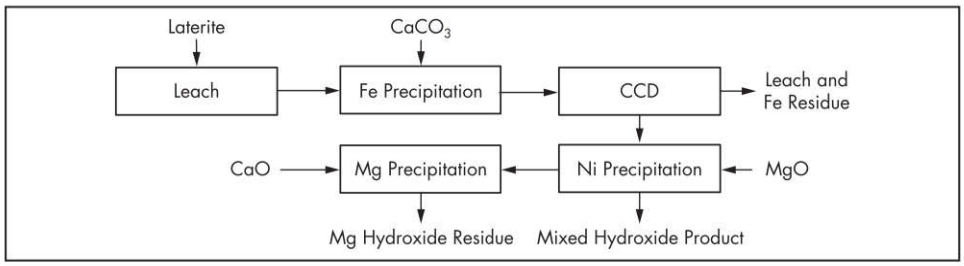


**Figure 10 Block flow diagram of the laterite circuit**

a mixture of oxides of the valuable metals, goethite, hematite, magnesium oxide, and silica.

The knowledge that goethite is dissolved and hematite is not enables the calculation of the amount of goethite required to give the observed overall consumption of sulfuric acid. This is a simple acid balance.

In molar units, 1,000 kg of dry ore contains the following:

- 0.187 kmol of NiO
- 0.006 kmol of CoO
- 0.001 kmol of CuO
- 1.440 kmol of MgO
- 1.522 kmol of iron, split between FeOOH and $Fe_2O_3$

The total consumption of $H_2SO_4$ is 210 kg, or 2.141 kmol per 1,000 kg of ore. The dissolution of NiO, CoO, CuO, and MgO accounts for 1.634 kmol of the acid, leaving the balance for the dissolution of FeOOH, making the amount of FeOOH dissolved 0.338 kmol per 1,000 kg of dry ore. Assuming the percentage dissolution of FeOOH to be the same as those measured for nickel, cobalt, and copper (92%) and that the dissolution of MgO is also 92% gives the mineral assemblage listed in Table 3. Hematite accounts for the difference between the total iron and the iron present as goethite. Silica is simply the difference between 100% and the sum of the other components. This mineral assemblage correctly reflects the available measured data because the feed sample was not assayed for silica, hence the use of silica as the difference between the total mass and the mass of the other minerals. In more detailed work, the silica assay would also be available and the mineral assemblage would very probably be somewhat more complex, but this example still illustrates the principle.

**Modeling calculations for laterite processing.** Formulating a conceptual process includes choosing the form of the products and by-products. For example, a laterite deposit could be processed to an intermediate hydroxide product containing the nickel and cobalt, or all the way to metallic products. Selling prices need to be assigned to each product and by-product so the potential revenue from the deposit can be estimated.

The next step would be to define one or more potentially suitable process routes and evaluate the potential cost of processing the ore for each route selected. When an envisaged process is hydrometallurgical, that generally requires laboratory leaching tests to measure the extractions of valuable metals and the consumption of reagents such as acid. It is reasonable (but not essential) to calculate the consumption of, say, acid from the mineral suite and knowledge of the chemistry of the various minerals before commissioning laboratory tests. It is, however, always prudent to obtain experimental confirmation of the leach at an early stage.

In this example, the circuit entails leaching with sulfuric acid, neutralization of the resulting slurry with limestone, solid–liquid separation, precipitation of a mixed nickel–cobalt hydroxide with magnesium oxide, and precipitation of magnesium and sulfate from the barren solution using lime. Figure 10 is a block diagram illustrating a basic circuit.

Two variations of the basic circuit are covered in this example: leaching in agitated tanks under atmospheric pressure (ATL) and leaching at high pressure and high temperature (HPAL) in autoclaves. For the ATL case, the leach chemistry is the same as that shown in Table 2.

Leaching laterite at elevated temperature and pressure (HPAL) is done when the ore is more limonitic in nature, meaning that most of the nickel is contained in goethite-like iron minerals and those minerals make up the bulk of the ore. For such laterite ores under atmospheric leaching conditions, dissolving essentially all the iron minerals to release the nickel into solution and converting the iron to dissolved ferric sulfate would require large amounts of acid and then large amounts of limestone to neutralize the leach solution and precipitate out the iron. At the elevated temperatures generally used in HPAL (typically 240°–270°C), most of the dissolved ferric iron hydrolyzes and is precipitated as hematite, releasing the acid consumed in its dissolution and thereby greatly reducing the overall acid requirement. Leaching laterite under HPAL conditions also greatly accelerates the leach reactions, relative to leaching at or below the atmospheric boiling point of the solution.

At the elevated temperatures of HPAL, the second dissociation of sulfuric acid essentially does not occur. The top half of Table 4 gives stoichiometry illustrating the HPAL leach chemistry. On cooling after the high temperature leach reaction, the bisulfate salts revert to sulfuric acid and sulfate salts, as illustrated by the stoichiometry shown in the bottom half of Table 4. Although the overall chemistry is the same as for the atmospheric leach, the behavior of sulfuric acid under HPAL conditions is such that more than half of the sulfuric acid added must be neutralized after the leach.

In saprolitic laterites, which contain higher levels of magnesium, the acid requirement in HPAL is high even though the dissolved iron is re-precipitated as hematite, because the magnesium dissolves but does not re-precipitate.

The extent of precipitation of ferric iron in HPAL is influenced by the amount of residual sulfuric acid remaining in the solution. Figure 11 shows published data relevant to the hydrolysis of ferric iron under HPAL conditions (Papangelakis et al. 1996). In these measurements, the slurry contained 22% solids and the temperature was 250°C. This can be used to calculate the acid consumption that leaching the mineralogy in Table 3 under HPAL conditions would require for the same dissolution of nickel as in the heap leach option, assuming the same

**Table 4 HPAL stoichiometry**

| |
|---|
| $NiO + 2H_2SO_4 \rightarrow Ni^{2+} + 2HSO_4^- + H_2O$ |
| $CoO + 2H_2SO_4 \rightarrow Co^{2+} + 2HSO_4^- + H_2O$ |
| $CuO + 2H_2SO_4 \rightarrow Cu^{2+} + 2HSO_4^- + H_2O$ |
| $MgO + 2H_2SO_4 \rightarrow Mg^{2+} + 2HSO_4^- + H_2O$ |
| $2FeOOH + 6H_2SO_4 \rightarrow 2Fe^{3+} + 6\ HSO_4^- + 6H_2O$ |
| $2Fe^{3+} + 6\ HSO_4^- + 3H_2O \rightarrow Fe_2O_3 + 6H_2SO_4$ |
| $Ni^{2+} + 2HSO_4^- \rightarrow NiSO_4 + H_2SO_4$ |
| $Co^{2+} + 2HSO_4^- \rightarrow CoSO_4 + H_2SO_4$ |
| $Cu^{2+} + 2HSO_4^- \rightarrow CuSO_4 + H_2SO_4$ |
| $Mg^{2+} + 2HSO_4^- \rightarrow MgSO_4 + H_2SO_4$ |
| $2Fe^{3+} + 6\ HSO_4^- + 6H_2O \rightarrow Fe_2(SO_4)_3 + 3H_2SO_4$ |

Source: Dry 2013

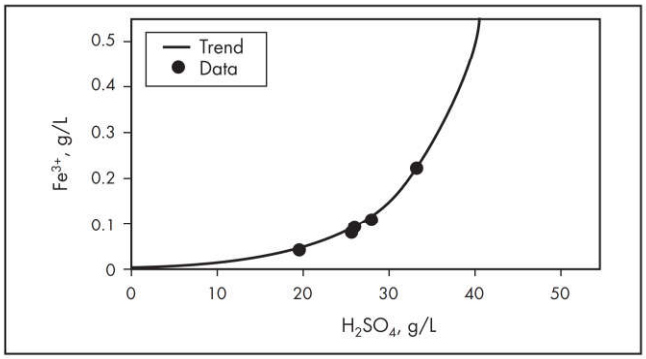


Source: Marsden and Botz 2017
**Figure 11 Ferric iron, hydrolysis data**

conversion for the first five reactions in Table 4 and adjusting the conversion of the sixth reaction at the same final acid concentration as for the atmospheric leach (5 g/L) in a leached slurry containing 25% solids, such that the dissolved ferric iron lies on the trend line shown in Figure 11. This calculation gives an acid requirement of 323 kg/t of ore, compared to 210 kg/t measured in the leach tests at atmospheric pressure. For generating the acid from elemental sulfur, the sulfur requirements would be 69 kg/t for the atmospheric leach and 106 kg/t for the HPAL case.

The pregnant liquor from the leach is treated with limestone ($CaCO_3$) to neutralize residual acid and to precipitate the dissolved iron. Table 5 shows the overall chemistry associated with the iron precipitation step. The amount of limestone consumed is fixed by the amount of iron dissolved in the leach and the level of free acid in the solution after leaching.

The nickel, cobalt, and copper are precipitated from the iron-free pregnant liquor as a bulk hydroxide, using magnesium oxide. Table 6 shows the overall chemistry assumed for this step. The precipitate would be washed, dried, and sold. Its nickel content would be about 50% by mass. The consumption of magnesium oxide is fixed by the amounts of nickel, cobalt, and copper precipitated and the amount of residual MgO in the precipitate.

Calculating the residual magnesium oxide in the mixed hydroxide precipitate (MHP) is straightforward, as follows:

**Table 5 Iron precipitation**

| |
|---|
| $H_2SO_4 + CaCO_3 \rightarrow CaSO_4 + H_2O + CO_2$ |
| $Fe_2(SO_4)_3 + 3CaCO_3 + H_2O \rightarrow 3CaSO_4 + 2FeOOH + 3CO_2$ |

Source: Dry 2013

**Table 6 Base metal precipitation**

| |
|---|
| $NiSO_4 + MgO + H_2O \rightarrow Ni(OH)_2 + MgSO_4$ |
| $CoSO_4 + MgO + H_2O \rightarrow Co(OH)_2 + MgSO_4$ |
| $CuSO_4 + MgO + H_2O \rightarrow Cu(OH)_2 + MgS_O4$ |

Source: Dry 2013

**Table 7 Magnesium precipitation**

| |
|---|
| $MgSO_4 + Ca(OH)_2 \rightarrow Mg(OH)_2 + CaSO_4 + 2H_2O$ |

Source: Dry 2013

- Ni dissolved from the laterite: 1.01 kg/t ore
- Assumed Ni in MHP: 50 mass %
- MHP produced: 0.202 kg/t ore
- $Ni(OH)_2$ in MHP: 0.160 kg/t ore
- $Co(OH)_2$ in MHP: 0.005 kg/t ore
- $Cu(OH)_2$ in MHP: 0.001 kg/t ore
- Therefore, MgO in MHP: 0.037 kg/t ore

From this calculation, the residual MgO in the MHP is small compared to the amount required to precipitate the base metals.

The barren solution remaining after precipitation of the base metals contains magnesium and sulfate that are precipitated with slaked lime, according to the chemistry shown in Table 7. This is necessary to avoid a buildup of magnesium sulfate in the circuit as the process water is recycled.

The amount of slaked lime required can be calculated from the amount of magnesium, which can be calculated from the amount of magnesium leached and the amounts of nickel, cobalt, and copper precipitated.

Lime (CaO) is produced by heating limestone ($CaCO_3$) to between 900°C and 1,000°C, driving off the carbon dioxide and leaving reactive calcium oxide. A conservative estimate of energy consumption for this is 6 mJ/kg CaO produced. One source of energy is coal. A typical heating value for coal is 30 mJ/kg, so a rough approximation of the amount of coal needed to produce 1 t of lime from limestone would be 200 kg.

Table 8 lists the amounts of sulfur, limestone, magnesia, and coal calculated for a circuit processing the laterite in this example, for ATL and HPAL technology, in kilograms per metric ton of the dry feed laterite.

For a venture to be commercially viable, the costs associated with any process need to be sufficiently less than the revenue generated. Commodity prices are not static; therefore, a single current price for any given commodity will probably not be reasonable in a study that would entail starting a commercial operation, say, 5–10 years into the future and operating it for the next two or more decades. One way around this problem is to use price ranges instead of single numbers for the different commodities. Figure 12 shows historical commodity prices (Kelly and Matos 2014) relevant to this exercise in constant 2013 U.S. dollars, over the past century for nickel, cobalt, sulfur, lime, and magnesia and over the past half century

for coal (U.S. Energy Information Administration 2018). The dashed lines on these charts are the long-term arithmetic average price, plus or minus one standard deviation. Although the various commodity prices have moved outside the "channels" depicted by the dashed lines in these graphs, they have always returned and each one has spent the bulk of the time covered within a standard deviation of the long-term average. In the absence of more detailed pricing for the relevant commodities, it is not unreasonable to assume the range indicated by the dashed lines for the relevant commodity.

Another cost item that needs to be included in these calculations is the cost of mining the laterite and delivering it to the processing facility. Laterite mines are usually opencast, and a mining cost model reference from the public domain (InfoMine 2018) gives a mining cost of US$7.32/t of ore mined. For the laterite in this example, that translates to US$0.33/lb of nickel in the hydroxide product.

Table 9 lists the variable costs from the spreadsheet model calculations and the commodity price ranges shown in Figure 12, along with the calculated revenue, assuming that

**Table 8 Reagent consumption from spreadsheet calculations**

| | Consumption, kg/t | |
|---|---|---|
| Reagent | ATL | HPAL |
| S | 69 | 106 |
| $CaCO_3$ | 214 | 172 |
| MgO | 7 | 7 |
| Coal | 17 | 17 |

Source: Dry 2013

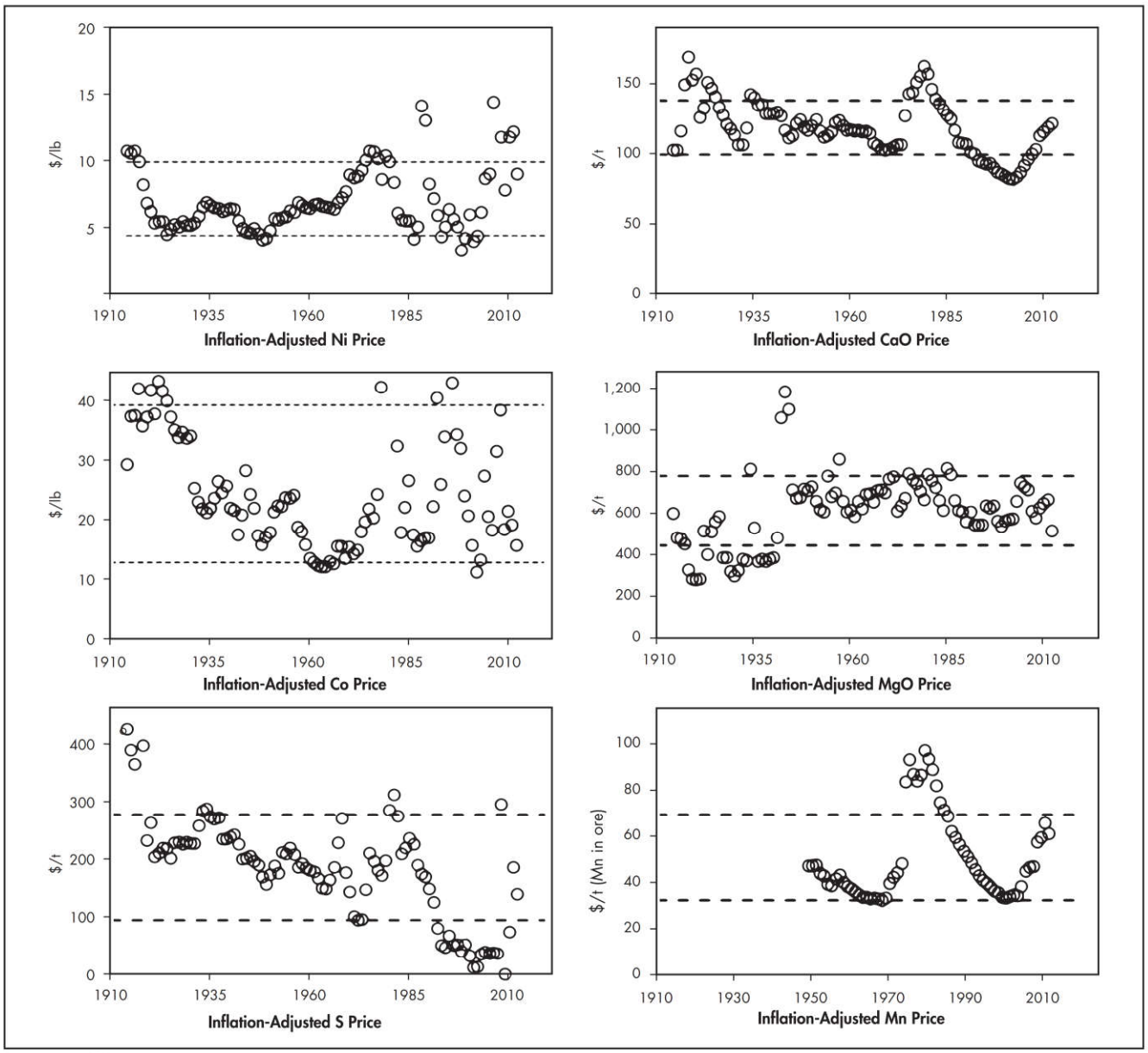


Source: Dry 2015

**Figure 12 Historical commodity prices**

**Table 9 Variable costs from spreadsheet calculations**

| | Consumption Ore, kg/t | | Reagent Price, $/t | | Variable Cost, $/lb Ni | | | |
|---|---|---|---|---|---|---|---|---|
| | | | | | ATL | | HPAL | |
| Reagent | ATL | HPAL | Low | High | Low | High | Low | High |
| S | 69 | 106 | 96 | 278 | 0.30 | 0.86 | 0.46 | 1.32 |
| $CaCO_3$ | 214 | 172 | 100 | 138 | 0.96 | 1.33 | 0.77 | 1.07 |
| MgO | 7 | 7 | 449 | 782 | 0.14 | 0.25 | 0.14 | 0.25 |
| Coal | 17 | 17 | 33 | 70 | 0.03 | 0.05 | 0.03 | 0.05 |
| Mining cost ($7.32/t ore) | | | | | 0.33 | 0.33 | 0.33 | 0.33 |
| Total calculated variable cost | | | | | 1.75 | 2.82 | 1.72 | 3.02 |
| Revenue for Ni hydroxide (75% of Ni price) | | | | | 3.33 | 7.48 | 3.33 | 7.48 |
| Revenue for Co hydroxide (75% of Co price) | | | | | 0.30 | 0.91 | 0.30 | 0.91 |
| Revenue minus variable costs | | | | | 1.88 | 5.57 | 1.90 | 5.37 |

Source: Dry 2013

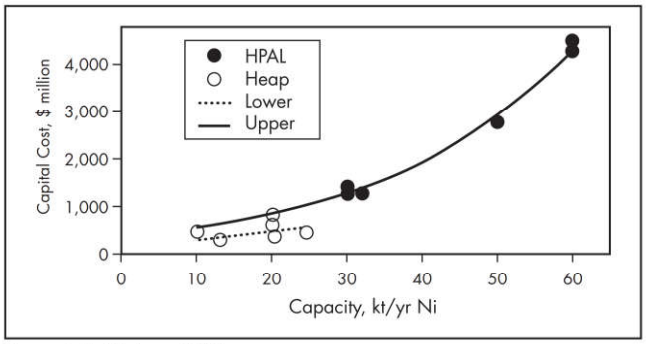


Source: Wedderburn 2010

**Figure 13 Capital costs for laterite projects**

the intermediate hydroxide precipitate can be sold for 75% of the price ranges shown for nickel and cobalt.

The calculated revenues exceed the calculated variable costs for both process routes examined. Had the variable costs approached or exceeded the revenue at this stage of the analysis, there would be no incentive to proceed further, apart from a careful check of the assumptions made and the calculations done. Since the calculated revenue does appreciably exceed the calculated variable costs, further evaluation is justified. The differences between the ATL and HPAL routes are not large enough, at this level of analysis, to differentiate between the two, so further examination of both is merited.

The costs for any venture are the variable operating cost, fixed operating cost, and capital cost. The fixed operating cost comes from salaries, spares, inventory, and so on. This number has to be estimated at this stage. For this exercise, the initial guess is 100 people at an average employment cost of US$50,000/yr, which translates to about $0.08/lb of nickel for 30,000 t of nickel per year.

The capital cost is a number that comes from engineering design work that has not even been contemplated at this stage of the exercise. However, an initial guess can be formulated using numbers from other similar projects. The capital costs shown in Figure 13 are for projects processing laterite to a mixed hydroxide intermediate via both HPAL and heap leaching.

Three of the data points for heap leaching are very close to the regression line through the HPAL data points (upper), whereas the other three lie well below this trend (lower). Assuming that the ATL capital cost can be approximated by the trend represented by the lower data points, extrapolating the lower regression line through these three points gives a capital cost of about US$600 million for 30,000 t/yr of nickel in the hydroxide product. Assuming HPAL for the leach step, interpolating the upper regression line to the same capacity gives a capital cost of about US$1,300 million.

Having evolved these very preliminary estimates for the costs and revenues associated with the laterite project chosen for this exercise, simple cash-flow analysis can be used to help decide whether the project is worth more substantial evaluation. Table 10 gives the results of this analysis for the case of ATL technology. The assumptions used are a two-year construction period with half of the capital expenditure in each of those years, followed by 20 years of production, with the throughput at 50% of design in year 3 and at 100% of design thereafter. Corporate tax was assumed to be 20% of the gross margin after recoupment of all the capital expenditure. For this calculation, the higher reagent costs and the lower metal prices were used.

The cash-flow analysis predicts an after-tax internal rate of return (IRR) of about 26% in the ATL case, for the average variable cost and revenue values.

Table 11 shows the cash-flow analysis for the HPAL case. For the average variable cost and revenue, the after-tax IRR comes to about 12%. The first conclusion to be drawn from these very preliminary calculations is that, for processing this laterite, the ATL case appears to be the stronger one, economically.

This process analysis does not require calculations that cannot be done quite easily on a spreadsheet, along with some rather persistent searching of open-domain information. The results can either greatly enhance confidence moving forward or rationally discourage further work if the numbers do not indicate a potentially viable project.

Whether these results lead to further effort would be a business decision based on information relevant to the project in question. These preliminary results will be taken as sufficient inducement to proceed to the next level of evaluation, which does get more sophisticated, computationally. From the preliminary numbers outlined in Table 11, it would seem logical to drop the HPAL option at this stage, but for completeness of the exercise, the HPAL option is also examined in more depth.

**Table 10 Cash-flow analysis for ATL case, US$ million**

| Year | 1 | 2 | 3 | 4 | 5 | 6 | 7 | 8 | 9 | 10–22 |
|---|---|---|---|---|---|---|---|---|---|---|
| Capital costs | 300 | 300 | — | — | — | — | — | — | — | — |
| Fixed costs | — | — | 17 | 17 | 17 | 17 | 17 | 17 | 17 | 17 |
| Variable costs | — | — | 75 | 151 | 151 | 151 | 151 | 151 | 151 | 151 |
| Revenue | — | — | 198 | 397 | 397 | 397 | 397 | 397 | 397 | 397 |
| Margin | –300 | –300 | 106 | 229 | 229 | 229 | 229 | 229 | 229 | 229 |
| Corporate tax | 0 | 0 | 0 | 0 | 0 | 38 | 46 | 46 | 46 | 46 |
| Profit | –300 | –300 | 106 | 229 | 229 | 190 | 183 | 183 | 183 | 183 |
| Internal rate of return: 26% | | | | | | | | | | |

Source: Dry 2013

**Table 11 Cash-flow analysis for HPAL case, US$ million**

| Year | 1 | 2 | 3 | 4 | 5 | 6 | 7 | 8 | 9 | 10–22 |
|---|---|---|---|---|---|---|---|---|---|---|
| Capital costs | 650 | 650 | — | — | — | — | — | — | — | — |
| Fixed costs | — | — | 17 | 17 | 17 | 17 | 17 | 17 | 17 | 17 |
| Variable costs | — | — | 78 | 157 | 157 | 157 | 157 | 157 | 157 | 157 |
| Revenue | — | — | 198 | 397 | 397 | 397 | 397 | 397 | 397 | 397 |
| Margin | –650 | –650 | 103 | 223 | 223 | 223 | 223 | 223 | 223 | 223 |
| Corporate tax | 0 | 0 | 0 | 0 | 0 | 0 | 0 | 0 | 28 | 45 |
| Profit | –650 | –650 | 103 | 223 | 223 | 223 | 223 | 223 | 195 | 178 |
| Internal rate of return: 12% | | | | | | | | | | |

Source: Dry 2013

**Process modeling for laterite processing.** One approach could be to first proceed with spreadsheet modeling of the process. When the results of the preliminary evaluation using spreadsheet calculations indicate a sufficiently strong business case for the project, the next stage can be pursued, which is to refine the calculated cost and revenue numbers so that the financial modeling can in turn be strengthened. At this stage, further experimental work becomes more than appropriate, as does a more detailed evaluation of the envisaged process. Process modeling can be used to generate and study a mass–energy balance of the envisaged circuit, optimally while more detailed experimental work is being done. This gives two major benefits: (1) a substantially enhanced understanding of the envisaged circuit enables the experimental work to be done much more cost effectively than would otherwise be possible; and (2) when experimental results become available, they can be incorporated into the mass–energy balance, which then becomes a very good basis for subsequent detailed engineering design and costing work, should the project reach that stage.

In this example, two detailed process models were constructed using commercially available process simulation software known as Aspen Plus, and the mass–energy balances generated were used to refine the analysis of the project. Figure 14 is a diagram of the ATL circuit modeled and Figure 15 is a diagram of the HPAL circuit. The process chemistry is the same as before. Incoming laterite is crushed and slurried with recycled and makeup water, the slurry is milled and the milled slurry is thickened, with the thickener overflow returning to the slurry makeup step and the underflow being pumped to the leach.

The process models include a standard sulfur burning acid plant. Incoming elemental sulfur is stockpiled as a solid, then reclaimed and melted in a sulfur melting pit. The molten sulfur is pumped to a sulfur burner and burned in air. The energy released is captured as high-pressure steam. The gas from the burner passes through three catalyst beds in which the sulfur dioxide is oxidized to sulfur trioxide. The oxidation is exothermic and the hot gas generated passes through heat exchangers, raising more high-pressure steam, between the catalyst beds. The gas from the third catalyst bed passes through an absorber in which the sulfur trioxide is captured into circulating strong acid and water, making 98% $H_2SO_4$, some of which is used to leach the milled laterite. The gas from the absorber passes through more heat exchangers and a fourth catalyst bed, then through another heat exchanger to a second absorber in which the sulfur trioxide is captured into the balance of the 98% sulfuric acid from the first absorber. The resulting strong acid returns to the first absorber and the residual gas is vented to a stack.

The leach is done at atmospheric pressure and 95°C in the ATL case, and at 250°C and elevated pressure in the HPAL case. In both situations, the leach is heated by injection of live steam from the acid plant, but in addition the HPAL case recycles steam flashed off after the leach to preheat the incoming slurry.

The residence time for atmospheric leaching was assumed to be 20 hours. For the HPAL case, the leach residence time was taken to be 75 minutes.

The leached slurry is pumped to a neutralization stage, where limestone is added to neutralize the residual free acid and precipitate the dissolved ferric iron. The incoming

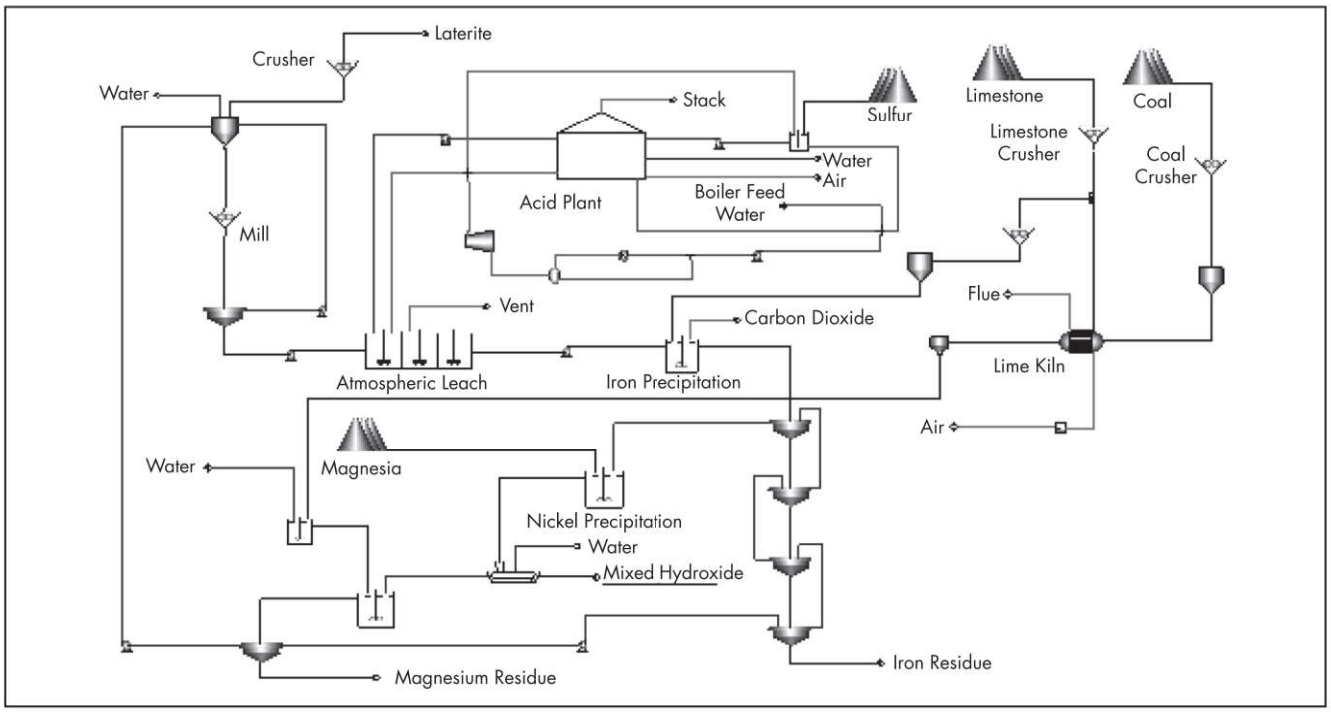


Source: Dry 2013

**Figure 14 Process model (ATL case)**

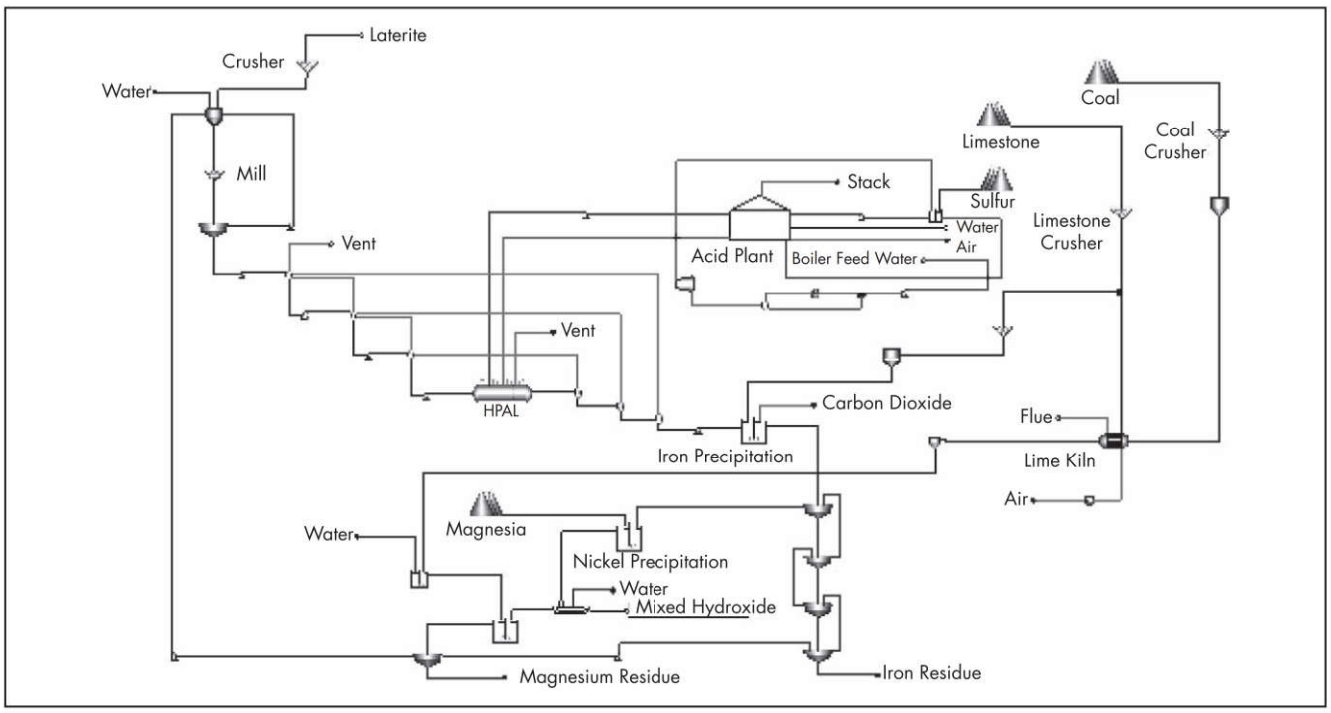


Source: Dry 2013

**Figure 15 Process model (HPAL case)**

limestone is crushed, and a part of the crushed limestone is used in the neutralization and iron precipitation step.

The neutralized slurry passes through a CCD train in which the solids are washed with recycled water. The washed solids leave the circuit. The supernatant from the CCD train is contacted with magnesium oxide to precipitate nickel, cobalt, and copper as a mixed hydroxide that is filtered out and washed with water. The washed hydroxide leaves the circuit as the desired intermediate product.

**Table 12 Reagent comparison, in kilograms per ton of laterite**

| | Atmospheric Leach | | HPAL | |
|---|---|---|---|---|
| Reagent | Spreadsheet | Process Model | Spreadsheet | Process Model |
| S | 69 | 69 | 106 | 106 |
| $CaCO_3$ | 214 | 227 | 323 | 348 |
| MgO | 7 | 8 | 7 | 8 |
| Coal | 17 | 22 | 17 | 22 |

Source: Dry 2013

The filtrate from the base metal precipitation step is contacted with slaked lime to precipitate the magnesium. The resulting slurry of magnesium hydroxide and calcium sulfate is thickened, the thickener underflow leaves the circuit, and the supernatant is recycled as wash to the CCD train and to the slurry step ahead of the leach. The slaked lime is made by calcining the crushed limestone not used in the iron precipitation step. A kiln was assumed for this duty, fired by coal and air. In this model, the ash from the coal accompanies the lime to the slaker.

The first comparison of interest between the results of the spreadsheet calculations and the balances from the process models is between the reagent consumption numbers, as shown in Table 12. The numbers for limestone are the sum of the amounts of calcium carbonate used directly in the iron precipitation step and the amounts needed to make the calcium oxide used in the magnesium removal step. Except for sulfur, the process models predict higher reagent consumption numbers than the spreadsheet calculation. The differences are because of the solution volumes in the case of $CaCO_3$ and MgO, and the heating of solids and air in the case of coal. These were ignored in the spreadsheet calculations.

Using the reagent consumption numbers from the process models in the cash-flow analyses done before reduces the IRR numbers by only 1%, which is not a significant difference at this level of evaluation. The relative differences in acid and limestone consumption predicted by the process models are in line with those from the purely stoichiometric calculations.

**Cost modeling for laterite processing.** Process engineering, equipment design, and cost estimation have traditionally been undertaken by different groups of specialists not automatically available to the people developing mining projects. Particularly in the case of junior mining companies, access to cost estimation has not been feasible until a substantial body of data has been generated, at which stage the investors allow the project team to commission engineering companies to do the necessary process engineering, equipment design, and cost estimation. The desired and anticipated outcome of this work is that the project in question is economically viable, but until the work is done, that outcome is uncertain, however much the project proponents believe in it. There is a risk that the time, effort, and money spent up to that stage of any given project will not result in a commercially viable operation.

A second consequence of the traditional separation between the process and estimation disciplines is that when there are alternative process options, comparison of options can be based more on opinion than on dispassionate evaluation, simply because dispassionate evaluation requires capital cost estimation, traditionally unavailable for reasons of cost and time. This is why approximately 80% of the capital cost of the process plant for any given project is sometimes determined by choices made in the conceptual design phase of the project, before any capital costs are known. In the modern world of global competition, investment decisions bringing projects to fruition faster, at less cost, and with minimum risk and uncertainty become ever more difficult.

It would be better to know sooner rather than later if a project is not sufficiently robust, economically, to justify its continued existence. It would also be better to know sooner rather than later that the most appropriate process option has been selected. Although perfect prescience is not achievable, it is quite possible to evaluate the capital and operating costs of a project, and hence the potential economic viability of that project, significantly earlier than has previously been practical. Just as process engineers have developed their tools, so have cost estimators. Equipment sizing and costing algorithms have been developed that generate equipment sizing and cost numbers from minimal process information. These algorithms have been embedded into modern computer software that can be used to automate the interface between process design, equipment sizing, and cost estimation. This enables the project team to iteratively evaluate project costs and compare options rapidly and cost effectively.

**Preliminary equipment sizing.** The following discussion illustrates the use of commercially available equipment sizing and costing software to estimate project costs. In the example used in this chapter, the two cases are similar except for the leach section. The cost estimation software automatically sizes the various pumps in the circuit, assuming standard design codes and carbon steel as the material of construction, but the material of construction can also be specified: stainless steel or rubber-lined carbon steel, for example. The various vessels in the circuit are automatically sized, assuming a specified residence time and default or specified material of construction.

The software used for this exercise is known as Aspen Process Economic Analyzer (APEA). This software can be activated directly from the Aspen Plus process simulation software; therefore, the entire mass–energy balance is electronically transferred from the process model to the corresponding process cost model. The various unit operations in the process model are computationally mapped to materials of construction and process equipment that is automatically sized, based on either default parameters or parameters that are specified for any item of equipment. The sizing calculations give the amounts of material and labor required to fabricate and install the process equipment, as well as the materials and quantities required for foundations, supporting structures and process piping, instrumentation, electrical wiring, and so on. In the exercise presented in this chapter, the software was set to give costs for a project in Africa. The equipment sizing was set up as follows.

**Ore preparation.** In the ore preparation section, incoming ore is crushed, slurried in water, and milled. The milled slurry is thickened, and the thickened slurry proceeds to leaching. The surplus water from the milled slurry is recycled.

The minimum process information required for the crusher by the sizing/costing algorithm is the power input, which can be approximated from the work index of the ore, the crushed product size, and the throughput. In this example, the work index has not been measured, so a number from the published literature must be used instead. One published number for an Indonesian laterite is 9.7 kW·h/t, and the ore throughput for this exercise is 360 t/h. Crushing the ore to

3-mm particles requires a crushing power of 638 kW (or 1.8 kW·h/t of ore). The crusher was assumed to be fed from a belt conveyor 100 m long and 1 m wide.

The information required for costing the mill is the internal diameter and the length. Outokumpu has published useful information on preliminary mill sizing, specifically a correlation linking the mill power to the mill type and dimensions. Assuming the same throughput and work index as for the crusher, and that the ore is milled from 3–100 mm, gives a milling power requirement of 2,854 kW (7.9 kW·h/t of ore). Using that and the standard factors tabulated in the Outokumpu pamphlet gives a mill diameter of 3.7 m and a length of 17 m.

The slurry tank between the crusher and the mill was assumed to be a carbon-steel agitated tank with a residence time of one hour, to allow the crusher to be run intermittently if necessary.

The mill thickener was assumed to be a standard thickener made from carbon steel. The thickening rate of the milled slurry not having been measured yet, 0.1 t/h/$m^2$ was assumed. The same number is used for the CCD train after leaching, which was inferred from published data from a pilot plant (detailed in the section on CCD later in this chapter).

**Acid plant.** The sulfur melting pit was assumed to be an agitated tank holding 2 hours of feed to the sulfur burner and heated by a steam coil using steam from the acid plant. The material of construction was set to stainless steel. The cost of the sulfur burner was approximated by the cost of a process furnace, the material of construction being stainless steel. The converters were sized from a standard design, assuming the same superficial gas velocity entering the first catalyst bed, which gave the vessel size and the volume of the catalyst beds. The catalyst bulk density and price were taken from a catalog of sulfuric acid catalysts. The various pumps and heat exchangers were sized automatically by the software. The material of construction was stainless steel throughout the acid plant.

**Atmospheric leach.** In the circuit using atmospheric leaching, the underflow from the mill thickener is pumped into the leach train, where it is leached for 20 hours. The reactors were specified as 10 agitated tanks, each having a residence time of 2 hours, with the tanks and agitators made of rubber-lined steel. At a height-to-diameter ratio of 2, that makes the diameter of each tank 9.5 m. The material of the pump after the leach train was specified as stainless steel.

**HPAL leach.** In the circuit using HPAL for the leach section, the milled and thickened ore slurry is passed through three direct-contact heat exchange towers in which it is progressively heated by condensing steam flashed from the hot leached slurry. These heat exchange towers were assumed to have a residence time of 10 minutes each, made of titanium-clad steel and lined with acid-resistant bricks to protect the vessel against erosion.

The preheated ore passes to the leaching step. The autoclave design was based on data from the Ambatovy (Madagascar) pilot plant. Anaconda's Murrin project had four autoclaves, each 35 m long and just less than 5 m in internal diameter, made from titanium-clad steel. The residence time in HPAL given in the work from the Ambatovy pilot plant is 75 minutes and the slurry into the preheating step contained 30% solids. That solids content and residence time translate to a required active volume of 1,500 $m^3$ for the 360 t/h throughput of the exercise in this chapter. Assuming the active volume to be 60% of the total internal volume of the autoclave, that requires four autoclaves similar to the ones used by Murrin. For costing purposes, each autoclave was assumed to be a multicompartment agitated horizontal tank reactor with the wall thickness designed for a working pressure of 40 bar, made from titanium-clad steel (8 mm titanium). The agitators were assumed to be six per autoclave, fitted with mechanical seals and made from titanium.

The hot pressure-leached slurry is flashed to atmospheric pressure in three let-down vessels. The residence time was left as the default, and the material of construction was set to titanium-clad steel lined with acid-resistant bricks.

**Iron precipitation.** The leached (and depressurized, in the case of the HPAL option) slurry is neutralized with solid limestone. The process equipment was assumed to be two agitated tanks in series. At a residence time of 20 minutes/tank and a height-to-diameter ratio of 2, the required tank diameter is 4.3 m. The material of construction for the tank and the agitators was set to rubber-lined steel.

The incoming limestone was assumed to be crushed to 3 mm and then milled to 100 µm. A typical work index for limestone is 103 kW·h/t and the limestone throughput is 82 t/h for the atmospheric leach case, giving a required crusher power of 153 kW and a mill of 3.7 m diameter and 4.1 m long.

**Countercurrent decantation.** The solids are separated from the neutralized leach solution and washed in a four-stage CCD train. The Ambatovy nickel project pilot-plant data were used to calculate a thickening rate, as follows:

- The working volume of the pilot autoclave was 30 L, the feed slurry contained 30% solids, and the residence time in the autoclave was 75 minutes. That gives a solids feed rate of 7.2 kg/h.
- The thickeners in the CCD train were 30 cm in diameter. Assuming the solids rates entering the autoclave and leaving the first neutralization step to be approximately the same means that each thickener settled about 7.2 kg/h of solids, and because the cross-sectional area of each thickener was 0.071 $m^2$, the solids settling rate was about 0.1 t/h/$m^2$.
- In the exercise presented here, the solids flows through the CCD train are 375 t/h for the atmospheric leach and 351 kg/h for the HPAL case. At the assumed settling rate of 0.1 t/h/$m^2$, that gives thickener diameters of 69 m for the atmospheric leach case and 67 m for the HPAL case.

The required parameters for thickener costing are the diameter and the total volume of the thickener. Assuming a sidewall depth of 3 m and a cone angle of 10° allows calculation of the total volume in the thickener. Optional specifications selected were that the bridge is from the center to the edge of the thickener, the drive and rake are heavy duty with overload alarm, a flocculation system is included, and the whole thickener is made from rubber-lined steel. Each thickener includes an underflow pump made from stainless steel.

**Nickel precipitation.** The supernatant from the CCD train is contacted with powdered magnesium oxide to precipitate the nickel, cobalt, and copper in two agitated tanks in series. The residence time in each tank was set to 20 minutes. The material of construction was left at the default, carbon steel. At a height-to-diameter ratio of 2, the required tank diameter is 10.5 m. The MgO was assumed to be purchased, stored in a conical bottomed hopper, and metered into the precipitation tanks via a screw feeder.

The resulting slurry is filtered. A rotary drum filter was specified for costing purposes. Since no filtration test results were available, the filtration rate was set to a default representing slow filtration. The material of construction was specified as epoxy-lined steel.

**Magnesium precipitation.** The filtrate from the nickel precipitation step is contacted with slaked lime to precipitate the dissolved magnesium. For this, crushed limestone is calcined in a coal-fired kiln, and the burnt lime is held in a surge vessel before being slaked with water in an agitated tank for 10 minutes. The slaked slurry overflows into a second nonagitated tank where it is diluted with more water, and grit is settled out and removed by a screw conveyor. The diameter of the two tanks is 2.5 m, and the height-to-diameter ratio is 2. The dry lime is fed into the first tank from one of two hoppers by a rotary feeder (24 hours of storage capacity, CaO bulk density of 0.5 t/m$^3$, and volume of 777 m$^3$ per hopper). The material of construction for this equipment was left as carbon steel throughout.

The filtrate and slaked lime are contacted in two agitated tanks in series (carbon steel, residence time 30 minutes each, height-to-diameter ratio 2, tank diameter 10.8 m).

In the absence of measured information, the thickening rate of the limed slurry was assumed to be the same as the rate in the CCD train, that is, 0.1 t/h/m$^2$. That gives a thickener diameter of 40 m for that thickener in both variations of the process. The optional parameters for this thickener were set to the same as the thickeners in the CCD train, except that in this thickener the material of construction was left as carbon steel.

**Infrastructure.** For ranking alternatives, the infrastructural cost components can be ignored because these items would be common to the competing alternatives. In this exercise, the infrastructural items were included because the capital cost for a new project does not consist only of the cost of the process equipment. The software also has cost models for various items of infrastructure.

The process model for the ATL case predicts 155 m$^3$/h solids and 615 m$^3$/h water in the leach residue plus the magnesium precipitate (45% solids by mass, combined). Assuming the final consolidated tailings to contain 80% solids, the volume would be 379 m$^3$/h. Taking a rise rate of 4 m/yr gives a tailings dam area of 793,000 m$^2$, with a perimeter of 3,567 m.

The process model for the HPAL case predicts 364 m$^3$/h of consolidated tailings. At the assumed rise rate of 4 m/yr, that gives a tailings dam area of just over 764,000 m$^2$ and a perimeter of 3,497 m.

A tailings slurry pump station and a pipeline 2,000 m long and 0.4 m in diameter were assumed for both cases. The pipe material was assumed to be fiberglass-reinforced polymer (more to illustrate that there is a variety of material in the cost modeling database than for any real reason).

For both cases, the tailings dam was assumed to require a starter dyke 5 m high. The base of the tailings dam was assumed to require brush clearing and excavation to a depth of 0.5 m. The bottom of the tailings dam was assumed to be a clay liner between two geosynthetic membranes, plus a grid of piping to assist drainage. Each year, the dyke would need to be raised by at least 4 m. The cost of the starter dyke (US$0.7 million) was thus added to the fixed operating cost to cover the annual raising of the dyke around the tailings dam.

The circulating process water was assumed to circulate through a fenced pond holding 48 hours of the process water circulating to the CCD stage as wash and to the feed preparation section to slurry the incoming crushed laterite.

Makeup fresh water was assumed to come from 25 km away via a pipeline and pumping station. Cooling water, 4,767 t/h in the atmospheric leach case and 1,197 t/h in the HPAL case, mostly for condensing the residual steam from the acid plant after electricity generation, was assumed to circulate through an evaporative cooling tower.

The project was assumed to require a heavy-duty rail link 80 km long and a paved road 20 km long. The required buildings were assumed to be a plant office and a laboratory, each 200 m$^2$. A parking lot (250 m$^2$) and a security fence (3 m high, 2,000 m long) were assumed. A power line (11 kV, 20 km) and a standby generator (1,500 kVA) were also assumed.

**Cost estimates.** Tables 13 and 14 show the cost estimates generated from the two mass–energy balances and the equipment sizing described previously, using the cost modeling software.

These costs exclude the capital cost for the mine, which would be the same in both cases. The direct field cost is the cost of the process equipment and its installation, including items like an electrical substation that the software adds automatically. The equipment costs are the material and labor costs for manufacturing and installing the various items of process equipment. Process piping, instrumentation, electrical wiring, foundations, and structural steel are from the default piping allocations, electrical allowances, foundation standards, and so on, in the software. These are based on data from numerous projects. When more detailed engineering work is done, these defaults are replaced by the results of the relevant work. The indirect field costs cover home-office costs, field supervision, start-up, and commissioning. The non-field costs are for freight, taxes and permits, basic and detailed engineering, procurement, overheads, and contract fees. These are all default numbers at this stage, but defaults based on extensive real data. The contingency of 15% was set to allow for the process being new.

Interestingly, although the extrapolations from published capital cost information predict that the HPAL case would cost about twice the cost of the ATL case, the numbers in the exercise presented here indicate that the total capital expenditure for the HPAL case will be only about one-third higher than the capital cost of the ATL case. A caveat here is that the cost database does not have cost information on the specialized slurry pumps needed in the pressure leach section, and these pumps were approximated by using cost information on less specialized pumps. This probably means that the capital cost for the HPAL case is underestimated.

The total installed equipment costs calculated are US$259 million for the ATL case and US$367 million for the HPAL case, or about 90% of the total direct field cost. The remaining 10% of the direct field cost covers items like electrical substations and other hardware added by the software.

Figure 16 shows how the installed equipment costs are distributed between the various parts of the process. The leach section makes up a much greater proportion of the total in the HPAL case, with the estimated cost of the HPAL autoclaves and ancillaries being about 10 times the estimated cost of the ATL reactors. The acid plant is also bigger and therefore more expensive in the HPAL case because of the higher overall acid requirement arising from the nature of sulfuric acid at the HPAL leach temperature, that is, having only one proton per $H_2SO_4$ instead of two at the lower temperature of the ATL.

**Table 13 Capital cost estimate for the ATL case, US$**

| Account | Worker-Hours | Wage Rate, $/h | Labor Cost, $ | Material Cost, $ | Total Cost, $ |
|---|---|---|---|---|---|
| Equipment | 23,257 | 29.88 | 694,875 | 96,680,284 | 97,375,159 |
| Piping | 284,527 | 29.62 | 8,428,760 | 34,890,531 | 43,319,291 |
| Civil | 1,939,524 | 24.22 | 46,982,556 | 85,233,942 | 132,216,498 |
| Steel | 7,397 | 27.79 | 205,591 | 1,157,698 | 1,363,289 |
| Instruments | 21,634 | 30.24 | 654,107 | 6,181,606 | 6,835,712 |
| Electrical | 24,446 | 29.17 | 713,103 | 3,271,639 | 3,894,742 |
| Insulation | 70,116 | 22.57 | 1,582,808 | 1,639,548 | 3,222,355 |
| Paint | 35,490 | 22.30 | 791,586 | 653,635 | 1,445,222 |
| **Direct field costs** | **2,406,390** | | **60,053,386** | **229,708,882** | **289,762,268** |
| **Indirect field costs** | **271,091** | | | | **86,243,305** |
| **Total field costs** | **2,677,481** | | | | **376,005,573** |
| Freight | | | | | 27,565,100 |
| Taxes and permits | | | | | 9,188,401 |
| Engineering and head office | 234,866 | | | | 25,088,702 |
| Other project costs | | | | | 27,395,372 |
| Contingency | | | | | 83,729,360 |
| **Non-field costs** | **234,866** | | | | **172,886,935** |
| **Project total costs** | | | | | **548,892,508** |

Source: Dry 2013

**Table 14 Capital cost estimate for the HPAL case, US$**

| Account | Worker-Hours | Wage Rate, $/H | Labor Cost, $ | Material Cost, $ | Total Cost, $ |
|---|---|---|---|---|---|
| Equipment | 39,595 | 29.93 | 1,185,033 | 168,614,804 | 169,799,837 |
| Piping | 595,940 | 28.40 | 16,927,161 | 67,948,917 | 84,876,078 |
| Civil | 1,820,265 | 23.95 | 43,601,902 | 85,879,760 | 129,481,662 |
| Steel | 9,743 | 27.77 | 270,587 | 1,533,526 | 1,804,113 |
| Instruments | 25,527 | 30.24 | 771,942 | 11,297,602 | 12,069,544 |
| Electrical | 31,101 | 29.20 | 908,251 | 5,040,725 | 5,948,977 |
| Insulation | 114,134 | 22.57 | 2,576,385 | 2,652,741 | 5,229,126 |
| Paint | 37,033 | 22.31 | 826,080 | 671,824 | 1,497,904 |
| **Direct field costs** | **2,673,337** | | **67,067,342** | **343,639,900** | **410,707,243** |
| **Indirect field costs** | **317,312** | | | | **96,176,705** |
| **Total field costs** | **2,990,649** | | | | **506,883,948** |
| Freight | | | | | 41,237,000 |
| Taxes and permits | | | | | 13,745,601 |
| Engineering and head office | 250,055 | | | | 26,650,802 |
| Other project costs | | | | | 35,664,822 |
| Contingency | | | | | 112,352,808 |
| **Non-field costs** | **250,055** | | | | **229,651,033** |
| **Project total costs** | | | | | **736,534,981** |

Source: Dry 2013

The algorithms inside the cost modeling software predict the fixed operating costs listed in Table 15. Inserting the capital and operating cost estimates generated by the cost modeling software into the cash-flow analyses done before gives the results shown in Dry (2013).

Results are shown in Table 16 for the ATL case and in Table 17 for the HPAL case. In this case the capital cost is the total capital cost calculated for the process plant plus the capital cost for the mine (US$14 million added to the cost of the process plant).

Even though the capital cost of the HPAL option decreased from the US$1,300 million assumed initially to the US$750 million calculated from the process and cost modeling exercise, the other changes to the reagent consumption numbers and fixed operating costs emanating from the modeling keep the HPAL case a distant second to the ATL case at best. The point is that the calculations based purely on the overall stoichiometry and interpolations from the literature gave results that appear to be reliable, certainly in light of the results from the process and cost modeling work. A reasonable generalization would be that if preliminary calculations

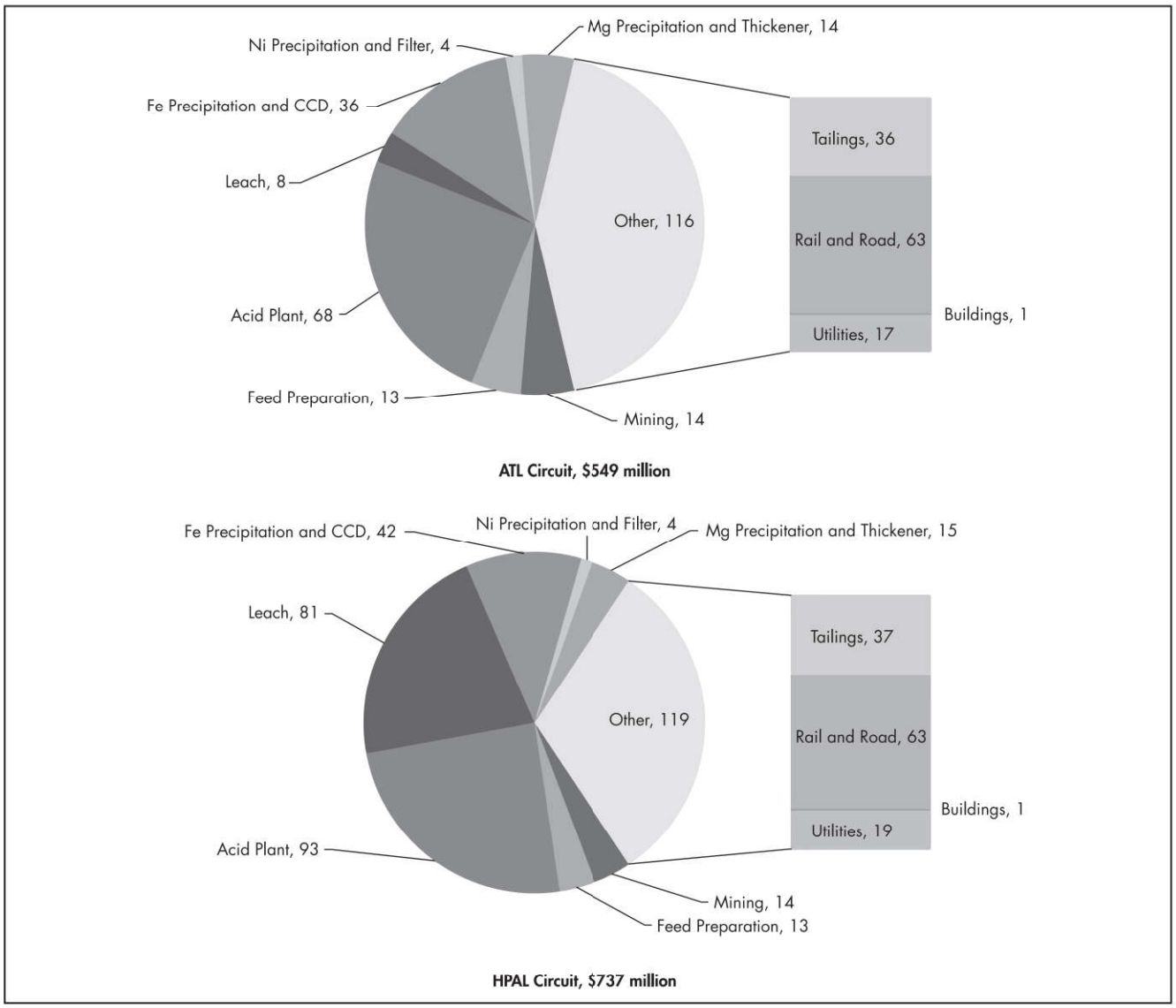


Source: Dry 2013

**Figure 16 Breakdown of the installed equipment costs**

indicate that the project is economically weak, it most probably is economically weak.

**Design changes.** After the process models and the costing models have been set up, it is quick and easy to evaluate different scenarios. For example, if the settling rates in the various thickeners are actually half or double the value assumed (i.e., 0.05 or 0.2 instead of 0.1 t/h/m$^2$) the thickener diameters would change accordingly, leading to a corresponding change in the estimated capital cost. Evaluating the impact of the thickening rate on the projected economics of the project is a simple matter of changing a few numbers in the thickener sizing calculations and the input to the cost model, rerunning the cost model, and saving the output to another spreadsheet.

To illustrate this, Figure 17 shows the impact of changing the settling rate on the installed equipment cost for the ATL case. The settling rate in the base case is 0.1 t/h/m$^2$; in the slow settling variation, it is 0.05 t/h/m$^2$; and in the fast settling variation, it is 0.2 t/h/m$^2$. The projected total capital cost changes from US$549 million in the base case to US$638 million for 0.05 t/h/m$^2$ instead of the assumed 0.1 t/h/m$^2$, and to US$504 million if the settling rate is 0.2 t/h/m$^2$. The cost of the equipment for the iron precipitation and CCD section

**Table 15 Fixed operating costs, US$ million/yr**

| Cost Item | ATL | HPAL |
|---|---|---|
| 25 operators/shift (S20/h, 4 shifts, 2,000 h/shift) | 3.5 | 4.0 |
| 2 supervisors/shift (S35/h, 4 shifts, 2,000 h/shift) | 0.6 | 0.6 |
| Maintenance cost | 3.9 | 5.8 |
| Utility cost | 9.0 | 16.1 |
| Operating charges, plant overhead, general and administrative | 9.9 | 9.9 |
| Tailings dam dike | 0.7 | 0.7 |
| Total operating cost | 26.0 | 3.7 |

Source: Dry 2013

**Table 16 Cash-flow analysis, ATL case, US$ million**

| Year | 1 | 2 | 3 | 4 | 5 | 6 | 7–22 |
|---|---|---|---|---|---|---|---|
| Revenue | — | — | 267 | 535 | 535 | 535 | 535 |
| Costs | 281 | 281 | 150 | 273 | 273 | 273 | 273 |
| Margin | –281 | –281 | 117 | 262 | 262 | 262 | 262 |
| Tax | 0 | 0 | 0 | 0 | 0 | 0 | 0 |
| Profit | –281 | –281 | 117 | 262 | 262 | 246 | 210 |
| Before-tax internal rate of return | | | 34% | | | | |
| After-tax internal rate of return | | | 32% | | | | |
| Capital cost estimate, $ million | | | 563 | | | | |
| Net present value at 10% discount rate, $ million | | | 808 | | | | |

Source: Dry 2013

**Table 17 Cash-flow analysis, HPAL case, US$ million**

| Year | 1 | 2 | 3 | 4 to 8 | 9 | 10 | 11–22 |
|---|---|---|---|---|---|---|---|
| Revenue | — | — | 266 | 533 | 533 | 533 | 533 |
| Costs | 375 | 375 | 212 | 387 | 387 | 387 | 387 |
| Margin | –375 | –375 | 54 | 146 | 146 | 146 | 146 |
| Tax | 0 | 0 | 0 | 0 | 7 | 29 | 29 |
| Profit | –375 | –375 | 54 | 146 | 139 | 117 | 117 |
| Before-tax internal rate of return | | | –5% | | | | |
| After-tax internal rate of return | | | –5% | | | | |
| Capital cost estimate, $ million | | | 750 | | | | |
| Net present value at 10% discount rate, $ million | | | –452 | | | | |

Source: Dry 2013

changes from US$35 million in the base case to US$61 million in the slow-settling variation and to US$23 million in the fast-settling variation. Settling rates in thickening steps are not always measured in preliminary experimental work, but given their potential impact on the capital costs, they should be. The point of this illustration is not that the settling rate is or is not any particular value; the point is that the settling rates in the various thickeners have an appreciable impact on the overall capital cost. Therefore, settling rates should be measured at as early a stage of the experimental work as can be arranged, even knowing that later work may well generate improved or more accurate settling rates. In this illustration, doubling the settling rate has a substantially smaller impact on the calculated capital cost than halving this number, which means that early-stage experimental work would be more focused on finding out whether the various slurries settle "normally."

If early work uncovers especially slow settling, appropriate work can be planned to improve the settling rate, confirm that it is slow enough to make the circuit of which it is a part unviable, or to find a better solid–liquid separation technique for the project in question. If reasonably fast settling rates are found early on, there would be little rational incentive for extensive experimental work aimed at further improving the settling rate, as the impact of further improvements on the capital cost of that project would be small.

**Capacity changes.** A question that commonly arises when processes are under evaluation is what effect the throughput has on the economics. If the changes in throughput are not excessively large, the fixed operating cost is, at least to a first approximation, unaffected and the variable cost is directly proportional to the throughput. That leaves the capital cost, which is traditionally scaled using the "0.6 rule"; that is, the baseline capital cost is multiplied by the ratio of the new throughput to the baseline, to the power 0.6. The cost modeling software used for the exercise presented in this chapter contains a feature that enables the effect of throughput on the capital cost to be evaluated more rigorously. As the capital cost is based on equipment sizing results that come from a numerically rigorous mass–energy balance, and that balance can be scaled linearly, the cost modeling software can easily recalculate the capital cost for throughputs other than the baseline by resizing the various items of process equipment, support structures, foundations, and so on, and recalculating the capital cost from the various quantities of material and labor so recalculated. If any item of process equipment, when resized, falls outside the range covered by the capital cost database, the software warns the user and then the user would specify duplicate items or make whatever other design change is required.

Figure 18 shows the results obtained by using the 0.6 rule and using the cost modeling software to calculate the capital cost of the ATL case, from half to double the baseline capacity of 30 kt/yr of nickel in the mixed hydroxide product. In this exercise, the mine cost was left unchanged.

The 0.6 rule gave rather good results for this exercise, compared to the more rigorous calculation from the cost modeling software (APEA; Aspentech 2018). The 0.6 rule does seem to underestimate slightly for scaling down, but the difference is unlikely to be significant at the preliminary stage of evaluation assumed for the exercise presented here.

By way of calibration of the process and cost modeling illustrated in this example, a press release in 2009 reports a

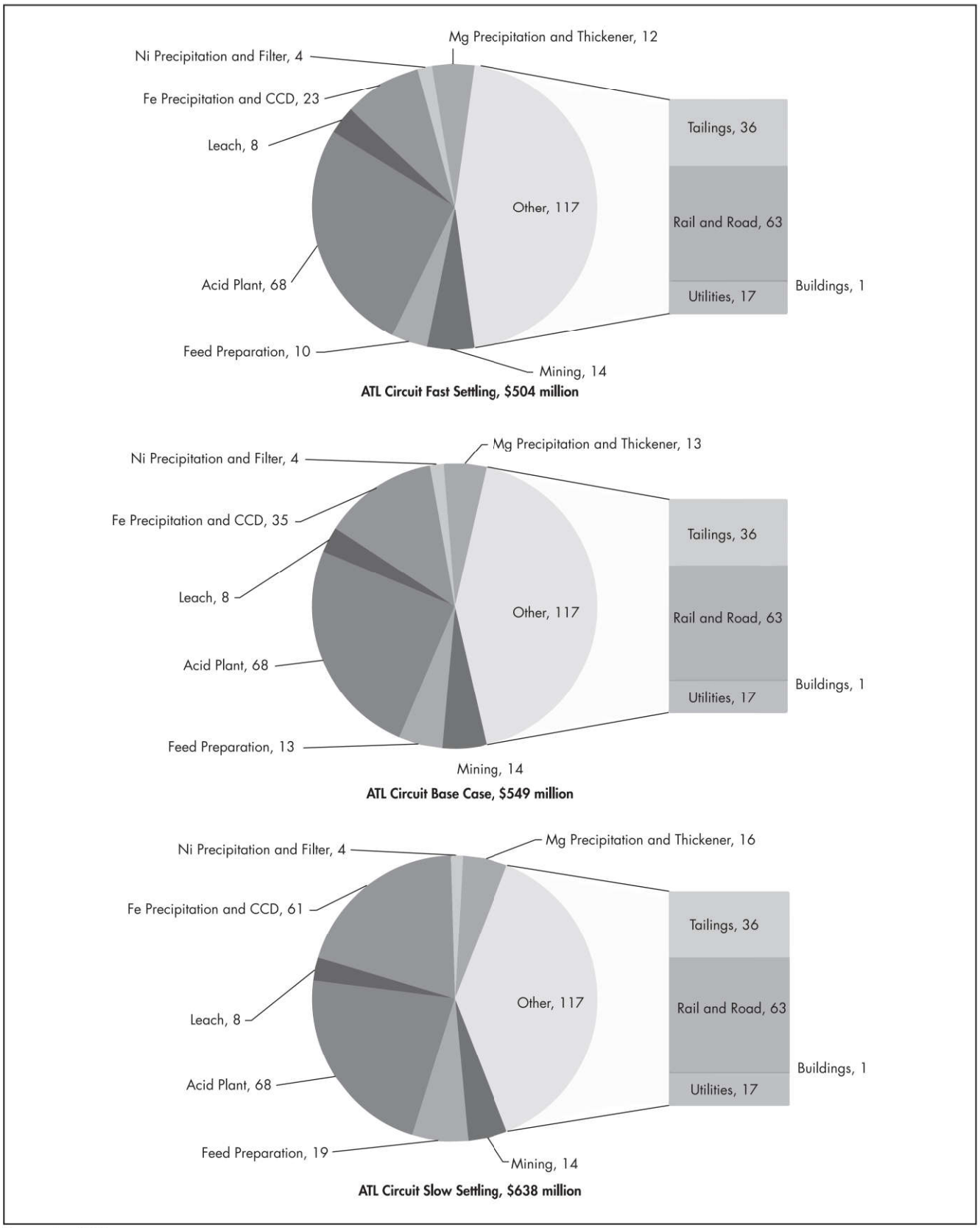


Source: Dry 2013

**Figure 17 Effect of settling rate, ATL case**

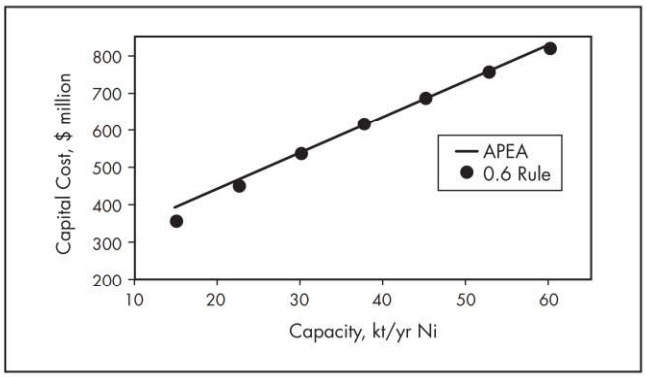


Source: Dry 2013
**Figure 18 Effect of capacity on capital cost, ATL case**

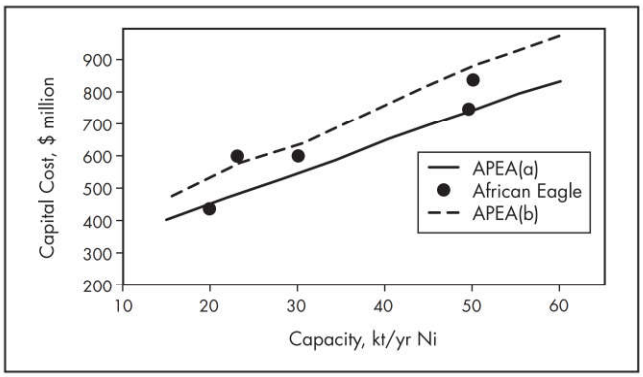


Source: Dry 2013
**Figure 19 Calculated and published capital costs**

capital cost estimate of US$435 million for Black Down Resources' Dutwa nickel project (Tanzania) (Dutwa Project 2018), at an annual throughput of 2 million t/yr of ore. Another press release from African Eagle, released in December 2010, gives a capital cost estimate of US$600 million for a production rate of 23 kt/yr of nickel. A third release gives capital costs of US$600 million and US$840 million for facilities producing 30 kt/yr and 50 kt/yr, respectively, of nickel in a mixed hydroxide precipitate.

In Figure 19, the symbols plot the capital costs published for the Dutwa nickel project (Dutwa Project 2018), and the lines are the capital costs calculated using the cost modeling software over the capacity range shown. The solid line is the capital cost calculated using the assumption that the settling rate in the various thickeners is 0.1 t/h/m$^2$, and the dashed line is the capital cost calculated assuming that the settling rate is 0.05 t/h/m$^2$.

The settling rate of 0.1 t/h/m$^2$ was inferred from HPAL pilot-plant data. In the HPAL, much of the iron is precipitated in the autoclave as hematite, which tends to have better settling properties than the goethite that is precipitated under the conditions found in the ATL circuit. Therefore, it would not be implausible to assume that the settling rate in the ATL circuit could be lower than the rate that would be expected in the HPAL circuit. If the settling rate is actually 0.05 t/h/m$^2$, the capital costs calculated in the exercise presented in this chapter pass through the numbers published by African Eagle, which, having been generated by process engineering companies, are most probably based on much more engineering design work than was used in the cost modeling exercise presented in this chapter.

Even without adjusting the settling rate, the capital cost numbers calculated using the capital cost modeling software are within 20% of the corresponding published numbers, except for one published number that is out of line with the others and about 26% off the corresponding number from the cost modeling software. That is well within the uncertainty generally associated with initial capital cost estimates.

The objective of the exercise presented in this example is not to show whether the Dutwa nickel project has business muscle. This project was chosen for mimicking because there is enough information published about it to enable sensible comparison between the calculated capital costs and corresponding published numbers that were generated more traditionally.

### *Conclusions in Hydrometallurgical Process Modeling*

The hydrometallurgical modeling example presented assumes that the quantity of ore is sufficient to sustain a viable rate of production over a useful project life. In the case of a new deposit, the calculation of reserves would entail fieldwork and consume substantial amounts of effort, time, and money. Doing calculations such as in the examples presented here, based on very preliminary experimental work, yields valuable information relevant to business decisions on whether to undertake the expense of proving up any particular deposit. If the process is not sufficiently strong economically, the size of the deposit is irrelevant and money spent proving the deposit is money wasted.

An important consideration in the example presented is what happens in the leach. The extraction of metals from ores necessarily involves minerals that are complex substances. The first experimental work necessary in developing any hydrometallurgical circuit is leaching tests. After information on the leaching behavior of the feed is available, either from appropriate experimental work or as knowledge from a suitable similar process, the modeling calculations become meaningful.

New projects can be sensibly evaluated early in the development cycle, as soon as enough is known about the ore to enable preliminary estimates of its overall composition and its leaching behavior. Preliminary calculations based on the overall stoichiometry and information in the open literature can inexpensively generate useful evaluations of whatever process options are under consideration. When the preliminary calculations and process modeling indicate a process option to be potentially viable, process and cost modeling can be used to predict rational capital and operating costs from limited hard data, and these numbers can be used to confidently rank process options and justify work or the termination of work on any given project much earlier in the development cycle than would be possible without these tools.

No skilled person would knowingly spend time, effort, and money on a doomed project, but all too often the realization that the project is doomed comes after the expenditure of considerable amounts of time, effort, and money. Since process modeling and cost estimation are inevitable steps in the development of a project, it would be wise to not commit to extensive experimental and engineering design work before doing the process and cost modeling that will be needed anyway to evaluate its economics. It is far better to use preliminary experimental results for setting up the process and cost

models and then use the models to evaluate the project and, assuming that the models predict sufficiently strong economics, use the models to guide the experimental work, feed the data back into the models, and so on.

In the case of viable projects, judicious use of process modeling can make the whole project development cycle much more cost- and time-effective, especially for dispassionately ranking process options and determining the best program of experimental work. Identifying and testing the parameters that most strongly affect the process economics is also possible using these tools, again leading to better results and less wasted effort.

## Applications of Process Modeling in Pyrometallurgy

Process modeling and simulation of pyrometallurgical processes require an in-depth understanding of high-temperature treatment of materials. Typical extractive operations in this category are calcining, roasting, smelting, and refining. In each case, physical and chemical transformations are brought about in materials at elevated temperatures.

Pyrometallurgy is extensively used in iron and steel production, refining precious metals, and extraction of base metals. About 90% of world copper output is produced pyrometallurgically from sulfide-based minerals, and in many cases from high-arsenic feedstock. Although some pyrometallurgical processes are relatively straightforward, others involve extremely complex reactions between multiple phases (gases, solids, and liquid slag and metal) that can lead to the release of large quantities of acidic, metallic, and other toxic compounds. In addition, the development and study of pyrometallurgical operations require very expensive piloting and laboratory test work. These factors, together with the need to evaluate pyrometallurgical processes thoroughly as part of their development, increase the importance and value of computer modeling and simulation. This section outlines modeling and simulation of pyrometallurgy and covers its application to the study of extraction of metals and the processing of other materials.

*Calcining* takes place in absence of air or oxygen to bring about thermal decomposition, a change of phase, or removal of a volatile fraction. The calcining process normally takes place at temperatures above the thermal decomposition temperature but below the melting point of the product materials. The *decomposition temperature* is usually defined as the temperature at which the standard Gibbs free energy for a reaction is equal to zero. For example, in limestone calcination (a decomposition process), the chemical reaction is

$$CaCO_3 \rightarrow CaO + CO_2(g) \quad \textbf{(EQ 10)}$$

The standard Gibbs free energy of limestone calcination reaction is approximated as $\Delta G°r = 177{,}100 - 158\ T$ (J/mol) (Mackinnon et al. 2003). The standard free energy of reaction is zero in this case when the temperature, T, is equal to 1,121 K, or 848°C, the temperature for decomposition of calcium carbonate.

*Roasting* involves more complex gas–solid reactions with carbonates and sulfides at elevated temperatures, with the aim of purifying the metal and eliminating unwanted carbon and sulfur, leaving behind a metal oxide that can be directly reduced. Roasting can be initiated by burning a fuel with the ore. This raises the temperature of the ore to the point where its sulfur content becomes the fuel. Roasting then continues autogenously, with no need for an external fuel source.

Before roasting, the metal concentrate is mixed with other materials to facilitate the process. Typical roasting thermal gas–solid reactions include oxidation, reduction, chlorination, sulfation, and pyrohydrolysis (Vahed 2004). In roasting, the ore or concentrate is treated with hot air. The sulfide is converted to an oxide, and sulfur is released in gaseous form. For example, roasting of chalcocite and sphalerite ores ($Cu_2S$ and ZnS) can be represented as

$$2Cu_2S + 3O_2 \rightarrow 2Cu_2O + 2SO_2 \quad \textbf{(EQ 11)}$$

$$2ZnS + 3O_2 \rightarrow 2ZnO + 2SO_2 \quad \textbf{(EQ 12)}$$

The gaseous product, sulfur dioxide ($SO_2$), is often used to produce sulfuric acid. Many sulfide minerals contain other components, such as arsenic, that are released into the environment if there were no abatement measures.

*Smelting* is a form of pyrometallurgy for extraction of metal from its ore. It includes production of silver, iron, copper, and other metals. Smelting uses heat and a chemical reducing agent to decompose the ore, driving off unwanted elements as gases or slag, and leaving just the metal behind. The reducing agent is commonly a source of carbon, such as coke. The carbon or carbon monoxide produced during this process removes oxygen from the ore, leaving behind elemental metal. The carbon is usually oxidized in stages, producing first carbon monoxide and then carbon dioxide. As most ores are impure, it is often necessary to use flux, such as limestone, to remove the accompanying rock gangue as slag. Plants for the electrolytic reduction of aluminum are also generally referred to as smelters.

*Refining* is the step that follows smelting, with the purpose of purifying the metal. For example, the discharge stream from the copper converter contains a significant amount of dissolved oxygen and copper oxide. The oxygen is removed by adding a hydrocarbon as a reducing agent:

$$4CuO + CH_4 \rightarrow 4Cu + CO_2 + 2H_2O \quad \textbf{(EQ 13)}$$

### *Pyrometallurgy Modeling Regimes*

Types of pyrometallurgical process simulation can be categorized as follows:

1. Steady-state simulation based on known process reactions and equilibrium
2. Steady-state simulation with predictive modeling where chemical reactions and pathways are not clearly understood
3. Dynamic simulation based on known pyrometallurgical reactions and kinetics, to determine effects of process variables with time
4. Dynamic simulation where nature of chemical reactions and kinetics are not clearly known and must be predicted from thermochemical properties of the reactants

**Steady-state modeling in pyrometallurgy.** The simplest approach to modeling pyrometallurgical processes is when the process is clearly defined and the chemical reaction pathways and kinetics are well known. When Gibbs free energy is minimized, it means that a system has reached equilibrium at constant pressure and temperature. Therefore, it is a convenient indicator of the spontaneity of processes to proceed. For example, roasting of base metals such as zinc, iron, lead, and copper to their respective oxides is most effectively carried out in the temperature range 600°–700°C, because

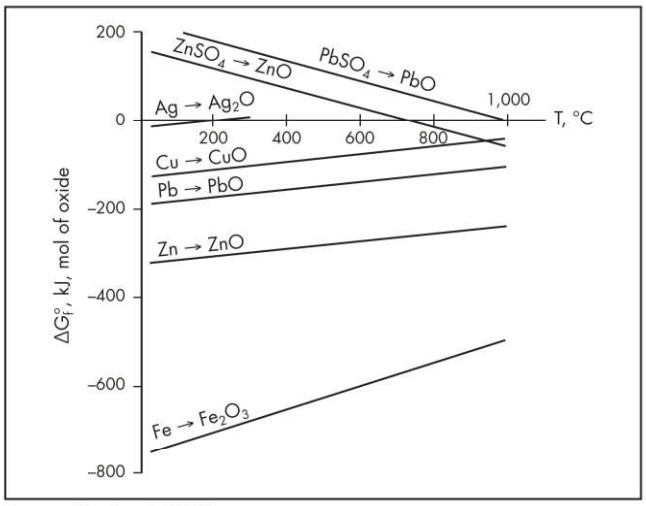


Source: Nicol et al. 1987

**Figure 20 Free energy of formation of metal oxides from elements and by decomposition of sulfates: $\rho SO_2$ = 0.001 atm**

the values of free energy of formation of metal oxides are negative at this range, enabling metal oxides to form. Hence, the temperature range for the process is predetermined and no predictive simulation is needed to identify the outcome. Figure 20 shows values of free energy of formation for metal oxides associated with refinery gold materials as a function of temperature for partial pressure of sulfur dioxide gas, $\rho SO_2$ = 0.001 atm (Nicol et al. 1987).

In similar fashion to hydrometallurgy, understanding of chemistry in pyrometallurgy is the first step, and the similar use of simulation packages could be beneficial in clarifying the chemical equilibrium associated with the process concept. Furthermore, in pyrometallurgy, performing test work and obtaining information from operating plants that are used to develop the conceptual process is costlier and challenging. Based on the same reasoning as in hydrometallurgy, process modeling can be used to perform chemical and equilibrium calculations for the aforementioned systems at elevated temperatures.

In similar fashion as use of Pourbaix diagrams (Gilchrist 1989) in hydrometallurgy, the standard Gibbs free energy for formation of a product in pyrometallurgy can be used to determine the chemical equilibrium for the reactions involved. The Ellingham diagram as shown in Figure 21 (Ellingham 1944) is a plot of the standard free energy of metal oxidation reactions as a function of temperature, and it determines the equilibrium composition of a pyrometallurgical process. These plots are useful in understanding the conditions under which extraction of metals is possible by pyrometallurgical process reactions of a gaseous phase (the oxidizing gas) with a pure solid or liquid phase (the metal and oxidized compounds). The Ellingham diagram also allows calculation of the equilibrium composition of the system and is useful in other ways: it can be an indicator of process conditions for reduction of a metallic oxide to pure metal, as well as partial pressure of oxygen that is in equilibrium with a metal at a set temperature. Also, the position of the line for a given reaction on the Ellingham diagram shows the stability of the metal oxide as a function of temperature. Reactions closer to the top of the diagram are for the most inert metals (e.g., gold and platinum), and their oxides are unstable and easily reduced. Toward the bottom of the diagram, metals become progressively more reactive and their oxides become harder to reduce.

Fundamentals of heat and mass balances in extractive metallurgy, described earlier in this chapter, also apply to pyrometallurgy. Many examples of steady-state modeling in pyrometallurgy include determination of energy balance based on known process design criteria, such as fraction of heat input lost to the surroundings. The following example is a heat and mass balance analysis for zinc roasting, based on previously determined conversion rates that determined 90% of total iron charged converted to $ZnO{\cdot}Fe_2O_3$. The goal of the steady-state calculation here could be to verify the furnace bed temperature at, for example, 10% heat lost to the environment. Table 18 shows the basis of this exercise.

Using quantities of each component for input and output streams, the associated sensible heat, and the heat of reaction, total heat liberated is calculated. This heat, minus the heat lost to the environment, is assumed to be available to raise the products' temperature in the furnace, and the temperature attained by the products is calculated. This simple steady-state modeling can be performed by any software program that can tally the chemical and physical changes and produce results with a steady-state heat and mass balance. For example, simple Microsoft Excel spreadsheets can be developed for a specific flow sheet such as a copper roaster. A review of kinetics of copper roasting processes for removal of impurities (Haque et al. 2012) also shows that when adequate kinetic data are available, impurity conversion levels obtained from test work can be used directly in steady-state models. In a 1997 study by Fan, conversion levels of arsenic as a function of time and roasting temperature were determined for arsenic-bearing copper concentrate in a fixed bed. Converted fractions of arsenic as a function of roasting time are shown in Figure 22 (Fan 1997). Similar test work can form the basis of arsenic conversions in roasting and afterburner sections of a pyrometallurgical plant. In addition to spreadsheets, simulation software programs such as METSIM, SysCAD, USIM PAC, and IDEAS are extensively used to provide a more user-friendly and understandable interface that provides access to previously identified component thermochemical and physical properties.

Here, as part of the steady-state model of the pyrometallurgical process, the intention can be to achieve an arsenic reduction target by partial roasting, and pilot tests can be conducted using high-arsenic concentrate to determine arsenic reductions in the roaster and the afterburner. The expected arsenic content in treated concentrate for commercial roasting is modeled based on this result. The heat and mass balance for the roaster package is based on typical design criteria for the roaster balance produced in a spreadsheet, as shown in Table 19.

Although its use is not prevalent, METSIM software can be used in pyrometallurgical process modeling in place of simple steady-state spreadsheets. Its advantage is that its array of unit operations includes several types of dryers, furnaces, and fluid bed reactors that can be modeled (Haque et al. 2012). The user provides details of these unit operations including number of stages, dimensions, area of heat transfer, bed area, feed solid characteristics, and flow rate. Heat input and losses can be provided to simulate heat transfer operation. Heat input or loss can be specified as a fraction of the local heat input to the unit operation. Heat generation as the result of

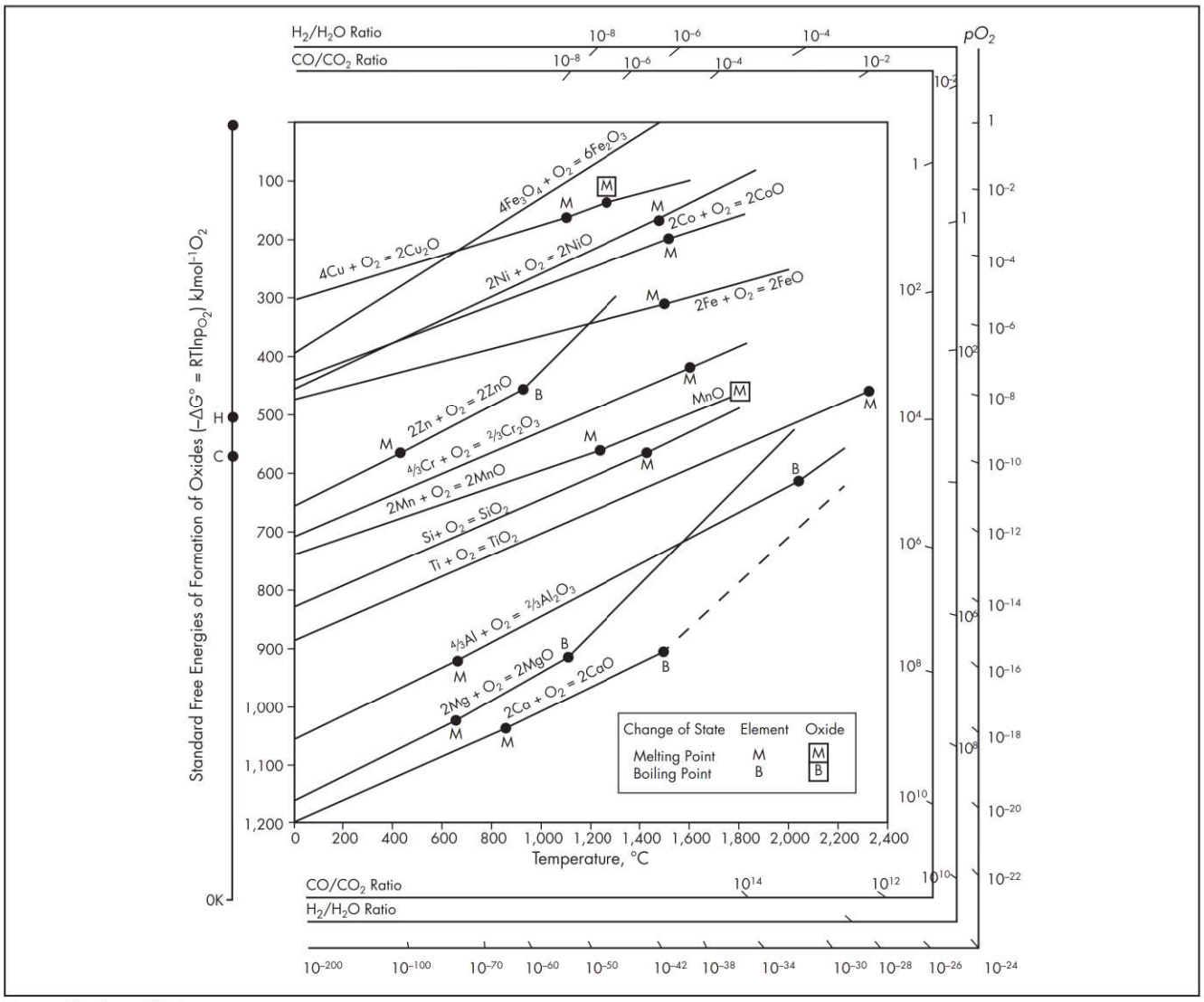


Source: Ellingham 1944

**Figure 21 Ellingham diagram**

**Table 18 Typical zinc concentrate roasting model design criteria**

| | Zinc Concentrate Roasting Design Criteria | | | | |
|---|---|---|---|---|---|
| Feed components | ZnS | FeS | PbS | $SiO_2$ | $H_2O$ |
| Weight % | 75 | 18 | 3 | 3 | 1 |
| Roaster reactions | $ZnS + 1½O_2 = ZnO + SO_2$ (99%); ($-\Delta H^o$ = 105,950 kcal/kg mol ZnO) | | | | |
| | $2FeS + 3½O_2 = Fe_2O_3 + 2SO_2$; ($-\Delta H^o$ = 292,600 kcal/kg mol $Fe_2O_3$) | | | | |
| | $PbS + 2O_2 = PbSO_4$; ($-\Delta H^o$ = 197,000 kcal/kg mol $PbSO_4$) | | | | |
| | $ZnO + Fe_2O_3 = ZnO{\cdot}Fe_2O_3$; ($-\Delta H^o$ = 4,750 kcal/kg mol $ZnO{\cdot}Fe_2O_3$) | | | | |
| | (Test work shows that 90% of total iron is tied up with ZnO.) | | | | |
| Heat losses | 10% of heat input is lost to the surroundings. | | | | |
| Feed rate | Material basis is 1,000 kg Zn concentrate feed | | | | |

Source: Dry 2013

pyrometallurgical rections is determined by METSIM, based on assumed conversion rates and thermochemical properties. This level of modeling can also be produced using IDEAS modeling software with capabilities over a range of industries. It can start with a simple steady-state model and end with predictive and dynamic modeling of the pyrometallurgical operation (Nikkhah and Anderson 2001).

**Predictive steady-state modeling for pyrometallurgical operations.** Before including enough detail about kinetics of pyrometallurgical reactions to observe the dynamic effect

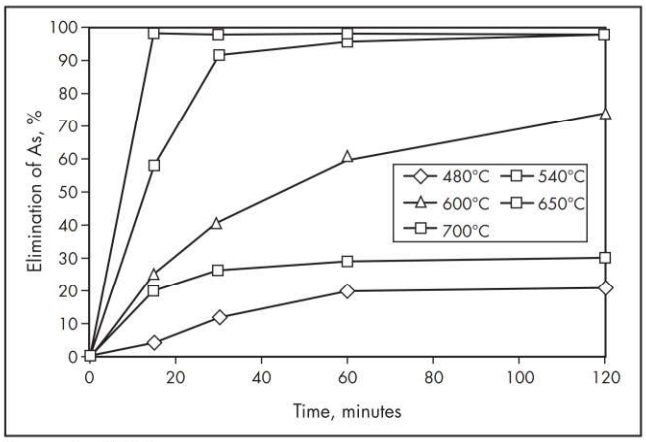


Source: Fan 1997

**Figure 22 Arsenic removal as a function of time and temperature during roasting of arsenic-bearing copper concentrate in a fixed bed**

**Table 19 Typical process design criteria for steady-state pyrometallurgical computer modeling (arsenic removal from copper concentrate)**

| Design Criteria | Roaster | Afterburner |
|---|---|---|
| Roasting temperature, °C | 670 | 250 |
| Air to concentrate mass flow rate ratio | 38.7/100 | 26/100 |
| Sulfur conversion, % | 95 | 95 |
| AsS oxidization, % | 5 | 5 |
| Arsenic fraction volatilized, % | 90 | 100 |
| Sulfur fraction volatilized, % | 20 | 100 |

Source: Dry 2013

of changes in process parameters such as feed type and flow rate, computer modeling can be used to predict the steady-state operation of a pyrometallurgical operation. Mintek's Pyrosim (Jones 1987) is an early example. Pyrosim software relied on the complete input of process conditions such as temperature, pressure, and heat losses, as well as knowledge of the process to be operated under isothermal or adiabatic conditions. Appropriate thermochemical attributes, such as enthalpy and entropy of formation and the heat capacity of minerals, were used to calculate the enthalpy of each component. Total enthalpy of each stream was then determined as the sum of the enthalpies of all components in each stream.

Pyrometallurgical operations take place at highly elevated temperatures. At these temperatures, reaching equilibrium is not prevented by kinetic limitations, and a general method for predicting composition at the process temperature is required. This is performed by minimizing the Gibbs free energy of the system, which is the fundamental description of chemical equilibrium, based on the fact that at a specified temperature and pressure, the most stable products are those associated with the lowest free energy. The Gibbs free energy of the system is defined as follows:

$$G = \sum_i \sum_p n_i^p \mu_i^p \quad \textbf{(EQ 14)}$$

where

$n_i^p$ = number of component i moles in phase p
$\mu_i^p$ = chemical potential of species i in phase p

Chemical potential is given by

$$\mu_i^p = \mu_i^0 + RT \ln a_i^p \quad \textbf{(EQ 15)}$$

where

$\mu_i^0$ = reference chemical potential for species i
$a_i^p$ = activity of species i in phase p

Assuming that $\mu_i 0 = 0$ for all elements in their standard states

$$\mu_i^0 = \Delta G_{fi}^\circ \quad \textbf{(EQ 16)}$$

where $\Delta G_{fi}^\circ$ is the Gibbs free energy of formation of species i at the process temperature.

**Dynamic modeling for pyrometallurgical operations.** Using the aforementioned principle of minimizing Gibbs free energy, IDEAS was used to develop a dynamic model of a Kivcet lead smelter (McGarry and Watson 1998) to assist in staging the ABB control system and in operator training. The Kivcet model began with existing IDEAS furnace and boiler modules, modified to suit the process requirement. Adding Gibbs free energy was a fundamental improvement to the furnace software module, along with the solution of more than 50 stoichiometric, equilibrium, and phase equilibria equations that accurately characterized the process. Results of the dynamic model were shown to be within 3% of values predicted by pilot-plant research and test work. This gave the furnace operators confidence in the proposed changes to the process control strategy. The dynamic model was successfully used as a testing platform for modifications to the smelter process control system.

IDEAS process simulation capabilities have been used for the entire pyrometallurgical plant: from initial design concept to start-up and process control verification and training of operators (Rajoria et al. 2014). IDEAS can extend from steady-state models that provide heat and mass balance to dynamic models that simulate material and energy flows over time (Nikkhah and Anderson 2001).

The goal of a process simulation model is to accurately represent real equipment operations. The better it does this, the higher its fidelity is said to be. IDEAS is a high-fidelity software, with accurate descriptions of material, chemical, and energy changes in pyrometallurgical processes.

The graphical nature of the IDEAS platform allows the user to construct a dynamic model by retrieving icon-based objects from various libraries and assembling them on a drawing-like worksheet. The user can develop a model by creating an intelligent process and instrumentation diagram of the process. Individual equipment characteristics are provided by filling in the process information for each object. Every time an object (unit operation) is retrieved from a library and placed onto a worksheet, a computer simulation of that unit is created. Each instance of the same object is identical in terms of the code (programming) executed when the model is used.

The objects can be connected in numerous plug-and-play combinations to create complex models. After the desired flow sheet is created, the necessary information is entered into input sheets (dialog boxes) and the simulation is started. Flows in different sections of the model at different temperatures and pressures throughout the model are solved and compiled in the output dialog boxes. These outputs are also used in the model's virtual plant and transmitters, controllers, and plotters. The IDEAS steady-state program structure can evolve

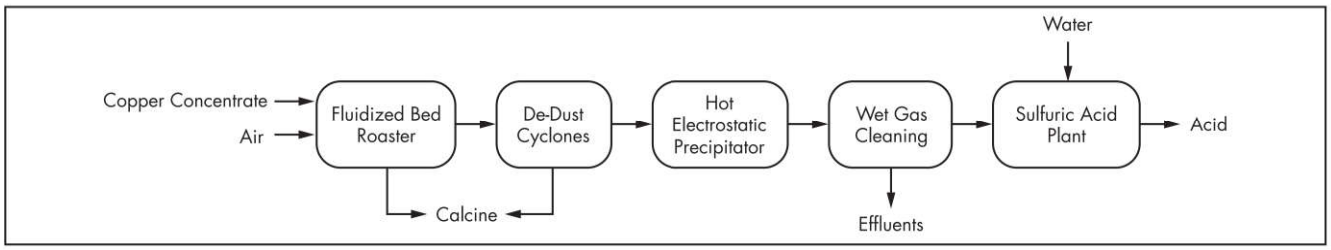


Source: Rajoria et al. 2014

**Figure 23 Simple block diagram of a high-arsenic copper concentrate roasting plant**

into a dynamic simulation that is highly accurate and can be used by the process engineering design team.

IDEAS' pyrometallurgy unit operations include a catalytic converter, drying tower, feed bin, packed-bed tower, post-combustion (afterburner), quench tower, radial flow scrubber, roaster, and the thermo analyzer ChemApp. ChemApp is a stand-alone thermochemistry programming software that has an extensive set of subroutines based on the thermodynamic phase equilibrium calculation module of FactSage (Bale et al. 2002). FactSage is used on a Microsoft Windows platform and as a dynamic link library. FactSage consists of a series of information, database, and calculation modules that enable utilization of databases for pure substances and mixtures of compounds. It can be used to perform a wide variety of thermochemical calculations and to generate tables, graphs, and figures of interest for pyrometallurgical processes. It allows the calculation of complex, multicomponent, multiphase chemical equilibria and their associated energy balances (Bale et al. 2002).

For pyrometallurgical process modeling, IDEAS software generally takes one of two approaches. When pyrometallurgical reactions are clear and well-defined, the standard IDEAS reactor object (either steady-state or dynamic) is used to calculate heat and mass balance based on first principles as described earlier in this chapter. Where pyrometallurgical reaction paths are unclear, ChemApp is used offline to calculate reaction paths and kinetics, which are then input to the IDEAS model. The latter approach was used to predict fluidized bed roasting of copper concentrates with high arsenic content (Rajoria et al. 2014).

### *Case Study: Application of Dynamic Modeling for Roasting of High-Arsenic Copper Concentrates*

A dynamic process model was used to predict the fluidized bed roasting of copper concentrates with high arsenic content, to show its benefits and to outline the steps required (Rajoria et al. 2014). Figure 23 shows a simple outline of this process. The model was used to eliminate arsenic from copper concentrate before smelting, and it included a fluidized bed roaster for conversion of copper sulfide concentrate to copper oxide and $SO_2$, along with the volatilization of arsenic and other impurities. The desulfurized product from the roaster was cooled and used as smelter feedstock to recover the metal. Off-gas from the roaster, containing sulfur dioxide, dust, and volatilized impurities, was de-dusted in cyclones, cooled, and then further de-dusted in a hot-gas electrostatic precipitator (ESP). Wet gas cleaning was used to humidify the de-dusted gas and scrub it in a radial-flow venturi. Arsenic was mostly captured in the scrubbing liquor, which was sent to effluent treatment. Residual impurities in the gas were removed in wet ESPs. $SO_2$ was converted to $SO_3$, and the $SO_3$ was absorbed in acid to produce sulfuric acid ($H_2SO_4$). Dust from the roaster hot-gas cleaning was cooled and stored for further processing.

The steps in constructing an IDEAS computer simulation model in this case were as follows:

1. Pyrometallurgical process mechanism determination
2. Thermodynamic analysis
3. Process model development

The roaster feed consisted of enargite ($Cu_3AsS_4$), pyrite ($FeS_2$), and covelite (CuS). The chemistry of decomposition of this type of roaster feed has been outlined in detail (Fan 1997; Rajoria et al. 2014) and is summarized in Table 20 (Jones 1987).

Based on earlier work by Devia et al. (2012), roasting reactions for any component, $X$, can be described as the product of a temperature-dependent kinetic constant, $k$, and a temperature-independent concentrate component concentration function in the following form:

$$\frac{dx}{dt} = -kf(X) \quad \textbf{(EQ 17)}$$

This approach essentially implies that the roasting reactions described in Table 20 follow first-order kinetics (Devia et al. 2012). The temperature dependency of $k$ is expressed by the well-known Arrhenius equation (Arrhenius 1889):

$$k = Ae^{-Ea/RT} \quad \textbf{(EQ 18)}$$

where

$A$ = Arrhenius constant
$Ea$ = activation energy
$R$ = gas constant
$T$ = absolute temperature

In addition to the heats of reaction for the roasting reactions obtained from ChemApp (ChemApp 2018; Bale et al. 2002), test results obtained by Devia et al. (2012) were necessary to determine the kinetic parameters needed in the process model. Rates of arsenic removal by roasting (Fan 1997) indicated that maximum arsenic volatilization takes place at 700°C.

Mass and energy balances were performed based on the roasting mechanism derived from thermodynamic data of species. The reaction rate data, obtained from pilot-plant studies (Devia et al. 2012), were used together with the reaction mechanisms to model the fluidized bed reactor using IDEAS, as shown in Figure 24. Roasting reactions shown in Table 20, and their kinetic parameters taken from pilot-plant studies at the University of Concepcion in Chile (Fan 1997), were used to model the roaster. The process model includes the

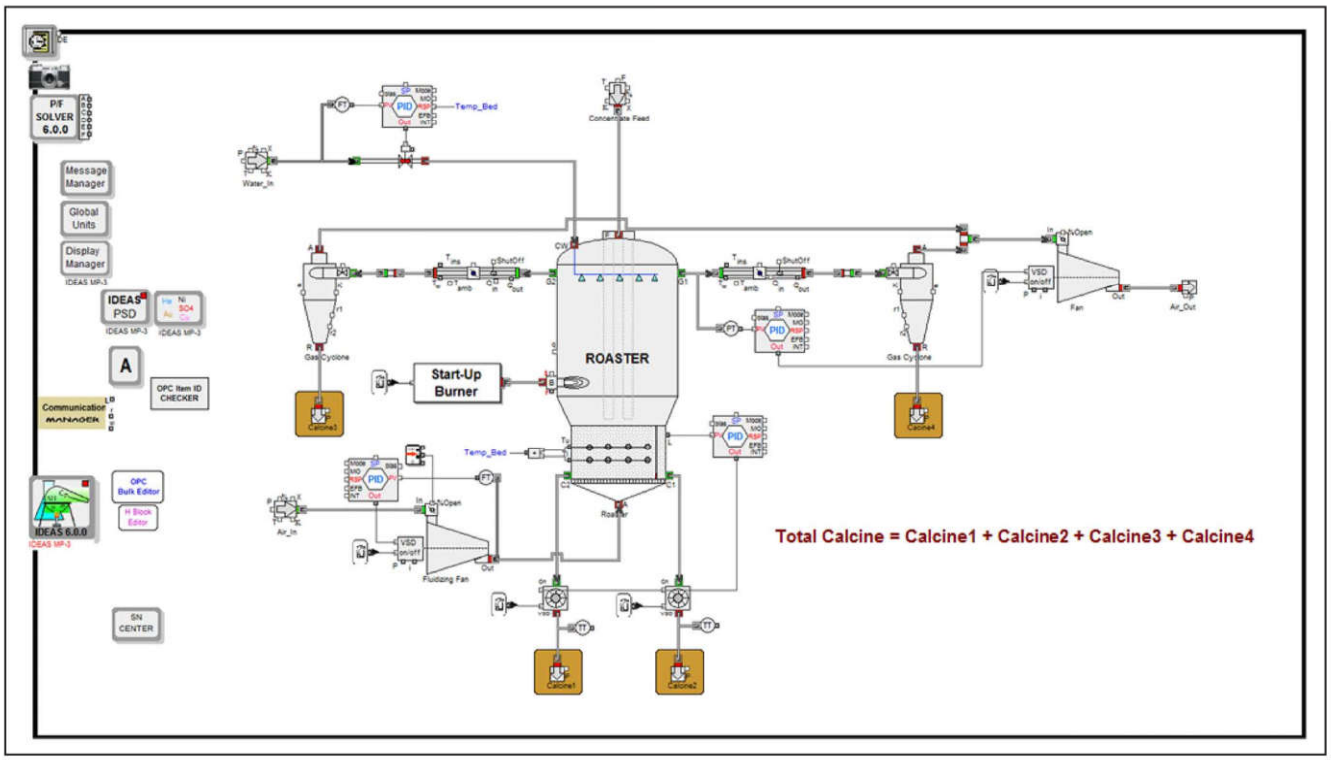


Source: Rajoria et al. 2014

**Figure 24 Outline of the IDEAS process model of a fluidized bed roaster**

roaster and the auxiliary units for collection of formed calcine. Concentrate is fed from top of the roaster. A start-up burner preheats the initial sand bed of the roaster. Bed temperature is controlled by water sprinklers. Discharged gases are then passed through cyclones to collect the entrained calcine. Pressure inside the roaster is controlled by a fan placed after the gas cyclones. Calcine is collected with the rotary feeders placed at the bottom of the roaster. The speed of these feeders is controlled by the level of the fluidized bed. This dynamic model was then used to investigate the case study outlined in this section.

Based on the pilot-plant study, the composition of the roaster concentrate feed, conditions and feed rates were used in the simulation model as outlined in Table 21 (Rajoria et al. 2014).

Typically, in a dynamic simulation of a pyrometallurgical process, effects of parameters such as feed rate, airflow rate, cooling water rate, and feed composition are of interest. In this case study, behavior of a copper concentrate roaster was simulated with the intention of investigating these parameters (Rajoria et al. 2014). Process conditions shown in Table 21 represent the steady-state operation of the fluidized bed roaster. However, during cold start-up, the roaster goes through several stages that IDEAS can model. Typically, the roaster burner is turned on to heat the fluidized bed with no concentrate and airflow. After the bed temperature reaches 450°C, airflow starts and is increased incrementally as concentrate feed rate and temperature also increase. Ultimately, as concentrate feed and airflow reach their steady-state levels, cooling water is used to maintain thermal equilibrium in the roaster. Figure 25 shows the dynamic computer simulation of the fluidized bed start-up and its transition to steady-state

**Table 20 Major copper concentrate reactions**

| Roaster Reactions | Heat of Reaction, kJ/kg |
|---|---|
| $2Cu_3AsS_4(s) = 3Cu_2S(s) + As_2S_3(g) + S_2(g)$ | –132.42 |
| $2FeS_2(s) = 2FeS(s) + S_2(g)$ | 1,118.32 |
| $4CuS(s) = 2Cu_2S(s) + S_{2(g)}$ | 455.96 |
| $10Cu_2S(s) + 4FeS(s) + S_2(g) = 4\ Cu_5FeS_4(s)$ | –257.75 |
| $0.6FeS(s) + O_2 = 0.2Fe_3O_4(s) + 0.6SO_2(g)$ | –6,457.35 |
| $S_2(g) + 2O_2 = 2SO_2(g)$ | –1,1255.48 |
| $2As_2S_3(g) = 9O_{2(g)} = As_4O_8(g) + 6SO_2$ | –6,160.16 |

Source: Fan 1997; Rajoria et al. 2014; Jones 1987

**Table 21 Composition of roaster feed and simulation model process conditions**

| Mineral | Weight % |
|---|---|
| $Cu_2S$ | 30 |
| $Cu_3AsS_4$ | 22 |
| $Cu_5FeS_4$ | 4.8 |
| $CuFeS_2$ | 7.3 |
| $CuS$ | 3.9 |
| $FeS_2$ | 26 |
| $SiO_2$ | 6 |
| **Process Conditions** | **Value** |
| Concentrate feed rate, t/h | 75 |
| Fluidized airflow rate, $Nm^3/h$ | 40,000 |
| Fluidized air temperature, °C | 250 |
| Fluidized bed temperature, °C | 700 |

Source: Rajoria et al. 2014

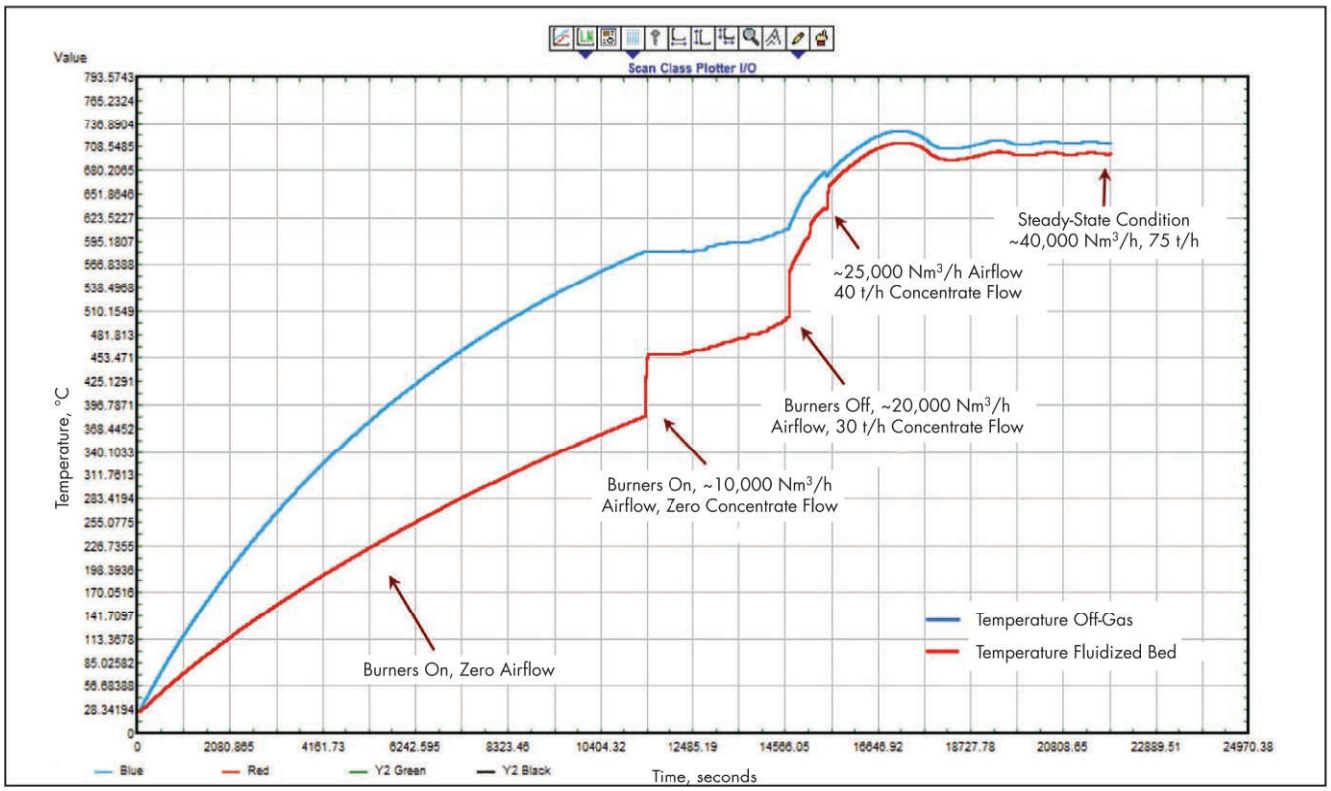


Source: Rajoria et al. 2014

**Figure 25 Dynamic process model of copper concentrate roaster start-up and transition to steady state**

behavior during a 6-hour period. The model also verified a 25°C gap between fluidized-bed and off-gas temperatures.

As part of this case study, several process conditions were modeled to understand the effect of variation of feed flow with constant airflow. The concentrate feed flow rate was varied between 55 and 90 t/h, while keeping airflow constant at 40,000 $Nm^3/h$ (Rajoria et al. 2014). The results are shown in Figure 26.

At the maximum concentrate flow rate of 90 t/h, the computer simulation verified that the temperature of the roaster starts to decrease. This is in line with actual operation of the roaster under these conditions; as during plant operation, insufficient oxygen to oxidize the concentrate sulfur content limits heat generation. Plant operators can use IDEAS to understand the effect of concentrate feed and airflow rates on the roaster temperature. Computer simulation showed that increasing airflow or decreasing the concentrate feed rate increased the roaster temperature.

Another behavior that can be investigated using IDEAS is the effect of variations in the fluidized airflow rate at constant concentrate feed rate. This is essential for the plant operator to understand the effect of air-flow rate on temperature profile and arsenic volatilization at a constant rate of concentrate feed. Figures 27 and 28 show these effects (Rajoria et al. 2014).

As the flow rate of fluidized air was increased to 55,000 $Nm^3/h$, the temperature of the fluidized bed increased to around 900°C (Figure 27). As more oxygen was passed through the bed, more sulfur was oxidized. When the flow of air was decreased to 35,000 $Nm^3/h$, the temperature of the bed started declining. With the change in the fluidized airflow rate, arsenic volatilization (weight % of arsenic going to off-gas) was also analyzed for all three cases and plotted as shown in Figure 28. The model provides a realistic depiction of arsenic volatilization rate with airflow rate as a function of time and temperature. Note that as the flow of air is reduced, off-gas arsenic content increases and, as a result, less arsenic is trapped in the calcine formed.

The model of the roaster operation was also used to study the effect of the flow of cooling water rate set-point on the roaster temperature profile. This is shown in Figure 29.

Figure 30 shows the effect of concentrate feed composition on temperature profile of the fluidized bed. The main change in feed composition was the arsenic content. A similar graph was plotted for the three cases with different feed compositions, and the same procedure was followed to cold-start the roaster as mentioned previously, to maintain a steady-state condition at 700°C with the concentrate flow of 75 t/h, with fluidizing air maintained at 40,000 $Nm^3/h$.

As shown in Figure 30, because of more heat generated from decomposition of enargite ($Cu_3AsS_4$) than that associated with decomposition of pyrite ($FeS_2$), the higher arsenic content of the concentrate results in more heat being generated.

### *Benefits of Process Modeling in Pyrometallurgy*

Steady-state modeling, leading to a material and energy balance of a process, is useful in determining flow-sheet alternatives and the flow rates of process input and output streams, as well as heating and cooling requirements. Dynamic process models have many additional uses, which include the following:

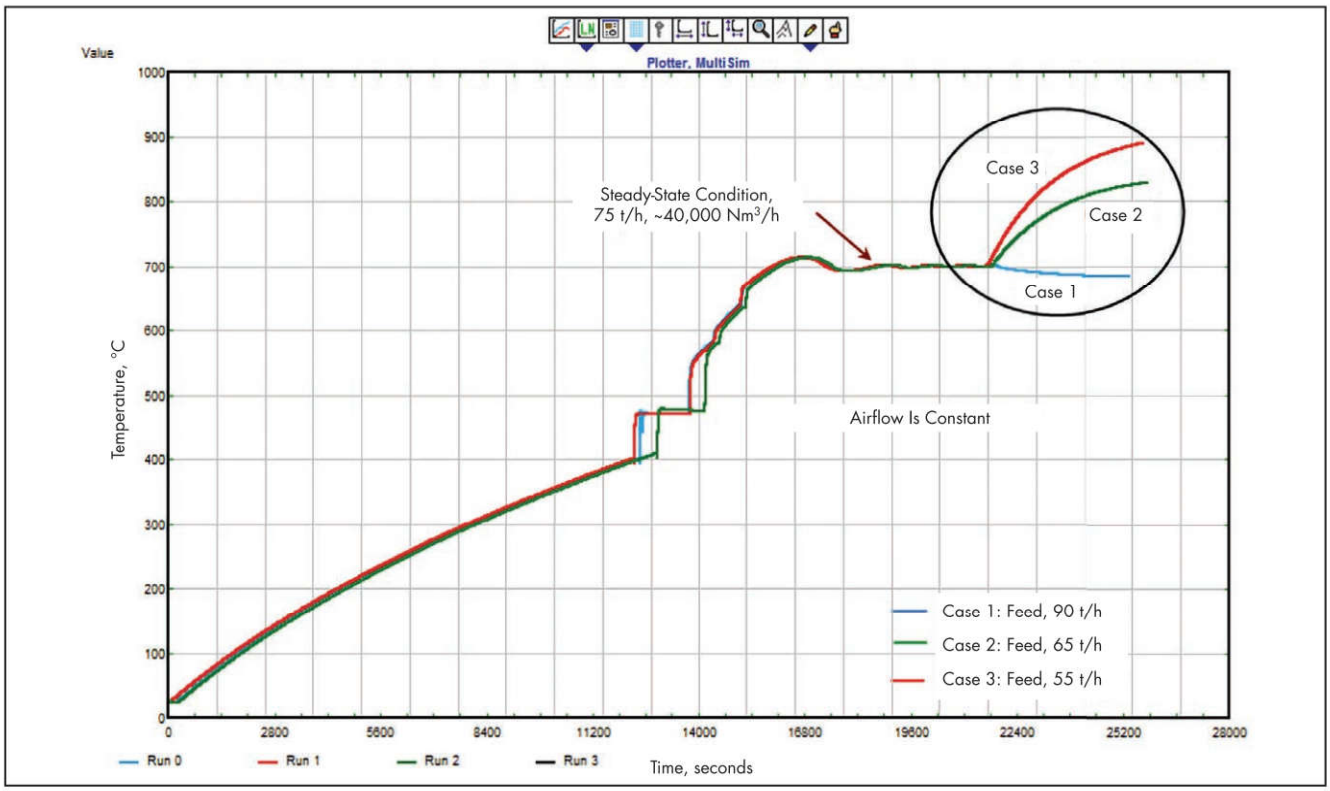


Source: Rajoria et al. 2014

**Figure 26 Effect of concentrate flow rate on roaster temperature**

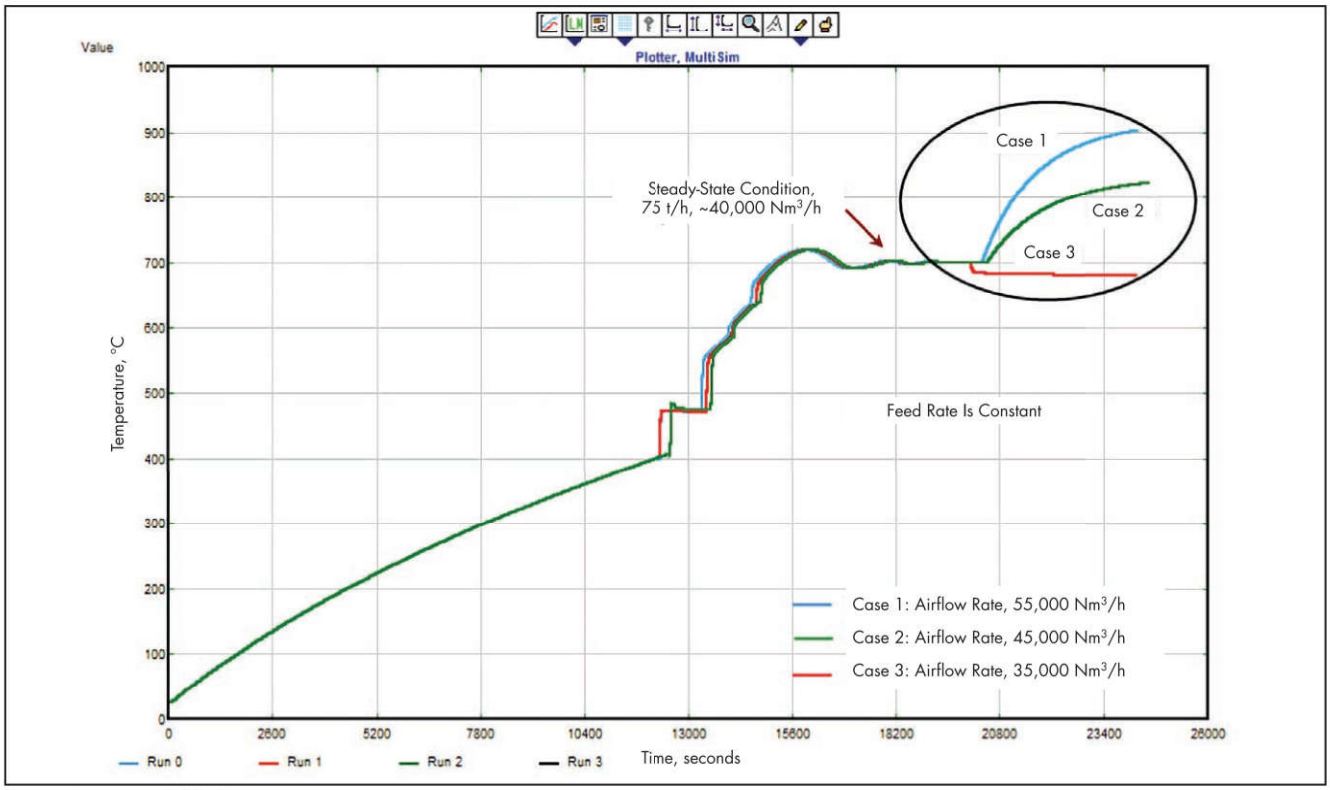


Source: Rajoria et al. 2014

**Figure 27 Effect of roaster airflow rate on process temperature at constant concentrate feed rate**

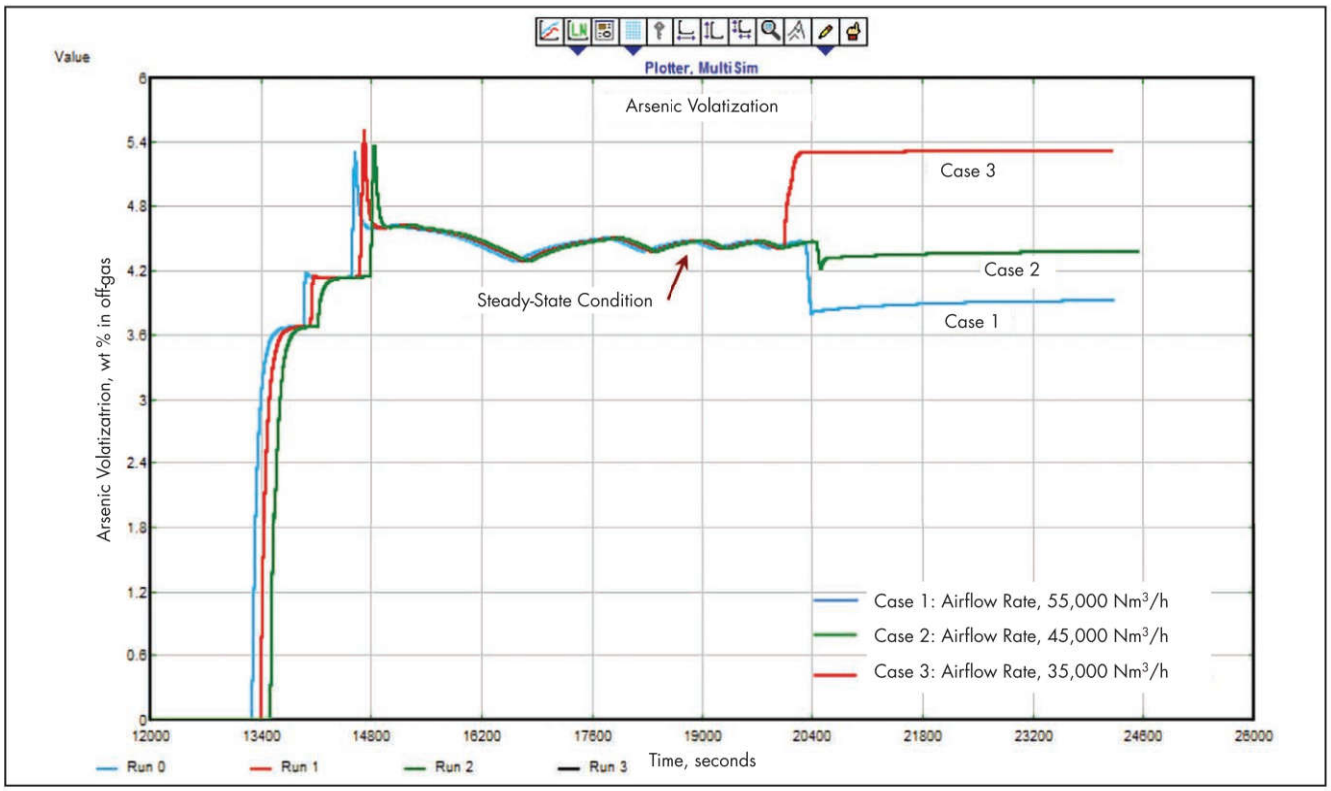


Source: Rajoria et al. 2014

**Figure 28 Effect of roaster airflow rate on arsenic volatilization at constant concentrate feed rate**

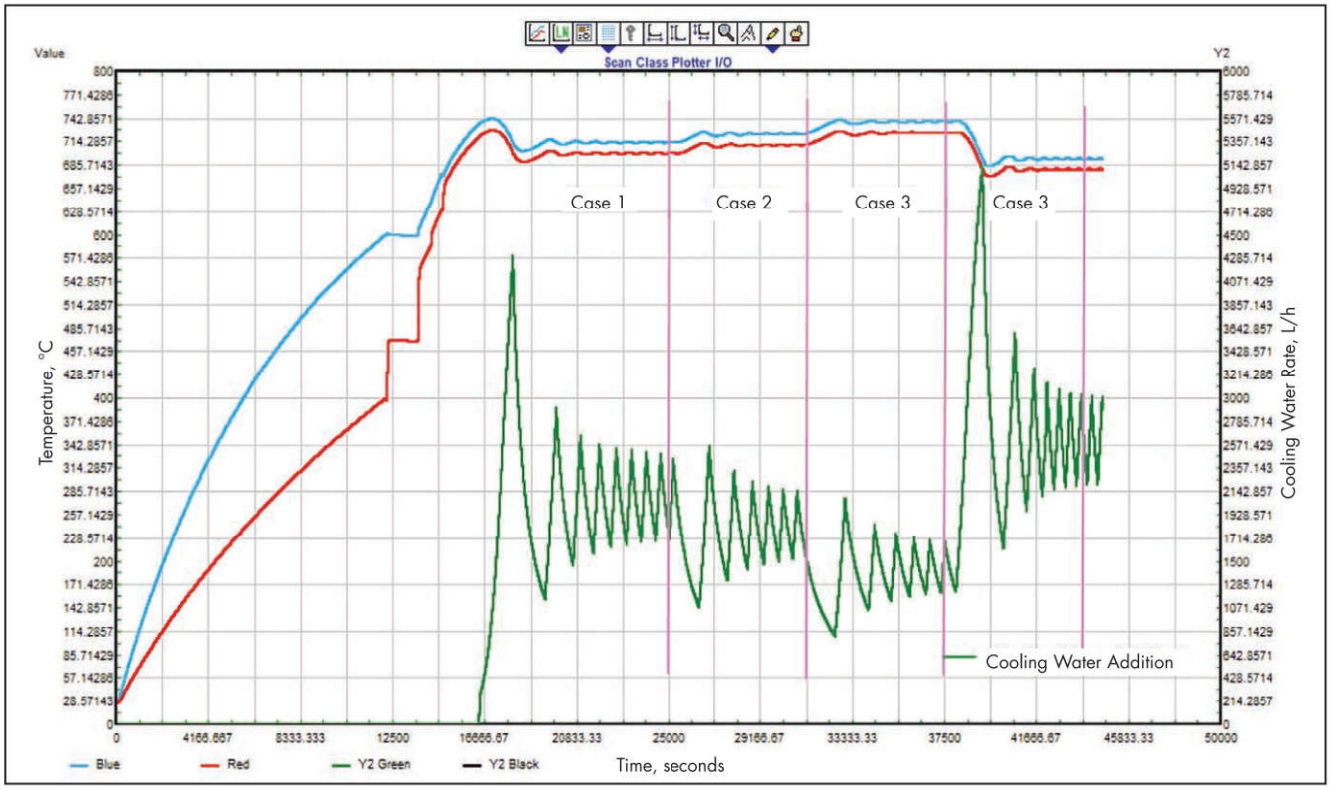


Source: Rajoria et al. 2014

**Figure 29 Effect of roaster temperature set-point variation on the cooling water rate**

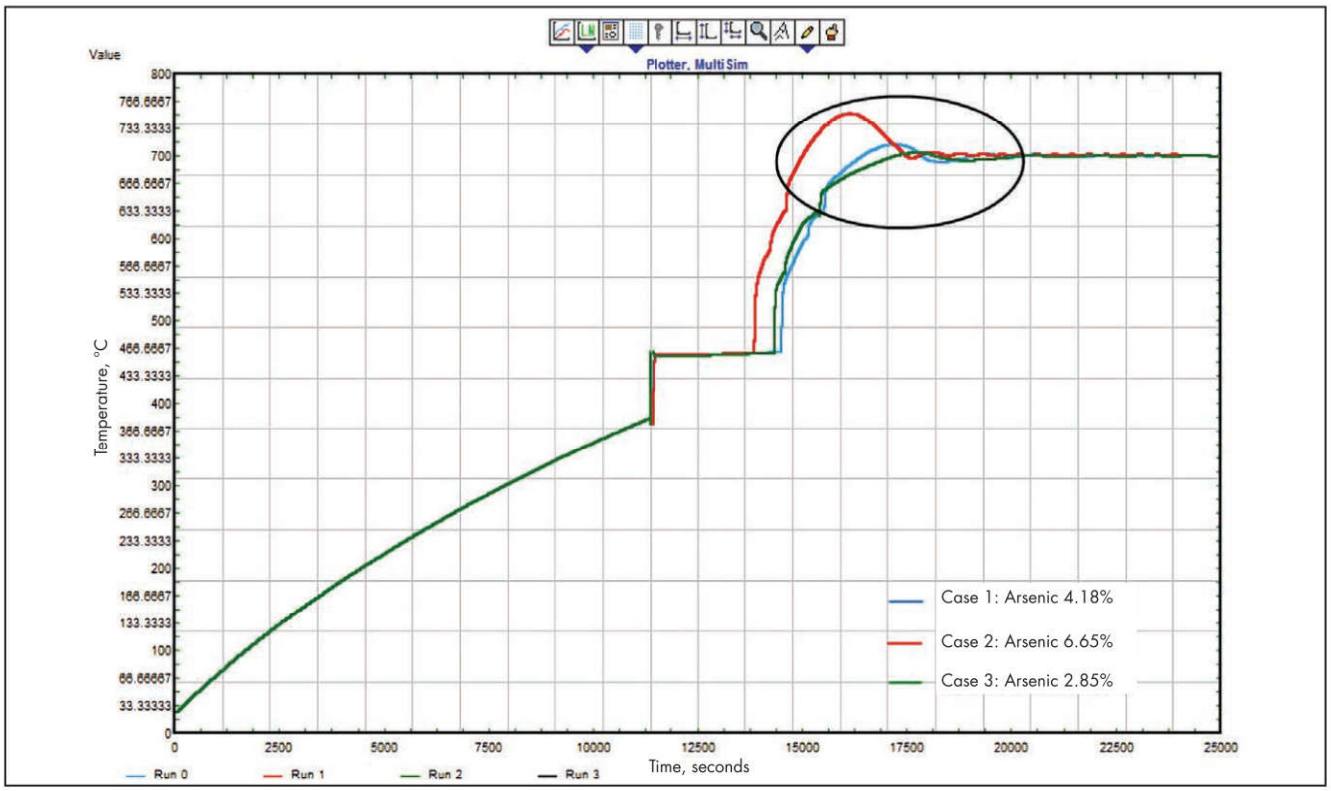


Source: Rajoria et al. 2014

**Figure 30 Effect of concentrate arsenic content on roaster bed temperature**

- **Validating operating procedures.** As part of dynamic modeling of a pyrometallurgical process, a virtual plant is created that can validate the operating process for unsteady-state conditions in real time. These include start-up, shutdown, and emergency situations such as loss of power or cooling water. In the case study of a fluidized bed roaster (Figure 24), the operating procedure for start-up was validated with the use of IDEAS.
- **Investigating what-if scenarios.** The simulation can test a pyrometallurgical process under different conditions and investigate their effect on the process. In the case study, several scenarios were tested (change in concentrate feed flow rate, airflow rate, cooling water rate, and concentrate feed composition), and their effects were shown on the temperature profile of the fluidized bed and arsenic volatilization.
- **Verifying process control logic.** The model can seamlessly interact with the control system—distributed control system and/or programmable logic controller—and be used for logic and control loop verification prior to the plant start-up.
- **Training operations personnel.** The dynamic model can be linked to the actual plant control system and used for operator training. Operators can use real control screens (human–machine interface) to be trained in operating the virtual plant, gaining an understanding of the process and equipment dynamics and interactions.

## REFERENCES

ABB. 2018. ABB Enterprise Software. http://new.abb.com/enterprise-software. Accessed February 2018.

AggFlow. 2018. AggFlow Design. https://aggflow.com/. Accessed February 2018.

Andersen, J.S. 1988. Development of a Cone Crusher Model. M. Eng. Sc. thesis, University of Queensland, Julius Kruttschnitt Mineral Research Centre, Brisbane, Australia.

Andritz. 2018. IDEAS software simulation downloads. www.andritz.com/products-and-services/pf-detail.htm?productid=18154. Accessed February 2018.

ANSYS. 2018. ANSYS Fluent. www.ansys.com/Products/Fluids/ANSYS-Fluent. Accessed February 2018.

Argyropoulos, S.A., Closset, B., and Valiveti, R. 1984. Documented Fortran programs for ball-mill modelling. *CIM Bull.* 870(77).

Arrhenius, S.A. 1889. Über die Dissociationswärme und den Einflusß der Temperatur auf den Dissociationsgrad der Elektrolyte. *Z. Physik. Chem.* 4:96–116.

Aspentech. 2018. AspenPlus. www.aspentech.com/products/engineering/aspen-plus/. Accessed February 2018.

Austin, L.G., Klimpel, R.P., and Luckie, P.T. 1984. *Process Engineering of Size Reduction: Ball Milling*. New York: SME-AIME.

Baes, C.F., and Mesmer, R.E. 1976. *The Hydrolysis of Cations*. New York: Wiley-Interscience.

Bale, C.W., Chartrand, E.P., Degterov, S.A., Eriksson, G., Hack, K., Ben Mahfoud, R., Melançon, J., Pelton, A.D., and Petersen, S. 2002. FactSage thermochemical software and databases, computer coupling of phase diagrams and thermochemistry (Calphad). *Int. Res. J. Calculation Phase Diagrams* 26(2):189–228.

Caspeo. 2018. USIM PAC. www.caspeo.net/USIMPAC. Accessed February 2018.

CFDEM Project. 2018. LIGGHTS open source discrete element method particle simulation code. www.cfdem.com/liggghts-open-source-discrete-element-method-particle-simulation-code. Accessed February 2018.

ChemApp. 2018. Home page. www.gtt-technologies.de/chemapp. Accessed February 2018.

CITIC SMCC Process Technology. 2018. Home page. www.citic-smcc.com. Accessed February 2018.

Daniel, M.J., and Morrell, S. 2004. HPGR model verification and scale-up. *Miner. Eng.* 17(May):1149–1161.

Devia, M., Wilkomirsky, I., and Parra, R. 2012. Roasting kinetics of high arsenic copper concentrates: A review. *Miner. Metall. Process*. 29(2):121–128.

Dry, M. 2013. Early evaluation of metal extraction projects. Presented at ALTA 2013, Perth, Australia, May 25–June 1.

Dry, M. 2015. Technical and cost comparison of laterite treatment processes, Part 3. Presented at ALTA 2015, Perth, Australia, May 23–30.

Drzymala, J. 2007. *Mineral Processing Foundations of Theory and Practice of Minerallurgy* [sic]. Poland: Wroclaw University of Technology.

Dutwa Project. 2018. Home page. www.blackdownresources.com/dutwa-overview.asp. Accessed February 2018.

EDEM. 2018. EDEM Software. www.edemsimulation.com/software. Accessed February 2018.

Ellingham, H.J.T. 1944. Reducibility of oxides and sulfides in metallurgical processes. *J. Soc. Chem. Ind.* 63(1944):125–133.

Fan, Y. 1997. Cinética y mecanismos de vaporización de sulfuros de arsénico desde concentrados de cobre. Tesis de magíster en ciencias de la ingeniería, Mención Metalurgia Extractiva, Universidad de Concepción, Concepción, Chile.

Fourie, P. 2007. Modelling of separation circuits using numerical analysis. In *Proceedings of the 6th International Heavy Minerals Conference "Back to Basics."* Johannesburg: Southern African Institute of Mining and Metallurgy. pp. 1–6.

Gilchrist, J.D. 1989. *Extraction Metallurgy*, 3rd ed. Oxford: Pergamon Press.

Haque, N., Bruckard, W., and Cuevas, J. 2012. A techno-economic comparison of pyrometallurgical and hydrometallurgical options for treating high-arsenic copper concentrates. Presented at the XXVI International Mineral Processing Congress (IMPC), New Delhi, India, September 24–28.

Hay, M.P. 2005. Using the SUPASIM® Flotation Model to Diagnose and Understand Flotation Behaviour from Laboratory through to Plant. In *Proceedings of 37th Annual Meeting of the Canadian Mineral Processors*. Montreal, QC: Canadian Institute of Mining, Metallurgy and Petroleum. pp. 463–479.

Herbst, J.A., and Pate, W.T. 2018. Dynamic simulation of size reduction operations from mine-to-mill. Kealakekua, HI: J.A. Herbst and Associates.

Herbst, J., Rajamani, R.K., Mular, A.L., and Flintoff, B. 2002. Mineral processing plant/circuit simulators: An overview. In *Mineral Processing Plant Design, Practice, and Control*. Edited by A.L. Mular, D.N. Halbe, and D.J. Barratt. Littleton, CO: SME. pp. 383–403.

Holland-Batt, A.B. 1989. Spiral separation: Theory and simulation. *Trans. Inst. Min. Metall.* 98(Jan.-Apr.):C46–C60.

InfoMine. 2018. Mining cost models. http://costs.infomine.com/costdatacenter/miningcostmodel.aspx. Accessed February 2018.

JKTech. 2018. Software. http://jktech.com.au/software. Accessed February 2018.

Jones, R. 1987. Computer simulation of pyrometallurgical processes, APCOM 87. In *Proceedings of the Twentieth International Symposium on Application of Computers and Mathematics in Mineral Industries*. Vol. 2: Metallurgy. Johannesburg: Southern African Institute of Mining and Metallurgy. pp. 265–279.

Kelly, T.D., and Matos, G.R. 2014. Historical statistics for mineral and material commodities in the United States (2016 version). US Geological Survey Data Series 140. http://minerals.usgs.gov/minerals/pubs/historical-statistics. Accessed February 2018.

King, R.P. 2001. *Modeling and Simulation of Mineral Processing Systems*. Oxford: Butterworth-Heinemann.

Leung, K. 1987. An energy based ore specific model for autogenous and semi-autogenous grinding mills. PhD thesis, University of Queensland, Australia.

Lishchuk, V. 2016. Geometallurgical programs: Critical evaluation of applied methods and techniques. Licentiate of engineering thesis in mineral processing, Luleå University of Technology, Sweden.

Luttrell, G.H., Barbee, C.J., Bethell, P.J., and Wood, C.J. 2005. *Dense Medium Cyclone Optimisation*. Final Technical Report to the U.S. Department of Energy, DOE Award Number DE-FC26-01NT41061.

Lynch, A.J. 1977. *Mineral Crushing and Grinding Circuits: Their Simulation, Optimization, Design and Control*. New York: Elsevier Scientific Publishing.

Mackinnon, S., Yan, D., and Dunne, R. 2003. The interaction of flash flotation with closed circuit grinding. *Miner. Eng.* 16 (11):1149–1160.

Maelgwyn Mineral Services Ltd. 2009. Limn: The Flowsheet Processor. www.maelgwyn.com/technology/limn-the-flowsheet-processor/. Accessed February 2018.

Marsden, J.O., and Botz, M.M. 2017. Heap leach modeling: A review of approaches to metal production forecasting. *Miner. Metall. Process.* 34(2):53–64.

MathWorks. 2018. MATLAB. www.mathworks.com/products/matlab.html?s_tid=hp_products_matlab. Accessed February 2018.

McGarry, M., and Watson, M. 1998. Dynamic simulation: A maturing technology generating real benefits. https://www.andritz.com/resource/blob/14790/d17a6ac5824afe0c442c065bb93a47c6/aa-automation-simulation-maturing-technology-benefits-data.pdf. Accessed February 2018.

Metso. 2008. Bruno: Metso's simulating tool. www.metso.com/miningandconstruction/mm_segments.nsf/WebWID/WTB-081113-2256F-FD63A/$File/Bruno_presentation.pdf. Accessed February 2018.

Mineral Technologies International. 2010. MODSIM: Modular simulator for mineral processing plants. www.mineraltech.com/MODSIM/. Accessed February 2018.

Moly-Cop. 2018. Moly-Cop Tools 3.0 Software. www.molycop.com/supporting-customers/molycop-tools. Accessed February 2018.

Nageswararao, K. 1990. Reduced efficiency curves of industrial hydrocyclones: An analysis for plant practice. *Miner. Eng.* 12(5):517–544.

Napier-Munn, T.J., Morell, S., Morrison, R.D., and Kojovic, T. 1996. *Mineral Comminution Circuits: Their Operation and Optimisation*. Indooroopilly, Queensland: Julius Kruttschnitt Mineral Research Centre.

Nicol, M.J., Fleming, C.A., and Paul, R.L. 1987. The chemistry of extraction of gold. In *Extractive Metallurgy of Gold*. Edited by G.G. Stanley. Monograph Series M7. Johannesburg: Southern African Institute of Mining and Metallurgy. pp. 894–899.

Nikkhah, K., and Anderson, C. 2001. Role of simulation software in design and operation of metallurgical plants: A case study. SME Preprint No. 01-176. Littleton, CO: SME.

OpenCFD Ltd. 2017. About OpemFOAM. www.openfoam.com/. Accessed February 2018.

Papangelakis, V.G., Georgiou, D., and Rubisov, D.H. 1996. Control of iron during the sulfuric acid pressure leaching of limonite. In *Proceedings of the Second International Symposium on Iron Control in Hydrometallurgy*. Edited by J.E. Dutrizac and G.B. Harris. Montreal. QC: Canadian Institute of Mining, Metallurgy and Petroleum.

ProSim. 2018. Software and Services in Process Simulation. www.prosim.net. Accessed February 2018.

Proware. 2018. METSIM: The premier steady-state and dynamic process simulator. www.metsim.com/. Accessed February 2018.

PTC. 2018. PTC Mathcad. www.ptc.com/engineering-math-software/mathcad. Accessed February 2018.

Rajoria, A., Lucena, L., Das, S., Szatkowski, M., and Wilkomirsky, I. 2014. Dynamic simulation of processing high arsenic copper concentrates in a fluidized bed roaster. SME Preprint No. 14-071. Englewood, CO: SME.

Schwarz, S., Alexander, D., Whiten, W.J., Franzidis, J.P., and Harris, M. 2006. JKSimFloat V6: Improving flotation circuit performance and understanding. Presented at the XXIII International Mineral Processing Congress, Istanbul, Turkey.

Schwarz, S., and Richardson, J.M. 2013. Modeling and simulation of mineral processing circuits using JKSimMet and JKSimFloat. Presented at the SME Annual Meeting, Denver, CO.

STABCAL. 2015. Stability Calculation for Aqueous and Nonaqueous System. Version 2015. Butte, MT: Montana Tech.

SysCAD. 2018. Plant simulation software. www.syscad.net/. Accessed February 2018.

Tian, J., and Morrell, S. 2015. Operation and process optimization of Sino Iron's AG milling circuits. Presented at SAG Conference 2015, Vancouver, British Columbia, Canada.

Triple Point. 2018a. Algosys Bilmat: Accurate and timely data reconciliation. www.tpt.com/bilmat. Accessed February 2018.

Triple Point. 2018b. Algosys Metallurgical Accountant: Powerful metal accounting tool. www.tpt.com/metallurgical-accounting. Accessed February 2018.

U.S. Energy Information Administration. 2018. Coal. www.eia.gov/coal/. Accessed February 2018.

Vahed, A. 2004. Development of a fluid bed pyrohydrolysis process for Inco's Goro Nickel Project. Presented at the TMS Annual Meeting, Charlotte, NC.

Valery, W., Jr., and Morrell, S. 1995. The development of a dynamic model for autogenous and semi-autogenous grinding. *Miner. Eng.* 8(11):1285–1297.

VSMA (Vibrating Screen Manufacturers Association). 2014. *VSMA Vibrating Screen Handbook*. Milwaukee, WI: Association of Equipment Manufacturers.

Wedderburn, B. 2010. Nickel heap leaching study. Presented at the ISNG Environmental and Economics Session, April 27. www.insg.org/presents/Mr_Wedderburn_Apr10.pdf.

Weiss, N.L., ed. 1985. *SME Mineral Processing Handbook*. Littleton, CO: SME-AIME

Whiten, W.J. 1972. Simulation and model building for mineral processing. PhD dissertation, University of Queensland, Australia.

Whiten, W.J. 1974. A matrix theory of comminution machines. *Chem. Eng. Sci.* 29:589–599.

Wills, B.A. 1997. *Mineral Processing Technology*, 6th ed. Oxford: Butterworth-Heinemann.

Yan, D., Wiseman, D., and Dunne, R. 2005. Predicting the performance of a flotation circuit that incorporates flash flotation. Presented at the Centenary of Flotation Symposium, Brisbane, Queensland, Australia.